Institut für Informatik

Christian-Albrechts-Universität zu Kiel

future ocean
KIEL MARINE SCIENCES

Surrogate-Based Optimization for Marine Ecosystem Models

Dipl. Phys. Malte Prieß - mpr@informatik.uni-kiel.de

Supervisors: Prof. Dr. Thomas Slawig, Prof. Dr. Andreas Oschlies, Prof. Slawomir Koziel, Ph.D.

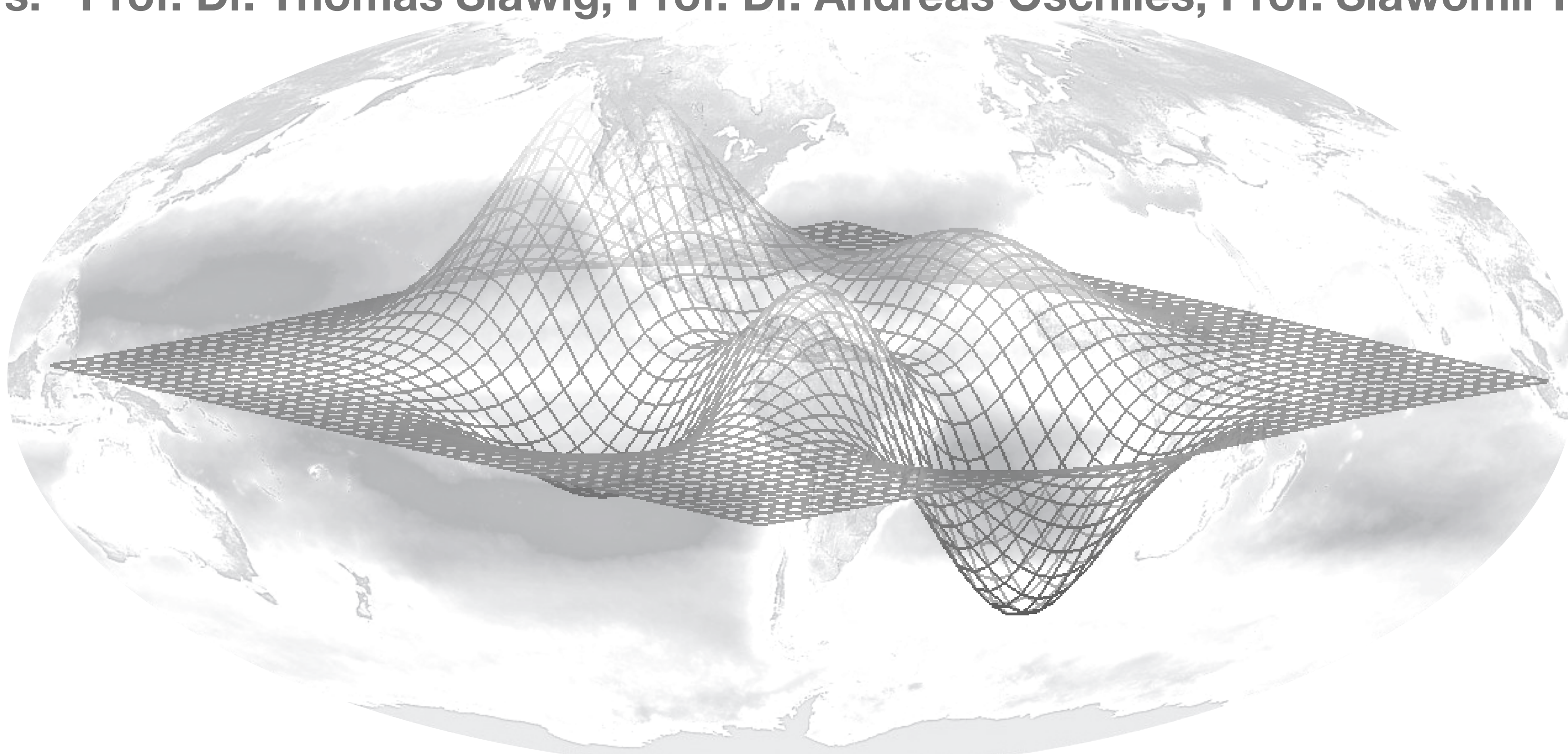

Defense

31/01/2012 - Kiel

computationally efficient calibration of marine ecosystem models at low computational costs

Outline

- The importance of marine ecosystems
- Marine ecosystem models
- Why model calibration?
- Surrogate-based optimization
- Study design
- Marine ecosystem models: Two examples
- Surrogate-based optimization: Numerical results
- Summary and outlook

Outline

- The importance of marine ecosystems
- Marine ecosystem models
- Why model calibration?
- Surrogate-based optimization
- Study design
- Marine ecosystem models: Two examples
- Surrogate-based optimization: Numerical results
- Summary and outlook

The importance of marine ecosystems

- Global warming is hardly scientifically doubted ➔ CO_2 as one main contributor
- 2010: Global CO_2 emissions exceeded the most pessimistic forecasts of the IPCC

The importance of marine ecosystems

- Global warming is hardly scientifically doubted ➔ CO_2 as one main contributor
- 2010: Global CO_2 emissions exceeded the most pessimistic forecasts of the IPCC
- Natural "sinks": Natural removal of atmospheric CO_2
- Example: Removal through biogeochemical cycle among carbon and the ocean biota

  ➔ marine carbon cycle

Institut für Informatik

future ocean
KIEL MARINE SCIENCES

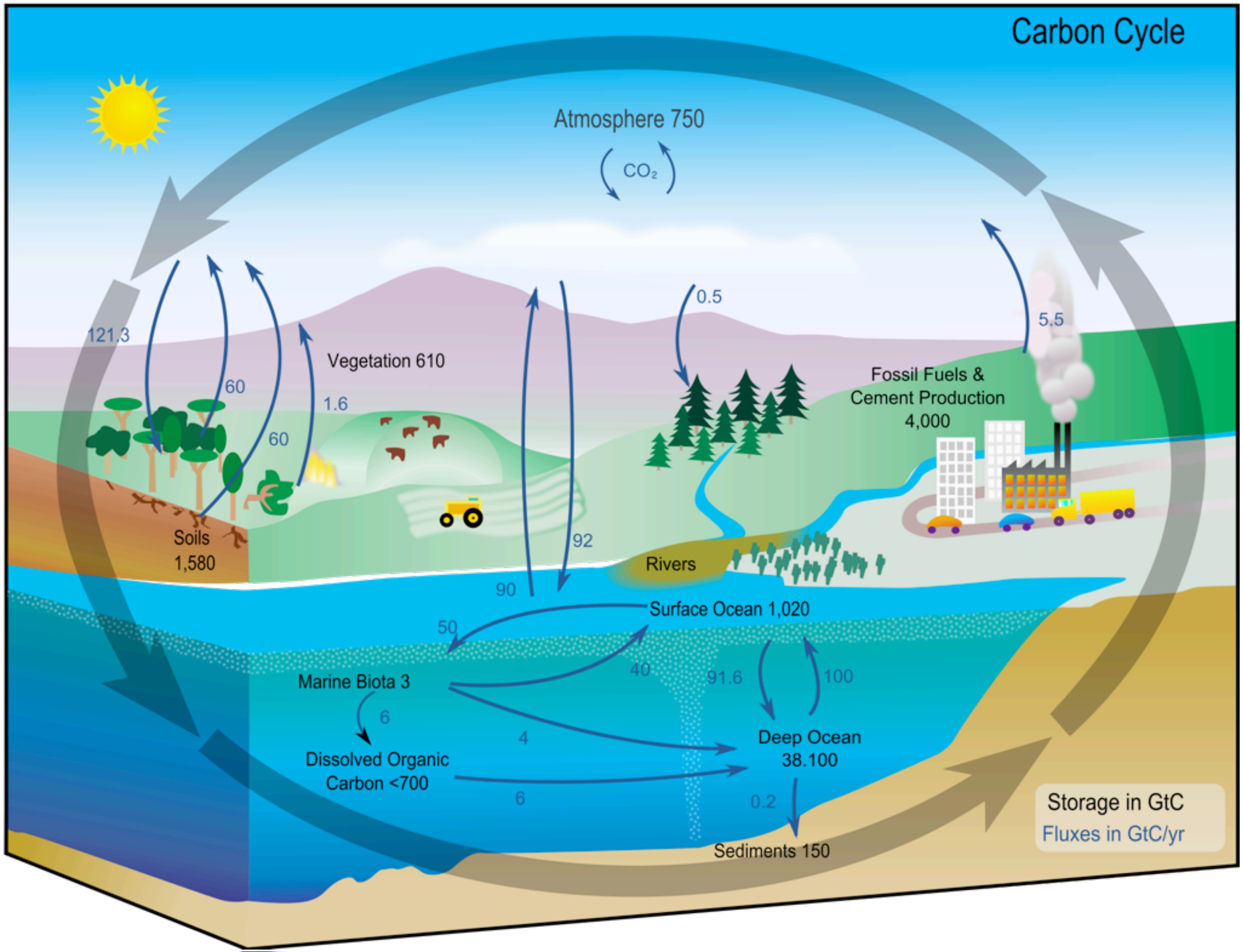

Picture source: NASA Earth Science Enterprise

Institut für Informatik
future ocean
KIEL MARINE SCIENCES

Clearly indispensible ...

- understanding relevant processes in the earth’s climate system
- understanding its responses to human impact
- projections of future dynamics

- Reliable representation of the past and today's observed quantities
  ➔ appropriate for prognostic simulations
- Modeled processes: Marine carbon cycle
- Time-dependent systems for transport, interactions, biogeochemistry
- Coupled with a hydrodynamic model (online/ offline)

- Reliable representation of the past and today's observed quantities
  ➔ appropriate for prognostic simulations
- Modeled processes: Marine carbon cycle
- Time-dependent systems for transport, interactions, biogeochemistry
- Coupled with a hydrodynamic model (online/ offline)

Hydrodynamic Model: ocean circulation, temperature and salinity distribution

↓ (↑)

Marine Ecosystem Model: transport, interactions, biogeochemistry

Outline

Institut für Informatik

future ocean
KIEL MARINE SCIENCES

- The importance of marine ecosystems
- Marine ecosystem models
- Why model calibration?
- Surrogate-based optimization
- Study design
- Marine ecosystem models: Two examples
- Surrogate-based optimization: Numerical results
- Summary and outlook

Why do we need model calibration (optimization)?

- Applicability for prognostic simulations
  ➔ depends on ability to resemble observed quantities

- Marine ecosystem models have to be calibrated
  ➔ identification of poorly known parameters

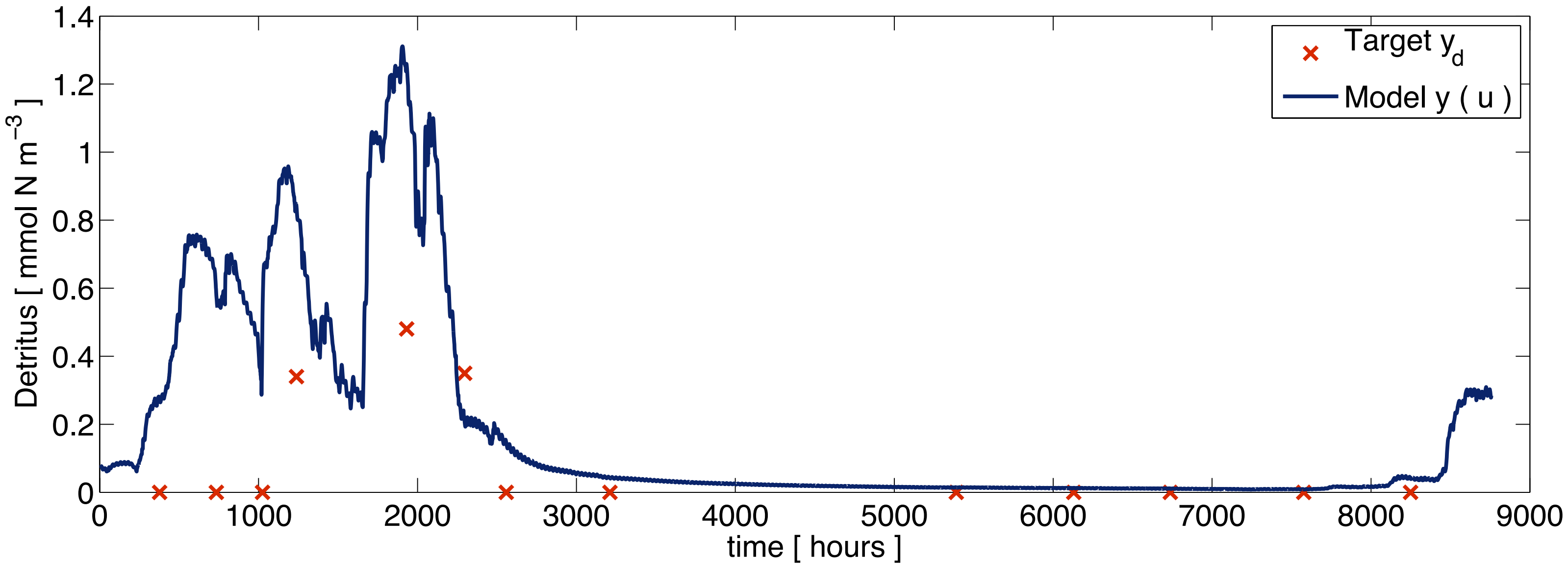

Why do we need model calibration (optimization)?

Institut für Informatik

future ocean
KIEL MARINE SCIENCES

- Applicability for prognostic simulations
  - ➔ depends on ability to resemble observed quantities
- Marine ecosystem models have to be calibrated
  - ➔ identification of poorly known parameters

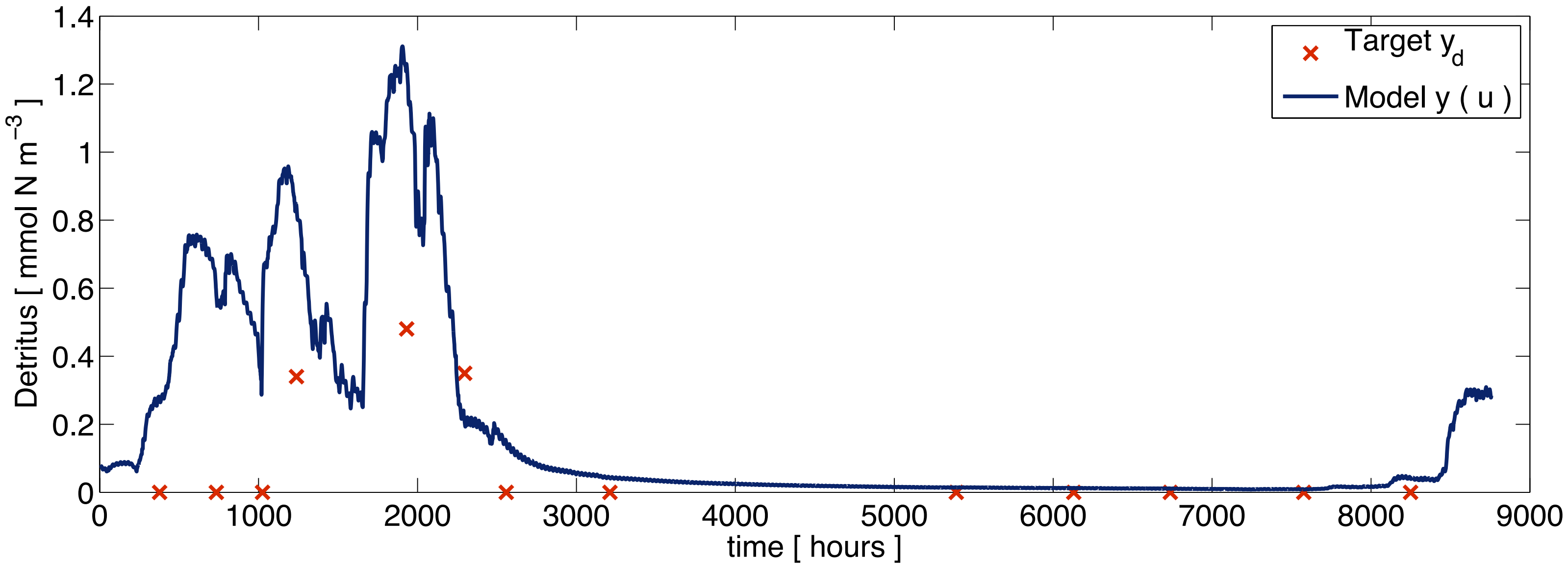

- Trade-off between high model complexity and simplified model formulation
- Assessment of models‘ quality ➔ calibration against observations

- Consider nonlinear optimization problems of the form: $\mathbf{u}^* = \underset{\mathbf{u}}{\operatorname{argmin}} \, J(\,\mathbf{y}(\mathbf{u})\,)$

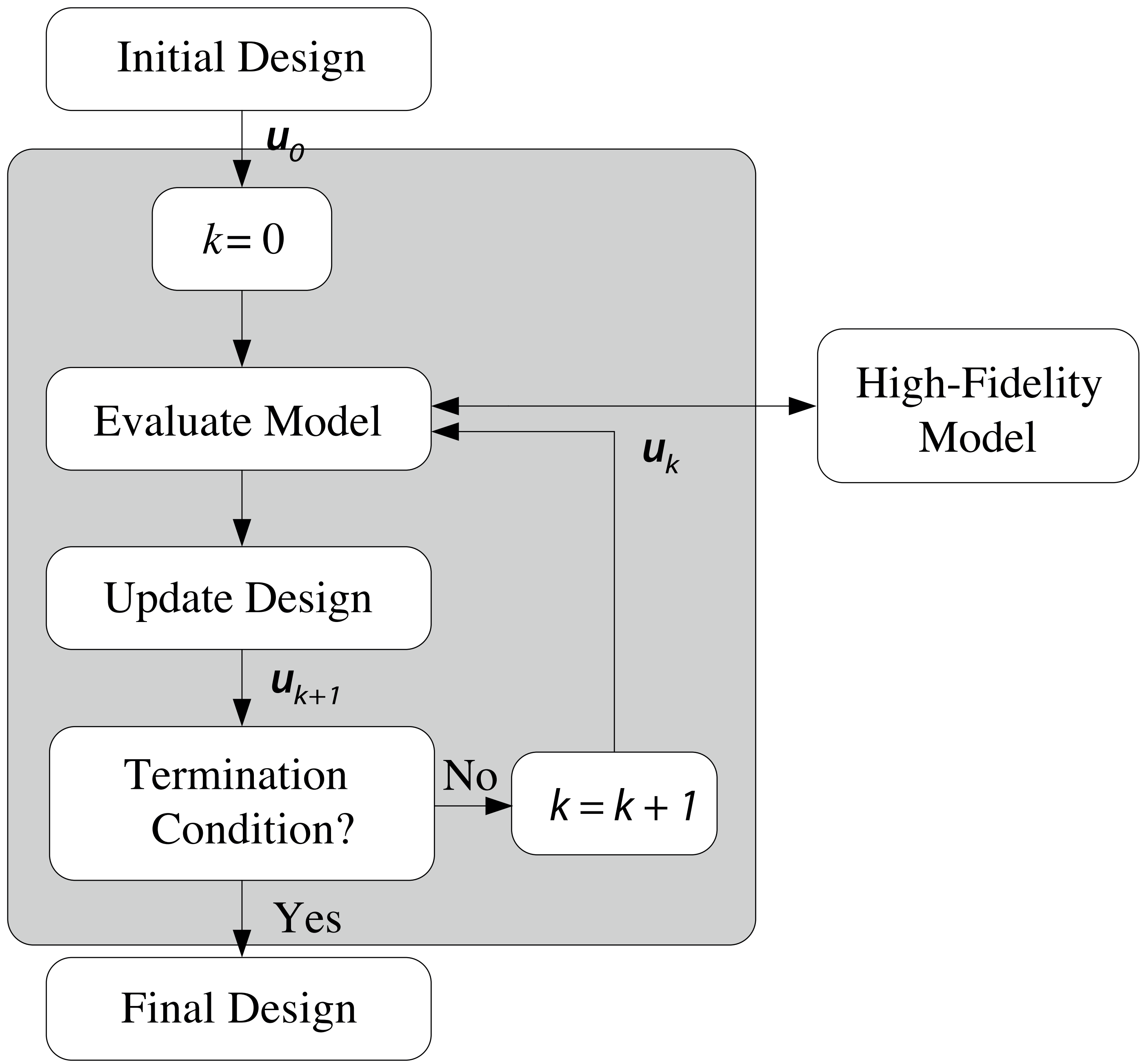

Picture source: cf. Koziel and Yang (2011), p. 196–198.

The direct optimization approach

- Consider nonlinear optimization problems of the form: $$\mathbf{u}^* = \underset{\mathbf{u}}{\operatorname{argmin}} \, J(\, \mathbf{y}(\mathbf{u})\,)$$

large number of objective function evaluations required

➔ possibly high computational costs

Picture source: cf. Koziel and Yang (2011), p. 196–198.

How to address the typically high computational burden

in direct optimization?

direct approach

$$\mathbf{u}^* = \underset{\mathbf{u}}{\operatorname{argmin}}\ J(\,\mathbf{y}(\mathbf{u})\,)$$

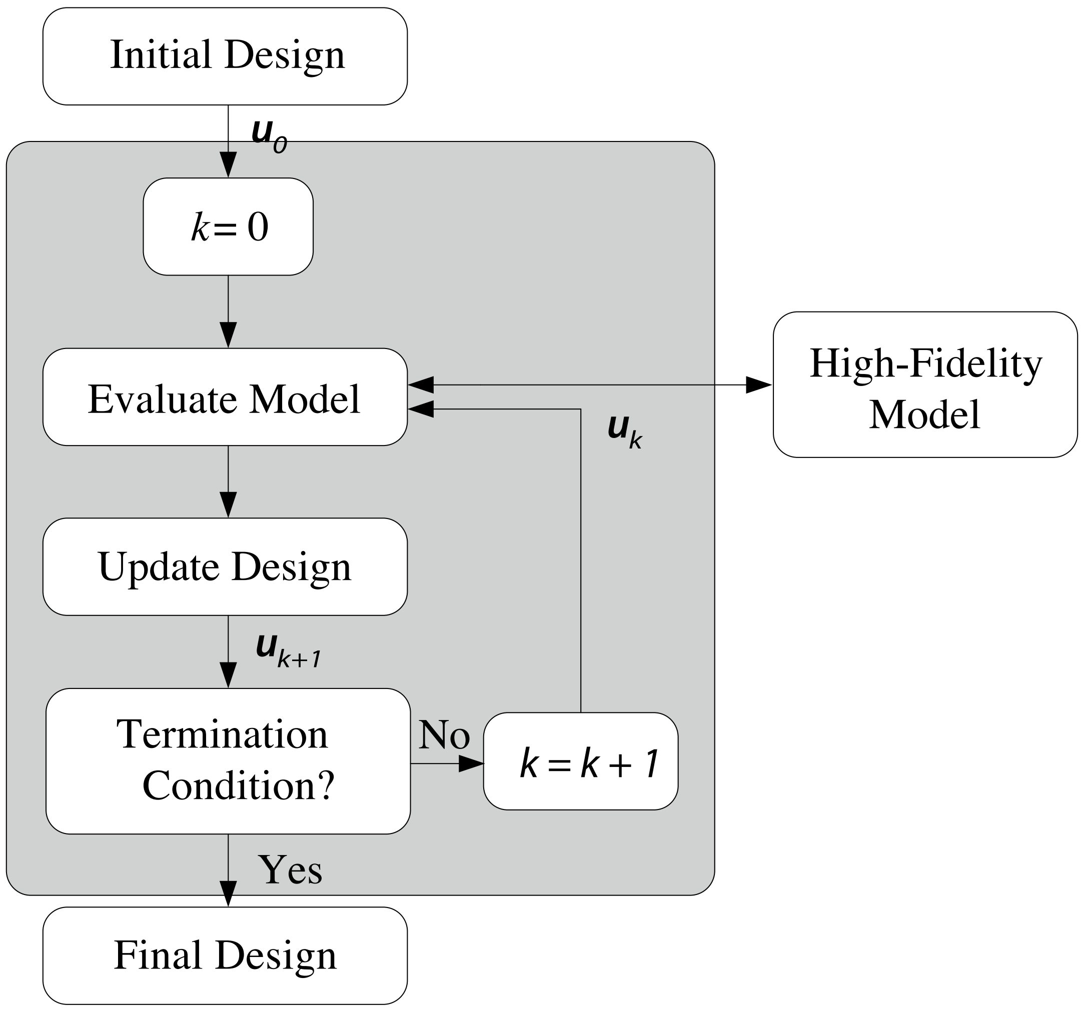

Picture source: cf. Koziel and Yang (2011), p. 196–198.

Institut für Informatik
future ocean
KIEL MARINE SCIENCES

direct approach

$$\mathbf{u}^* = \underset{\mathbf{u}}{\operatorname{argmin}}\ J(\,\mathbf{y}(\mathbf{u})\,)$$

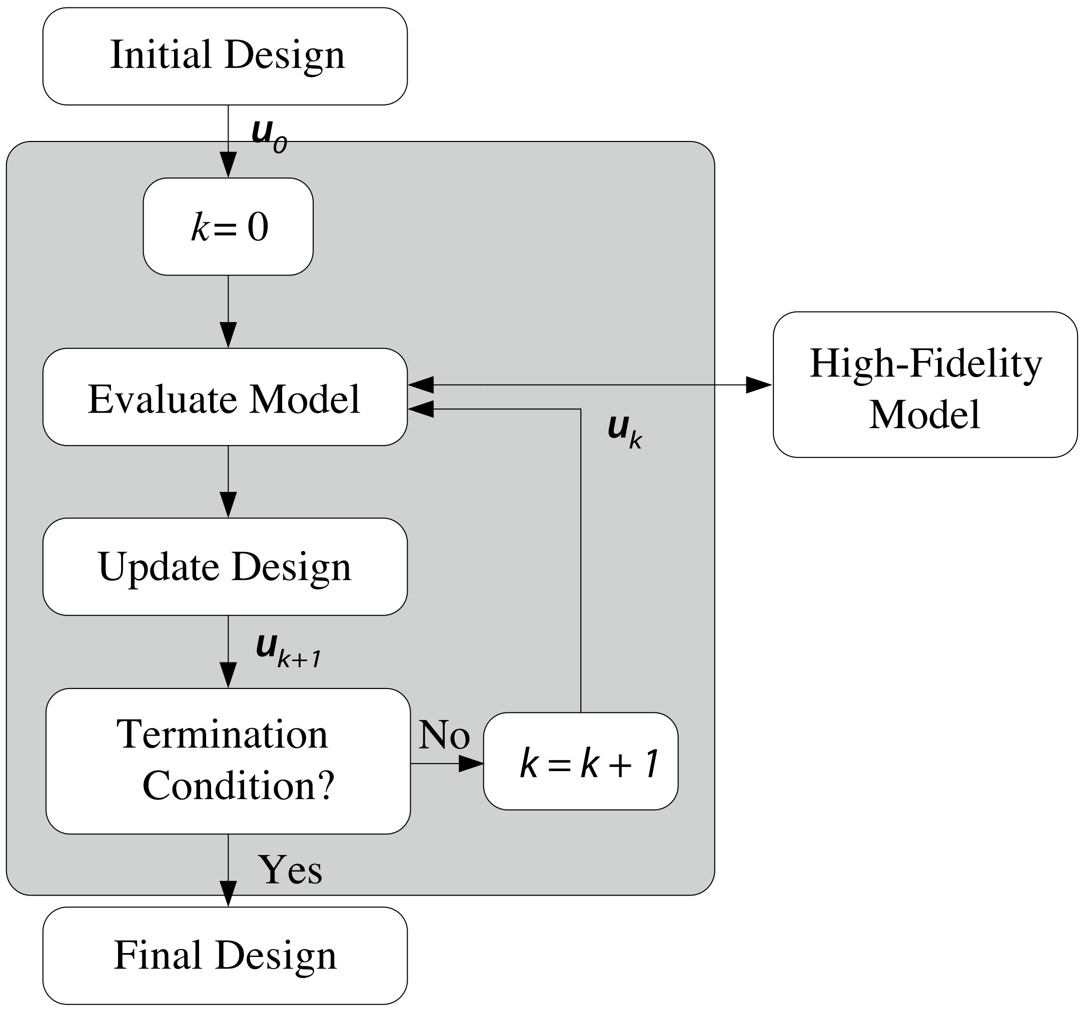

surrogate-based approach

$$\mathbf{u}_{k+1} = \underset{\mathbf{u}}{\operatorname{argmin}}\ J(\,\mathbf{s}_k(\mathbf{u})\,)$$

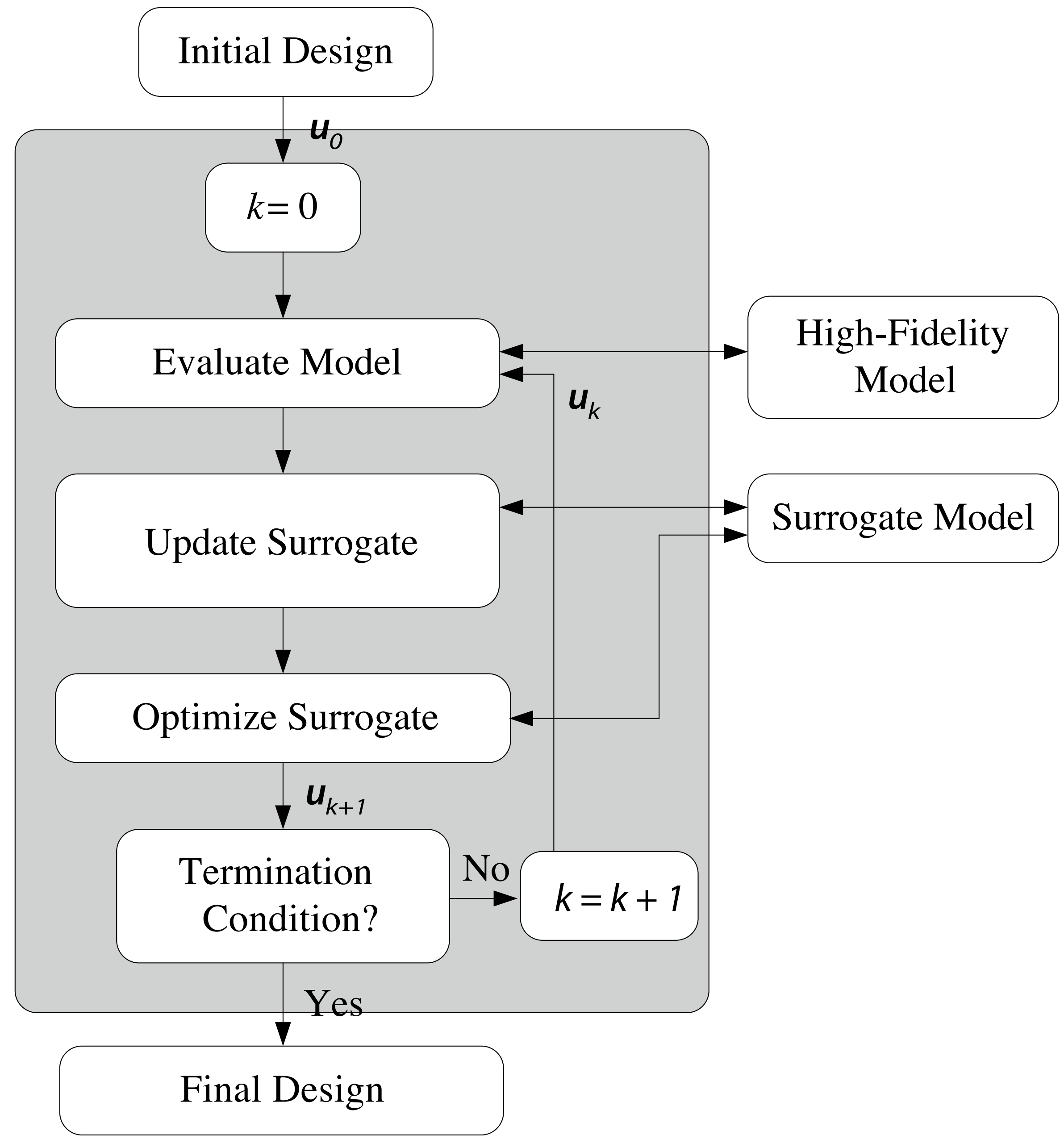

Picture source: cf. Koziel and Yang (2011), p. 196–198.

- Constructed from a physics-based low-fidelity (or coarse) model
  - Coarse discretization
  - Relaxed convergence criterion
  - Simplified physics
  - Analytical formulas

- Constructed from a physics-based low-fidelity (or coarse) model
  - Coarse discretization
  - Relaxed convergence criterion
  - Simplified physics
  - Analytical formulas
- Accuracy usually not sufficient for direct use
- Correction methods:

  Space Mapping [1], Response Correction [2], Manifold Mapping [3], Shape-Preserving Response Prediction [4], ...

[1] Bandler et al. (2004); [2] Søndergaard, J. (2003);
[3] Echeverria and Hemker (2008); [4] Koziel (2010b)

Advantages ...

- inherit relevant characteristics of fine model
- few fine model data necessary for sufficient accuracy
- generalization capability much better than for other types (functional surrogates)
- efficient: comparably small number of fine model evaluations required

  → overall optimization costs low

Outline

Institut für Informatik

future ocean
KIEL MARINE SCIENCES

- The importance of marine ecosystems
- Marine ecosystem models
- Why model calibration?
- Surrogate-based optimization
- Study design
- Marine ecosystem models: Two examples
- Surrogate-based optimization: Numerical results
- Summary and outlook

My work comprised ...

- surrogate-based optimization methodologies employing physics-based coarse models
- computationally efficient calibration of marine ecosystem models

My work comprised ...

- surrogate-based optimization methodologies employing physics-based coarse models
- computationally efficient calibration of marine ecosystem models

Aggressive Space Mapping

Multiplicative Response Correction

1D NPZD Model

3D N-DOP Model

Coarser Mesh Discretization

Truncated Spin-Up

Numerical Stability

My work comprised ...

- surrogate-based optimization methodologies employing physics-based coarse models
- computationally efficient calibration of marine ecosystem models

Aggressive Space Mapping

Multiplicative Response Correction

1D NPZD Model

3D N-DOP Model

Coarser Mesh Discretization

Truncated Spin-Up

Numerical Stability

Marine ecosystem models: Two examples under consideration

- One-dimensional, nitrogen-budget ecosystem model:

  Dissolved inorganic **n**itrogen, **p**hytoplankton, **z**ooplankton, **d**etritus [1]

  (12 model parameters)

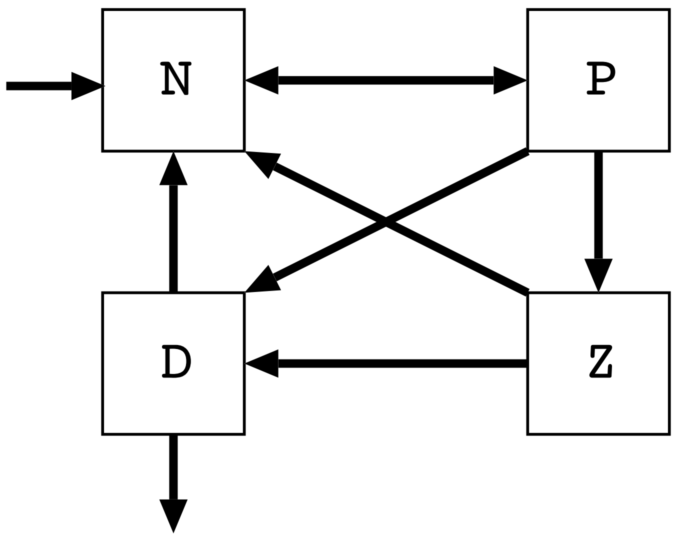

- Coupled (offline) with an ocean circulation model

- Time-dependent (non-periodic) forcing data + Euler time-stepping scheme

  ➔ transient run

[1] Oschlies and Garcon (1999); Bermuda Atlantic Time-Series Study, located at 31°N, 64°W - Schartau and Oschlies (2003)

- Three-dimensional simulation of phosphorus and dissolved organic matter [1] (7 model parameters)

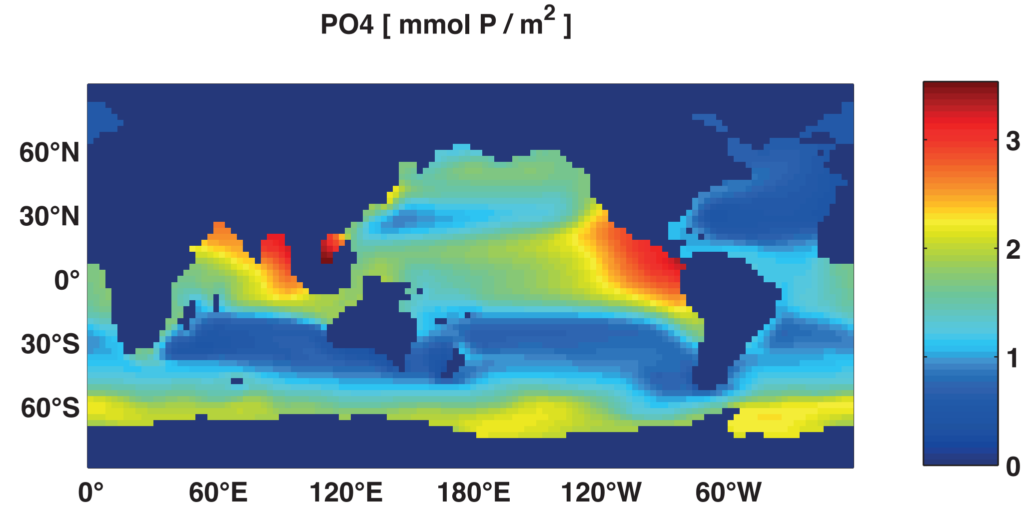

- Coupled (offline) with an ocean circulation model
  ➔ tracer transport matrices precalculated

- Transport Matrix Method [2] + classical fixed point iteration
  ➔ steady annual cycle

- Implemented as part of the simulation package of Metos3D [3]

[1] Kriest et al. (2010); Parekh et al. (2005); [2] Khatiwala et al. (2005);
[3] Piwonski and Slawig (2011)

Efficient model calibration by surrogate-based optimization:

Numerical results

Institut für Informatik
future ocean KIEL MARINE SCIENCES

- Basic idea:

$$\bar{\mathbf{s}}_k(\mathbf{u}) = \mathbf{a}_k\,\mathbf{y}_c(\mathbf{u}), \quad \mathbf{a}_k := \frac{\mathbf{y}_f(\mathbf{u}_k)}{\mathbf{y}_c(\mathbf{u}_k)}, \quad k = 1, 2, \ldots$$

- Consistency with fine model:

  Exact agreement in function values, derivatives expected to be at least similar

$$\bar{\mathbf{s}}_k(\mathbf{u}_k) = \mathbf{y}_f(\mathbf{u}_k), \quad \bar{\mathbf{s}}'_k(\mathbf{u}_k) \approx \mathbf{y}'_f(\mathbf{u}_k)$$

[1] Conn et al. (2000); Koziel et al. (2010)

- Basic idea:

$$\bar{\mathbf{s}}_k(\mathbf{u}) = \mathbf{a}_k\, \mathbf{y}_c(\mathbf{u}), \quad \mathbf{a}_k := \frac{\mathbf{y}_f(\mathbf{u}_k)}{\mathbf{y}_c(\mathbf{u}_k)}, \quad k = 1, 2, \ldots$$

- Consistency with fine model:

  Exact agreement in function values, derivatives expected to be at least similar

$$\bar{\mathbf{s}}_k(\mathbf{u}_k) = \mathbf{y}_f(\mathbf{u}_k), \quad \bar{\mathbf{s}}_k'(\mathbf{u}_k) \approx \mathbf{y}_f'(\mathbf{u}_k)$$

- Exact first-order consistency can be „forced“

$$\mathbf{s}_k(\mathbf{u}) = \bar{\mathbf{s}}_k(\mathbf{u}) + E_k\,(\mathbf{u} - \mathbf{u}_k), \quad E_k := \bar{\mathbf{s}}_k'(\mathbf{u}_k) - \mathbf{y}_f'(\mathbf{u}_k)$$

- Convergence: [1]

  Zero- and first order consistency + trust-region approach + „standard“ assumptions

[1] Conn et al. (2000); Koziel et al. (2010)

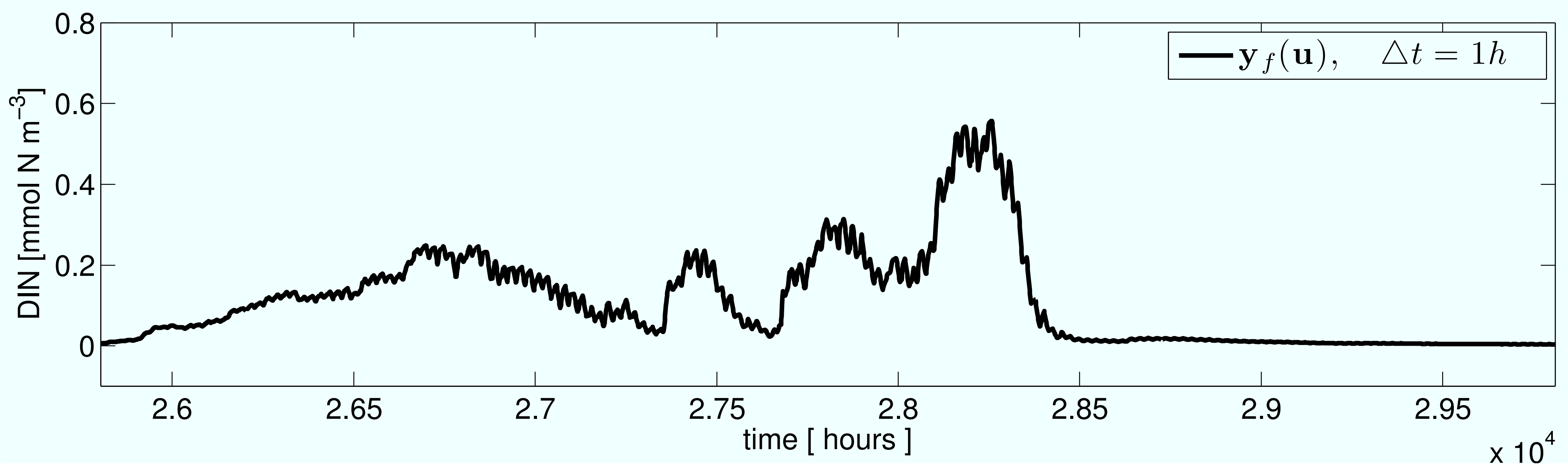

Figure: Raw fine and coarse model response.

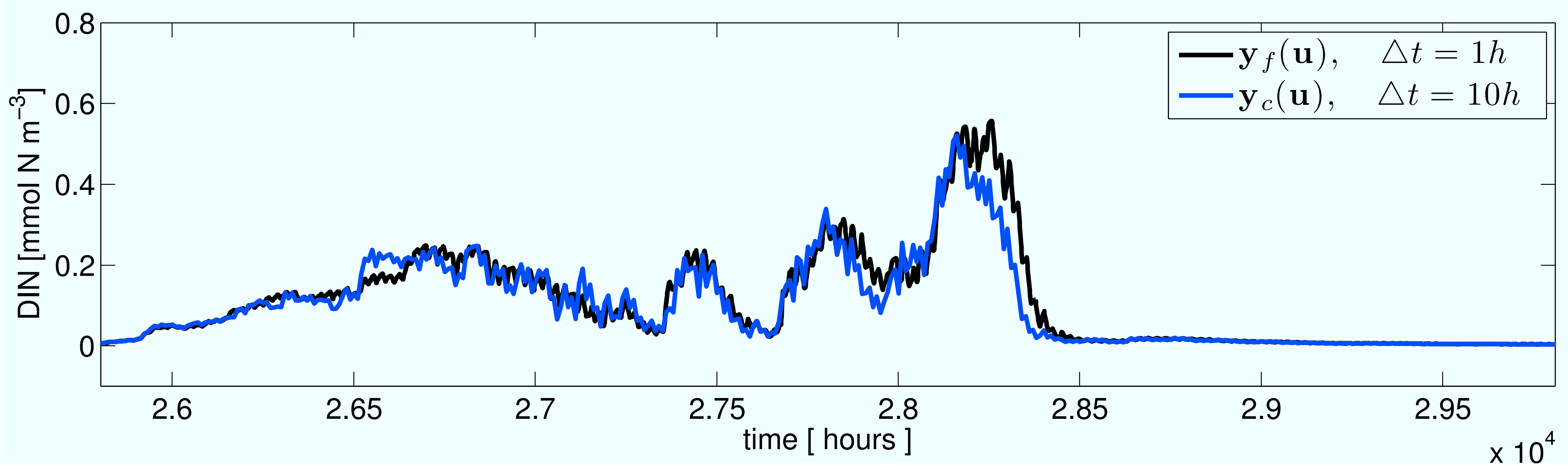

Figure: Raw fine and coarse model response.

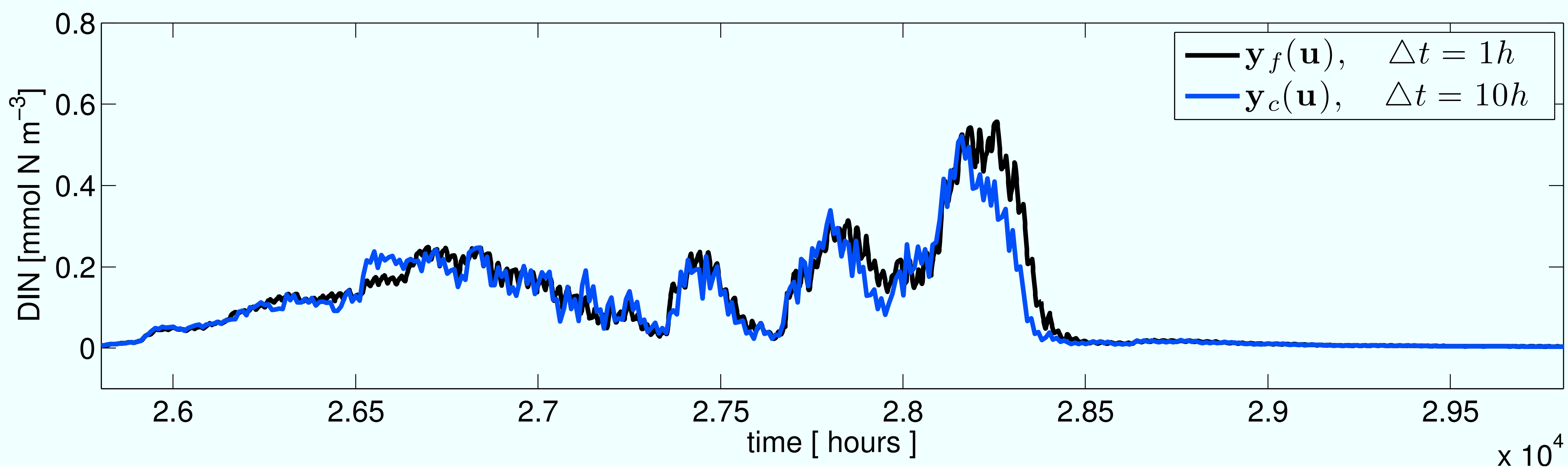

Figure: Raw fine and coarse model response.

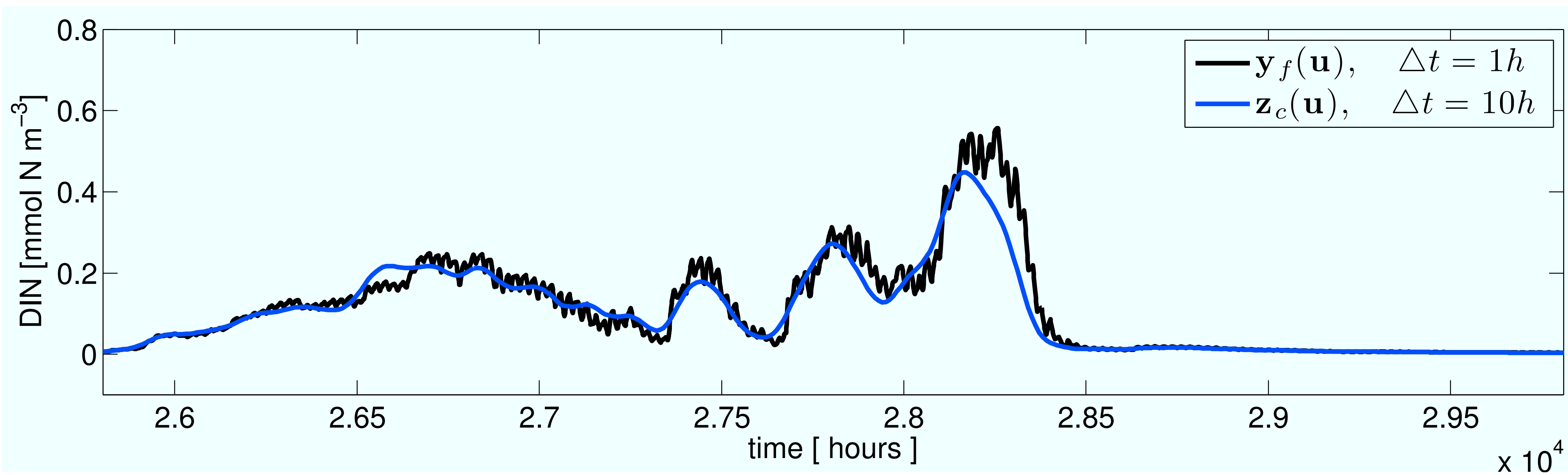

Figure: Smoothed fine and coarse model response.

1D NPZD model: Obtain a suitable coarse model

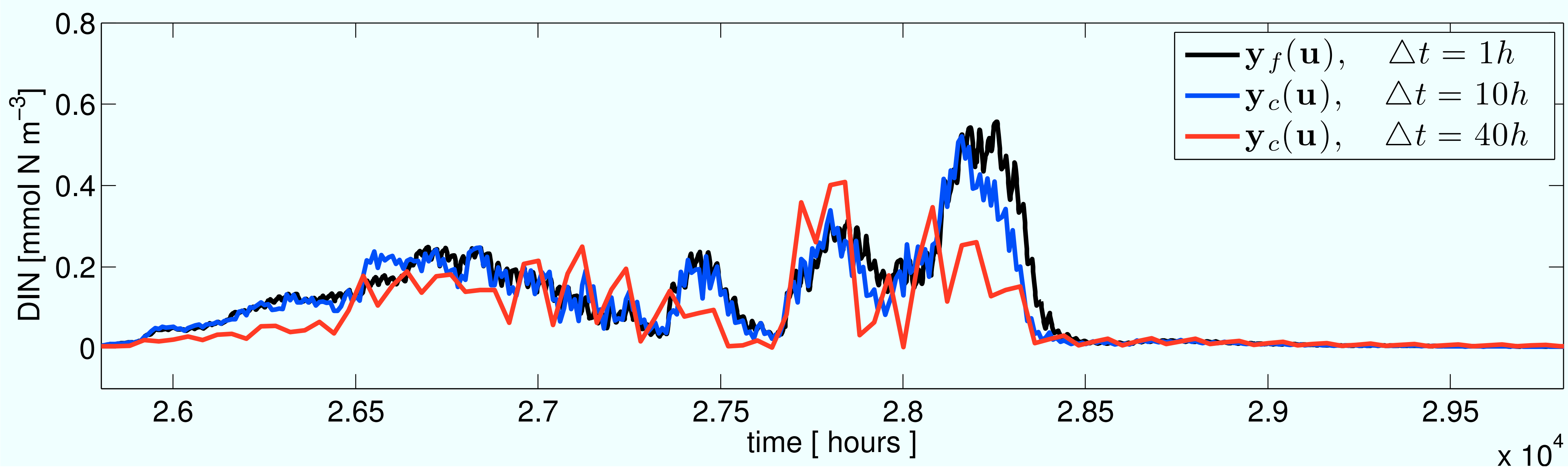

Figure: Raw fine and coarse model response.

smoothing

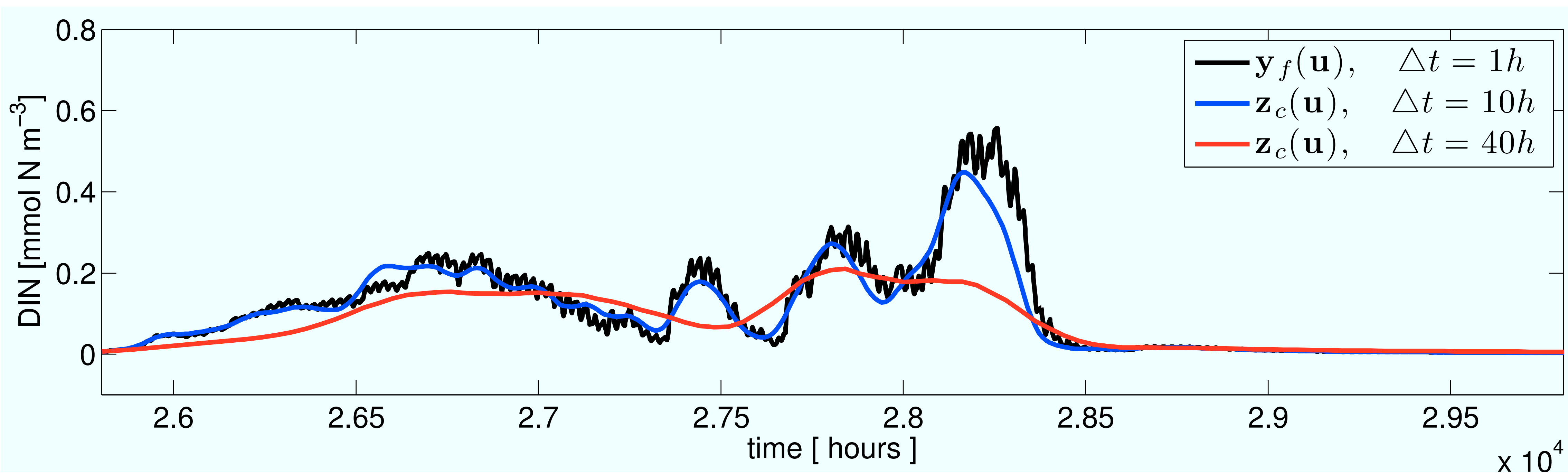

Figure: Smoothed fine and coarse model response.

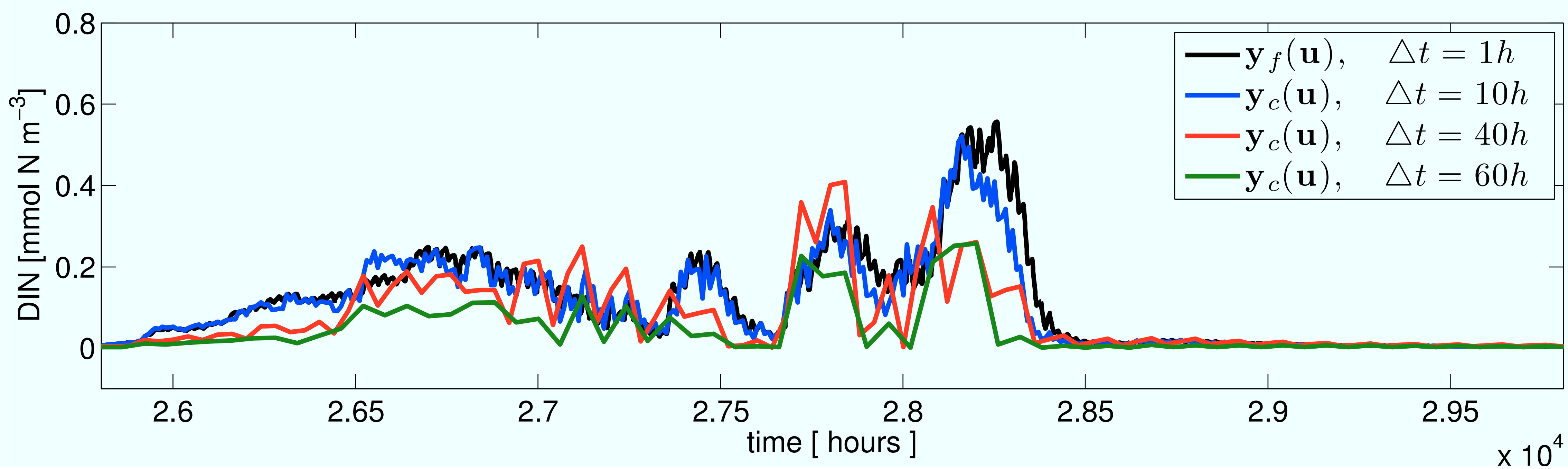

Figure: Raw fine and coarse model response.

smoothing

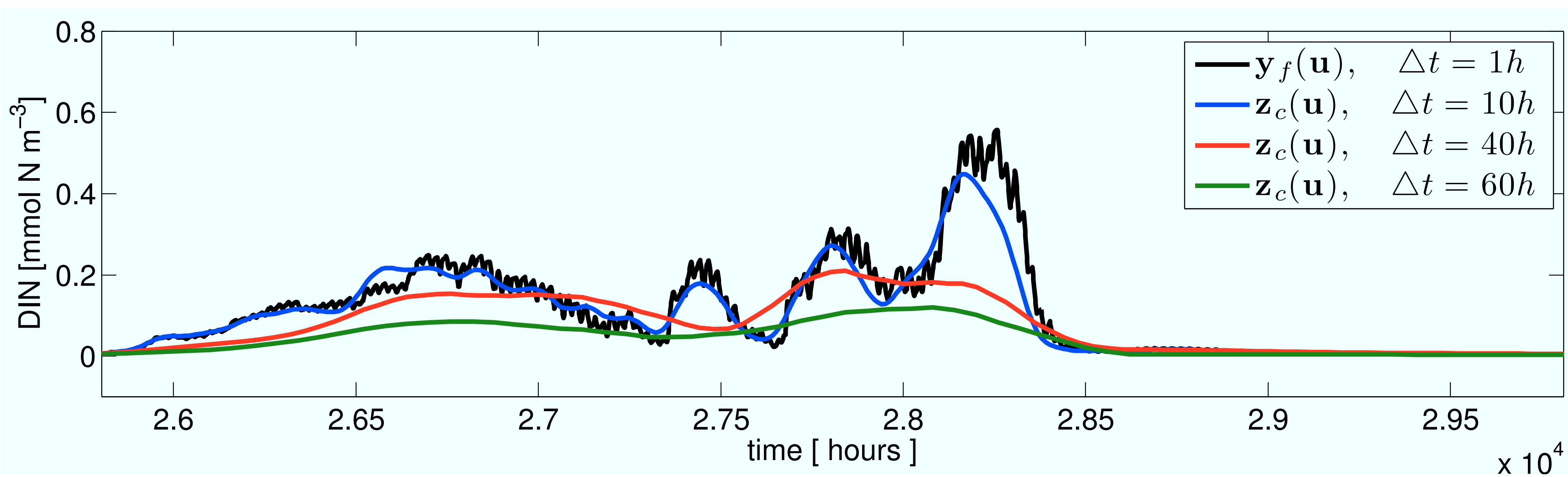

Figure: Smoothed fine and coarse model response.

- At iteration k in the optimization loop, with current parameter $\mathbf{u}_k$ ...

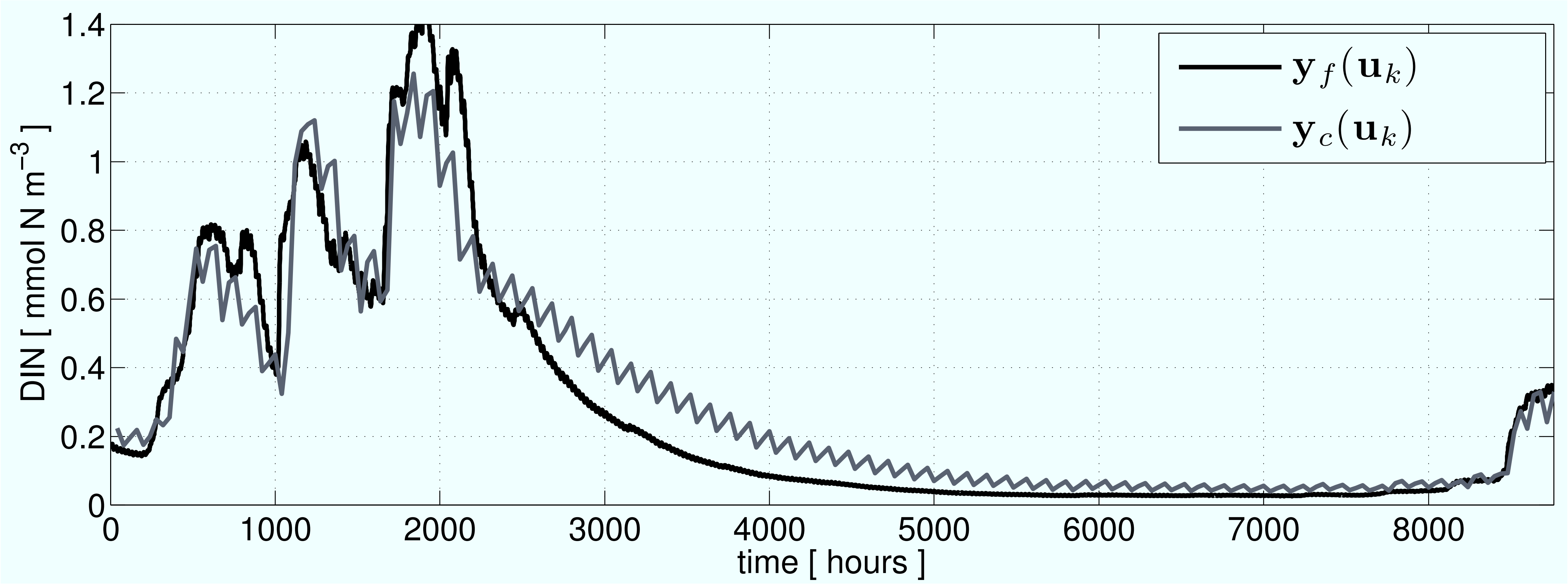

- At iteration k in the optimization loop, with current parameter $\mathbf{u}_k$ ...

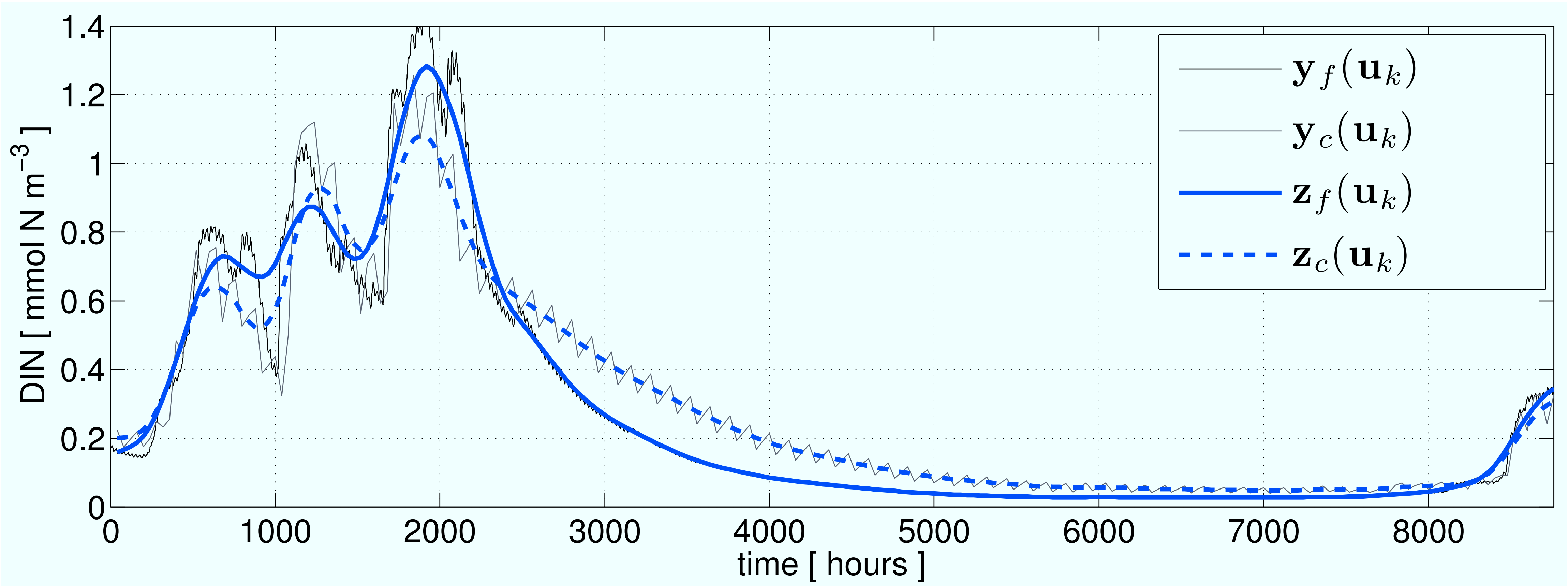

Institut für Informatik

future ocean KIEL MARINE SCIENCES

- At iteration k in the optimization loop, with current parameter $\mathbf{u}_k$ ...

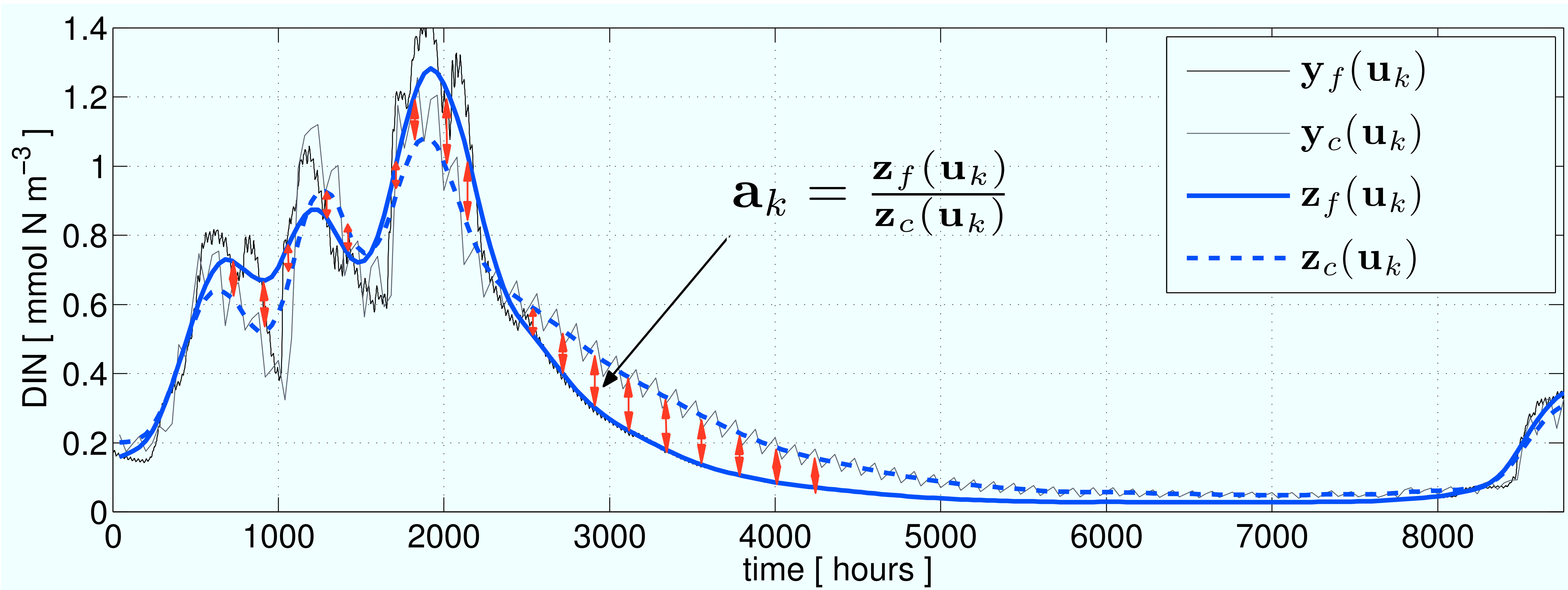

- At iteration k in the optimization loop, with current parameter $\mathbf{u}_k$ ...

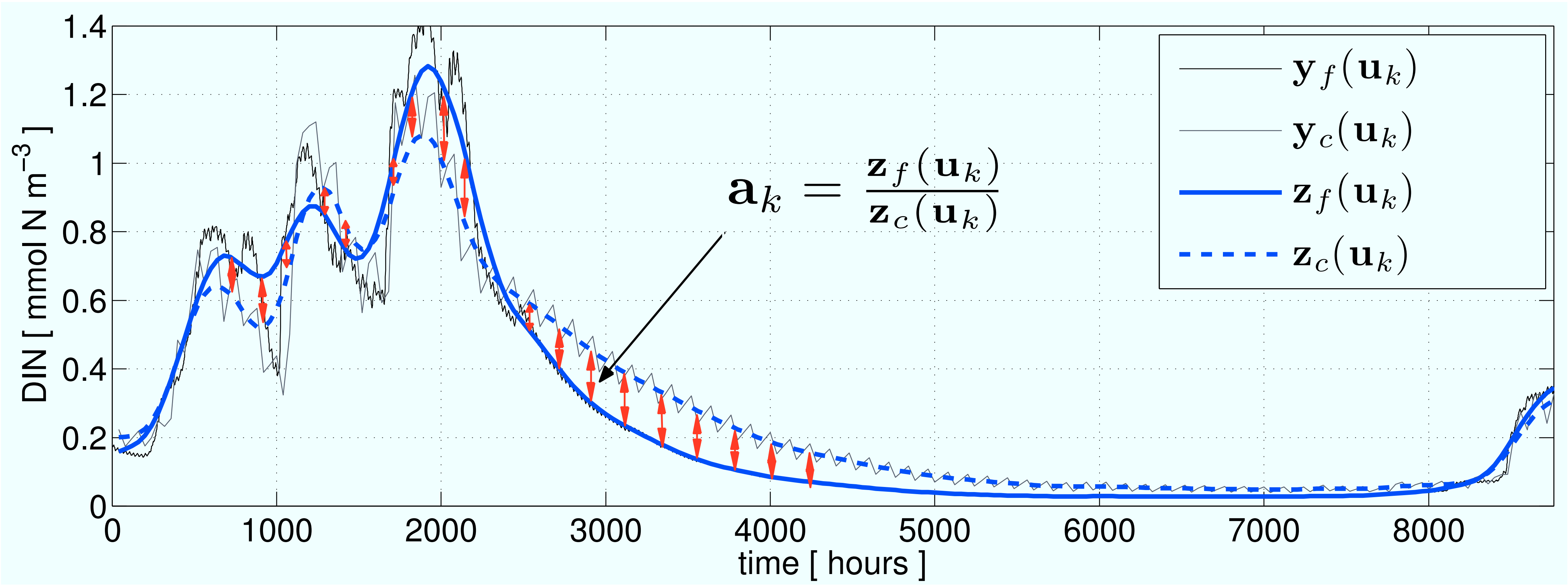

$$\Rightarrow \quad \bar{\mathbf{s}}_k(\mathbf{u}) = \mathbf{a}_k\, \mathbf{z}_c(\mathbf{u}) \quad \Rightarrow \quad \mathbf{u}_{k+1} = \underset{\mathbf{u}}{\operatorname{argmin}}\ J(\bar{\mathbf{s}}_k(\mathbf{u})) \quad \ldots$$

- Performance of the algorithm depends on:

  quality of surrogate's approximation of the fine model

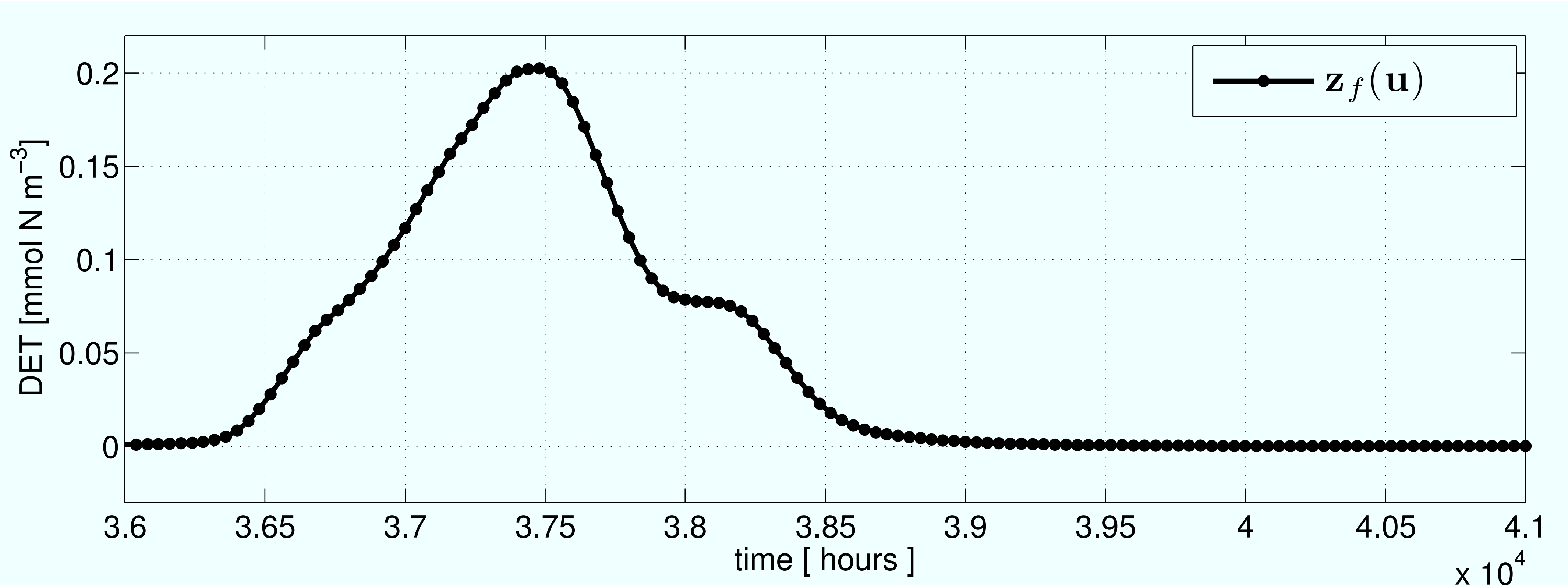

Figure: Fine, coarse model and surrogates' response (smoothed) at „construction point".

- Performance of the algorithm depends on:

  quality of surrogate's approximation of the fine model

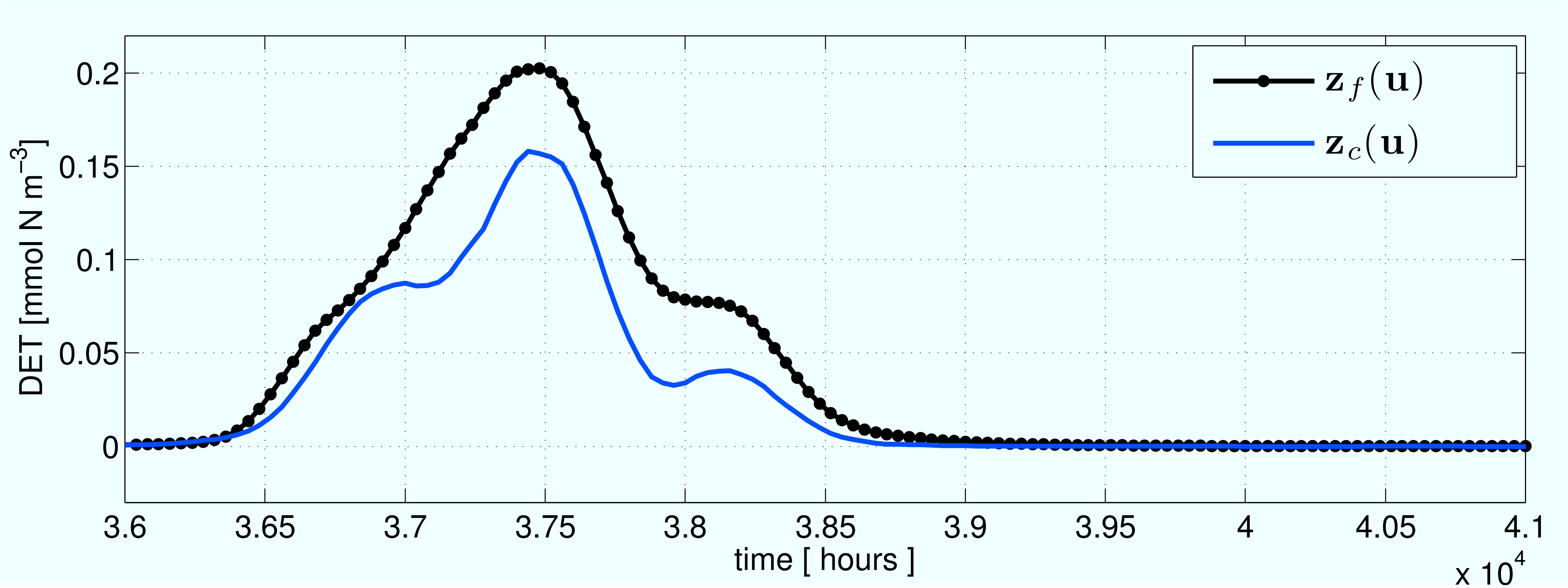

Figure: Fine, coarse model and surrogates' response (smoothed) at „construction point".

- Performance of the algorithm depends on:

  quality of surrogate's approximation of the fine model

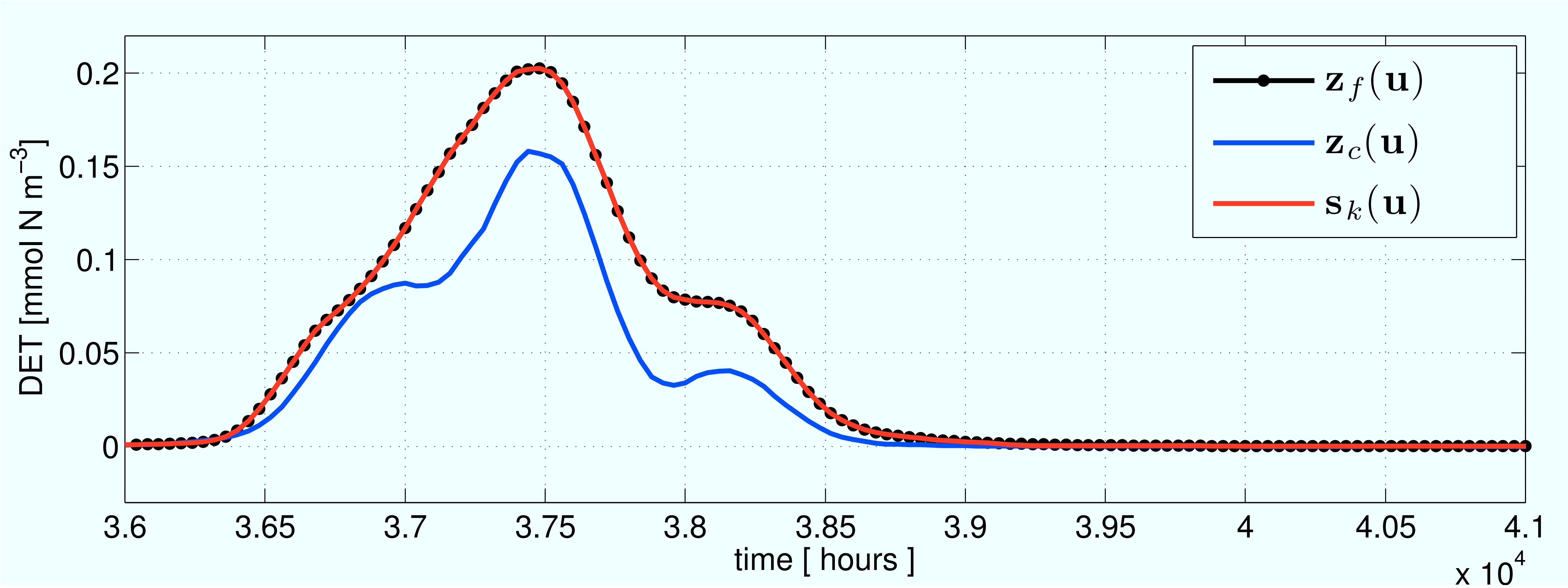

Figure: Fine, coarse model and surrogates' response (smoothed) at „construction point".

- Performance of the algorithm depends on:

  quality of surrogate‘s approximation of the fine model

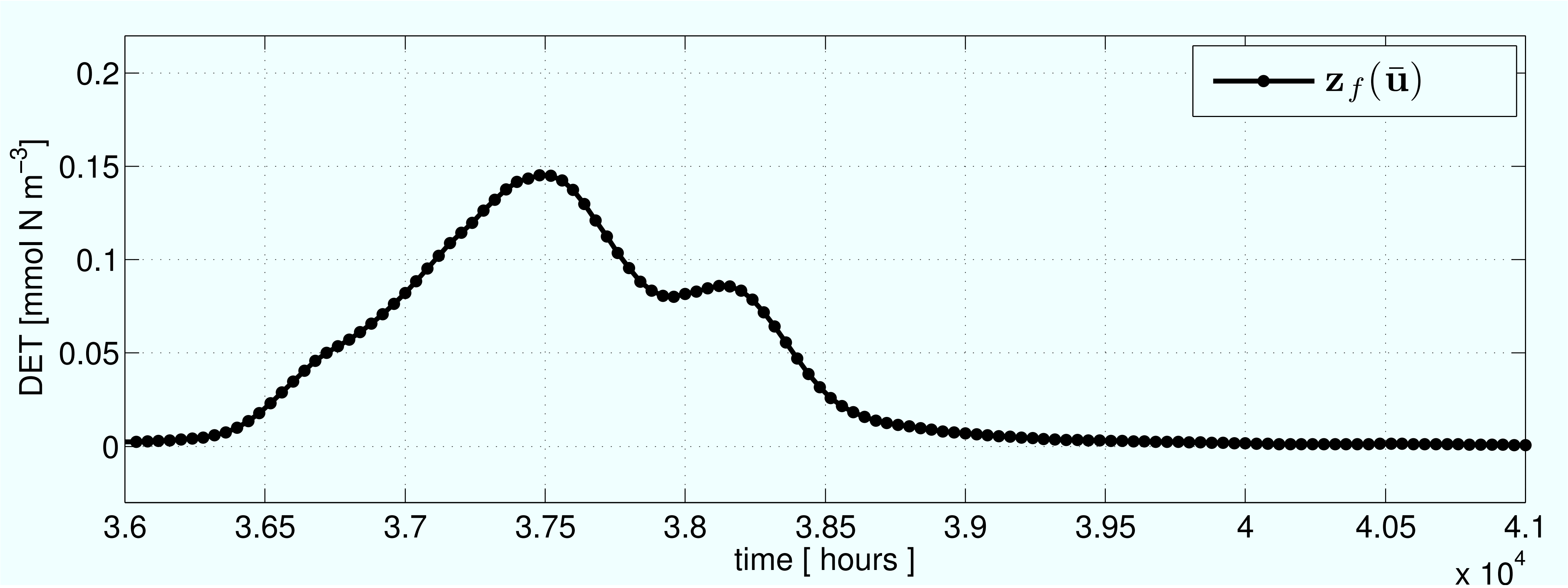

Figure: ... and in a neighborhood $\bar{\mathbf{u}}$.

- Performance of the algorithm depends on:

  quality of surrogate‘s approximation of the fine model

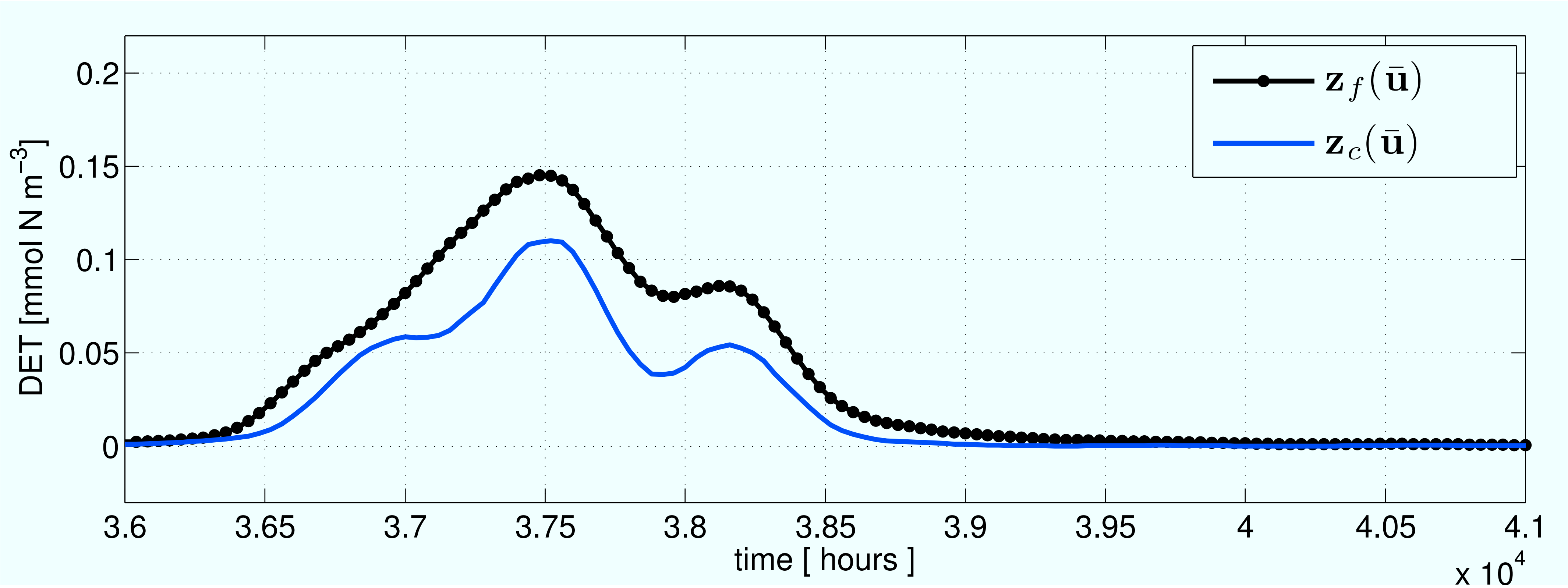

Figure: ... and in a neighborhood $\bar{\mathbf{u}}$.

- Performance of the algorithm depends on:

  quality of surrogate‘s approximation of the fine model

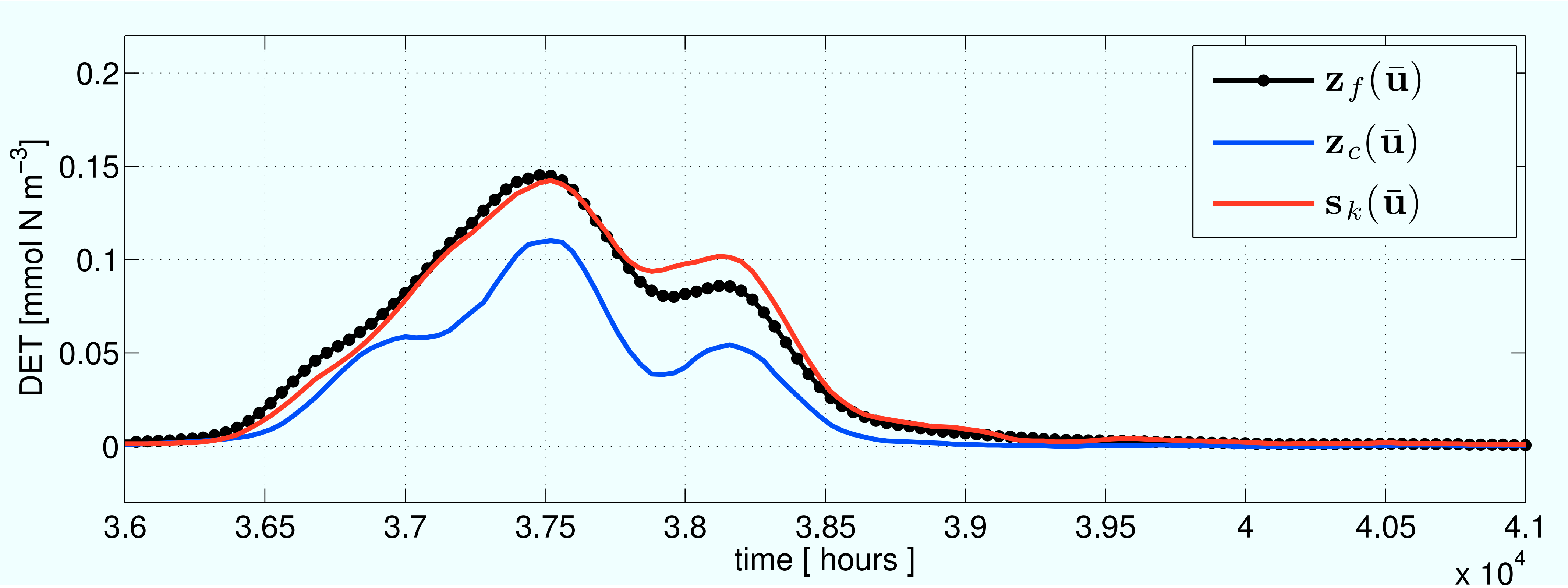

Figure: ... and in a neighborhood $\bar{\mathbf{u}}$.

1D NPZD model: Numerical results

Verification by model generated data

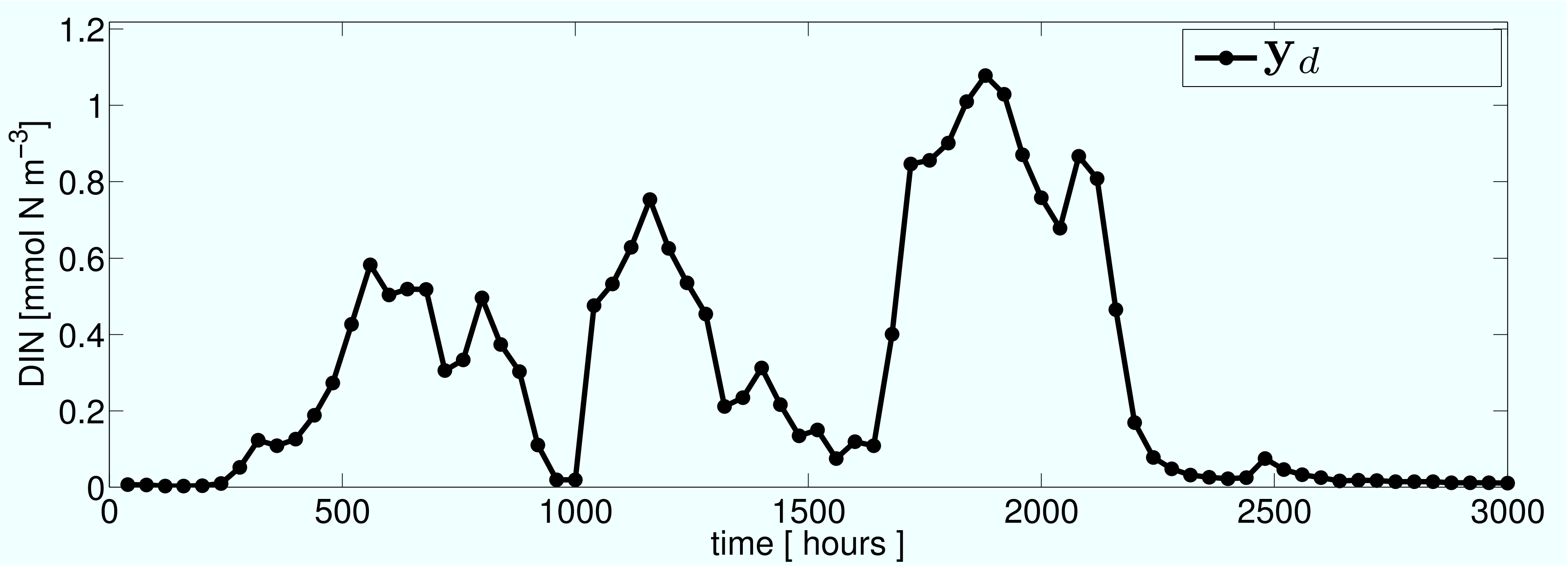

Figure: Fine, coarse model and surrogate optimization: Optimal solutions.

1D NPZD model: Numerical results

Verification by model generated data

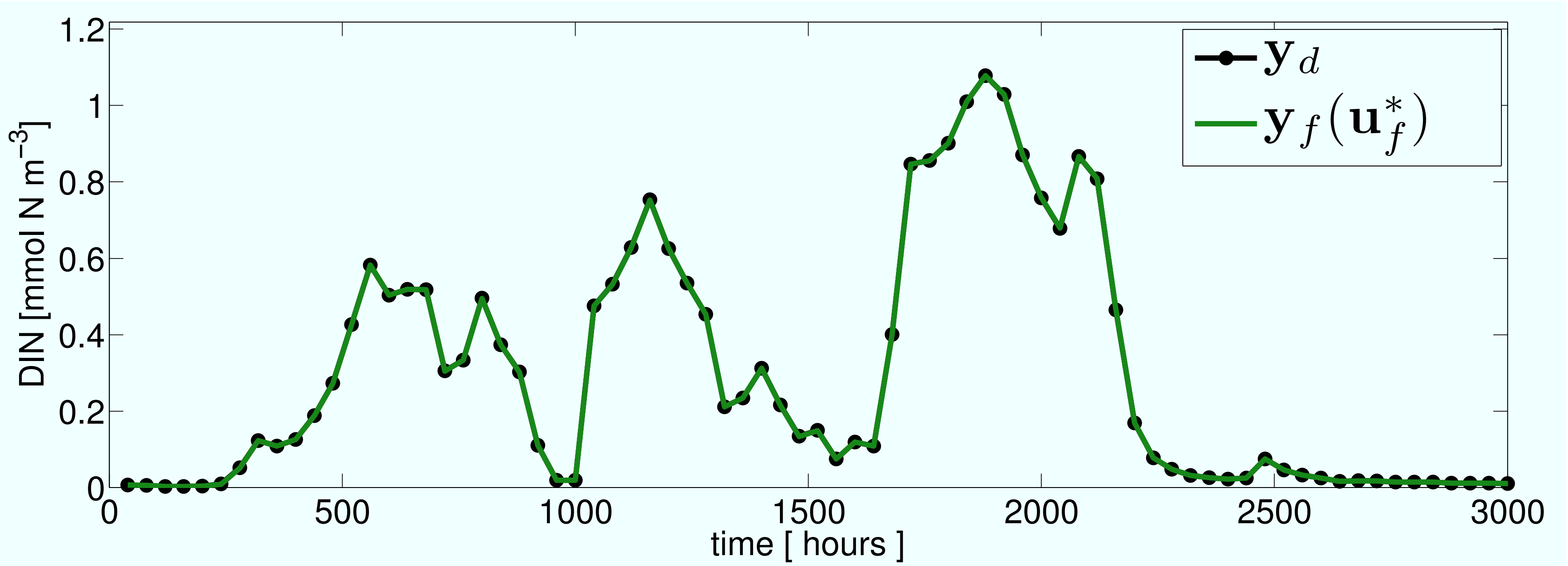

Figure: Fine, coarse model and surrogate optimization: Optimal solutions.

Institut für Informatik

future ocean KIEL MARINE SCIENCES

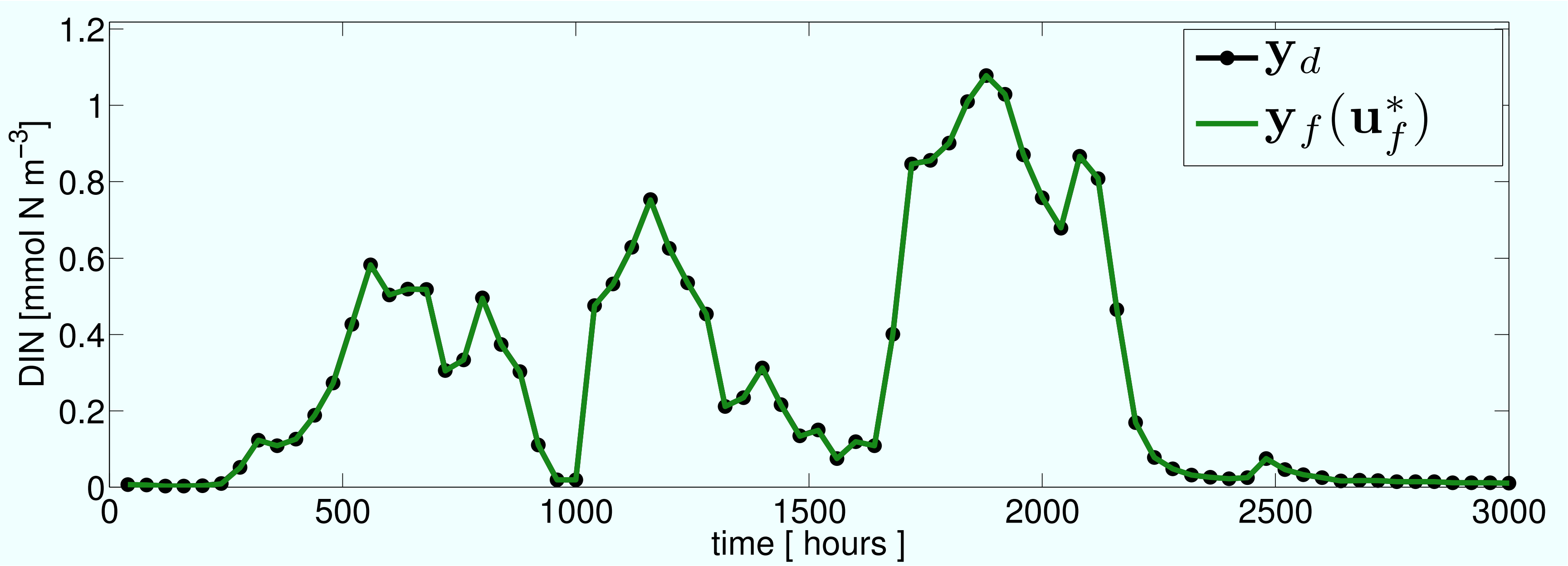

Figure: Fine, coarse model and surrogate optimization: Optimal solutions.

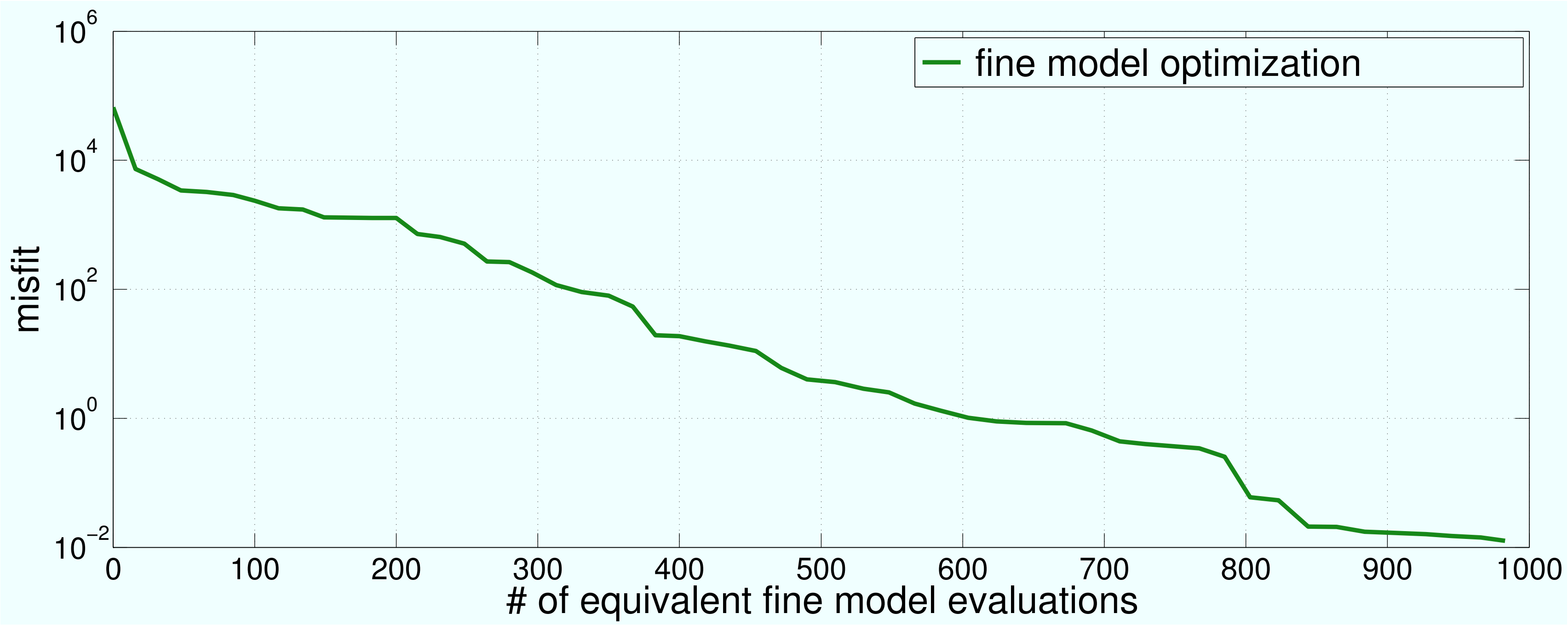

Figure: Convergence history of cost function.

1D NPZD model: Numerical results

Verification by model generated data

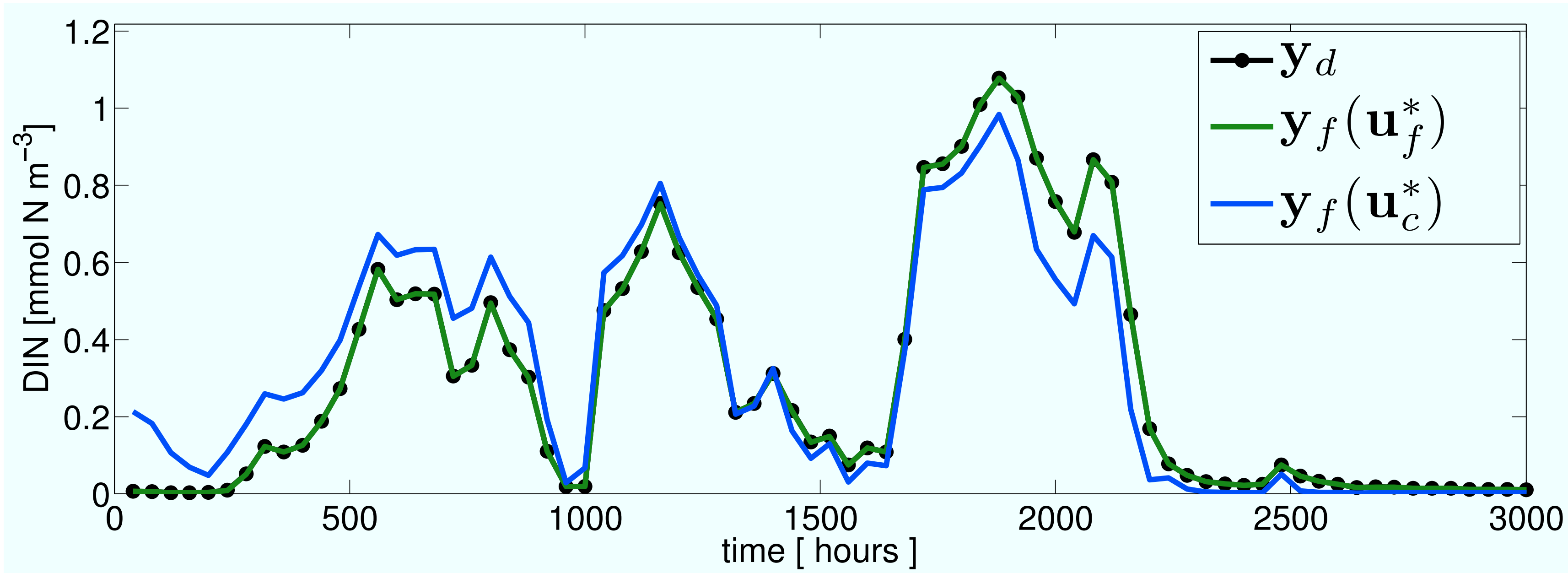

Figure: Fine, coarse model and surrogate optimization: Optimal solutions.

Figure: Convergence history of cost function.

Verification by model generated data

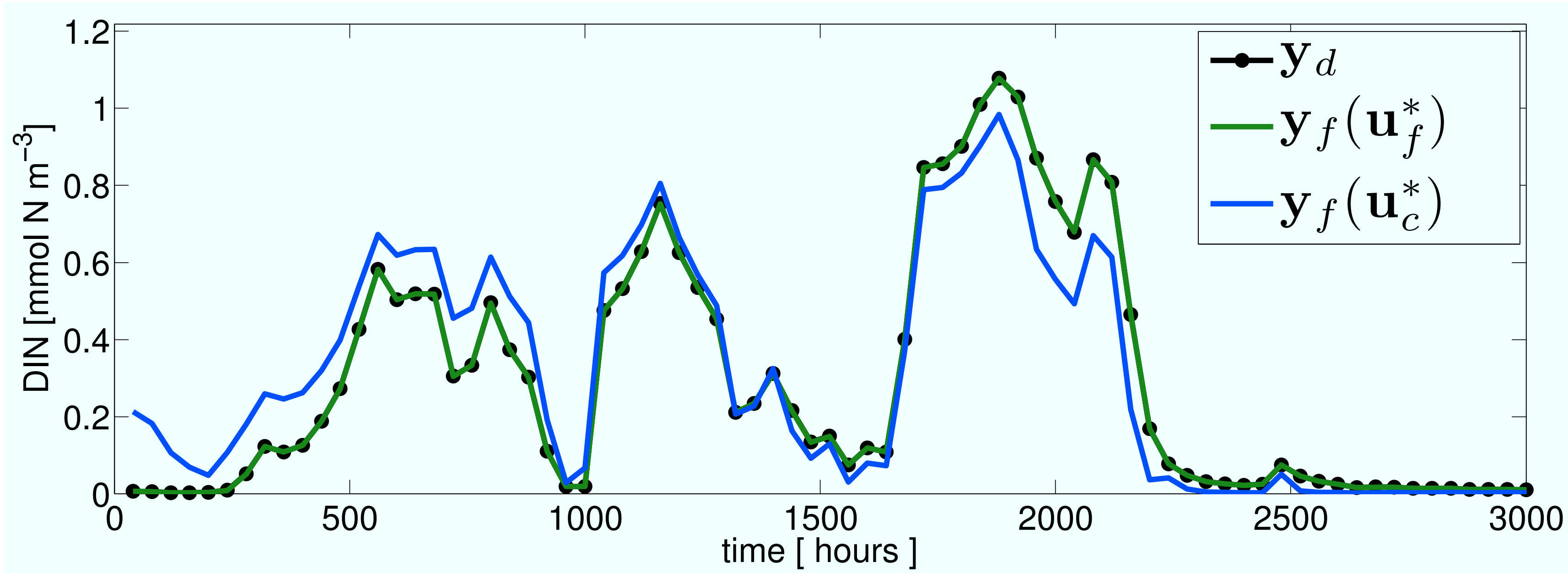

Figure: Fine, coarse model and surrogate optimization: Optimal solutions.

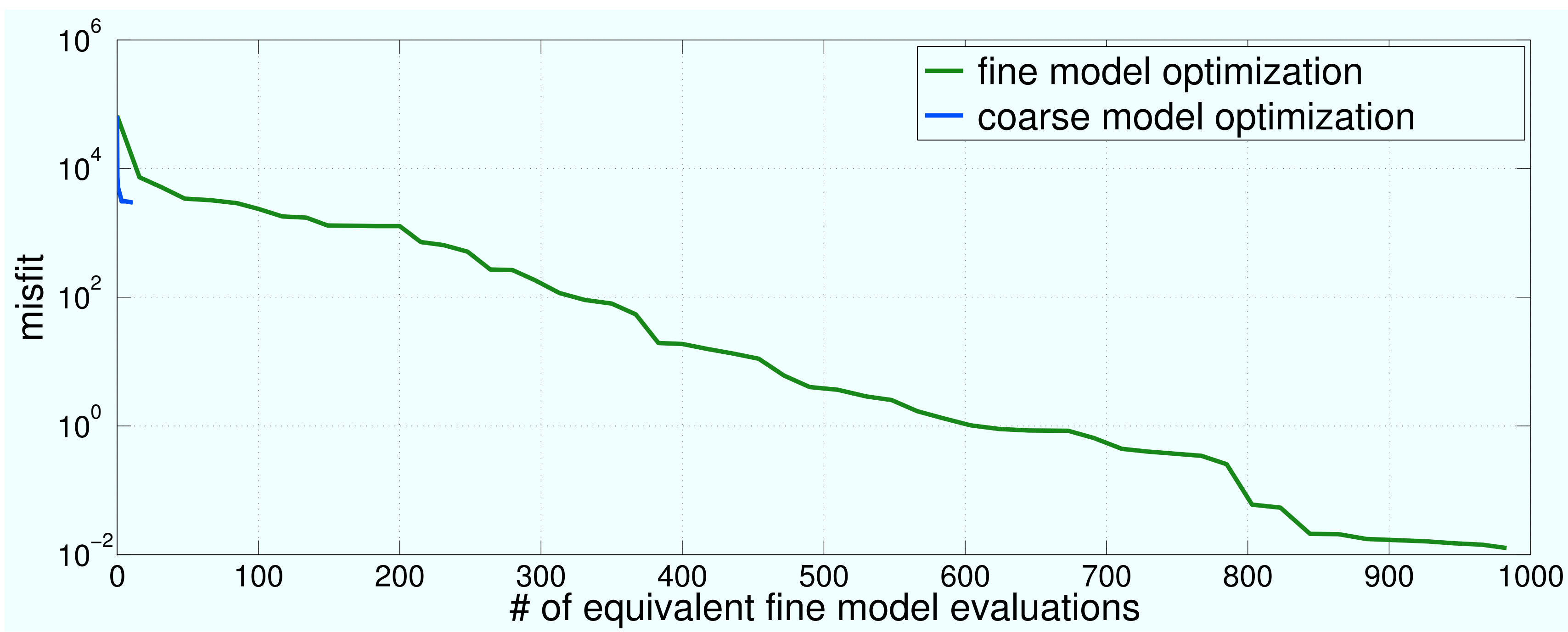

Figure: Convergence history of cost function.

1D NPZD model: Numerical results

Verification by model generated data

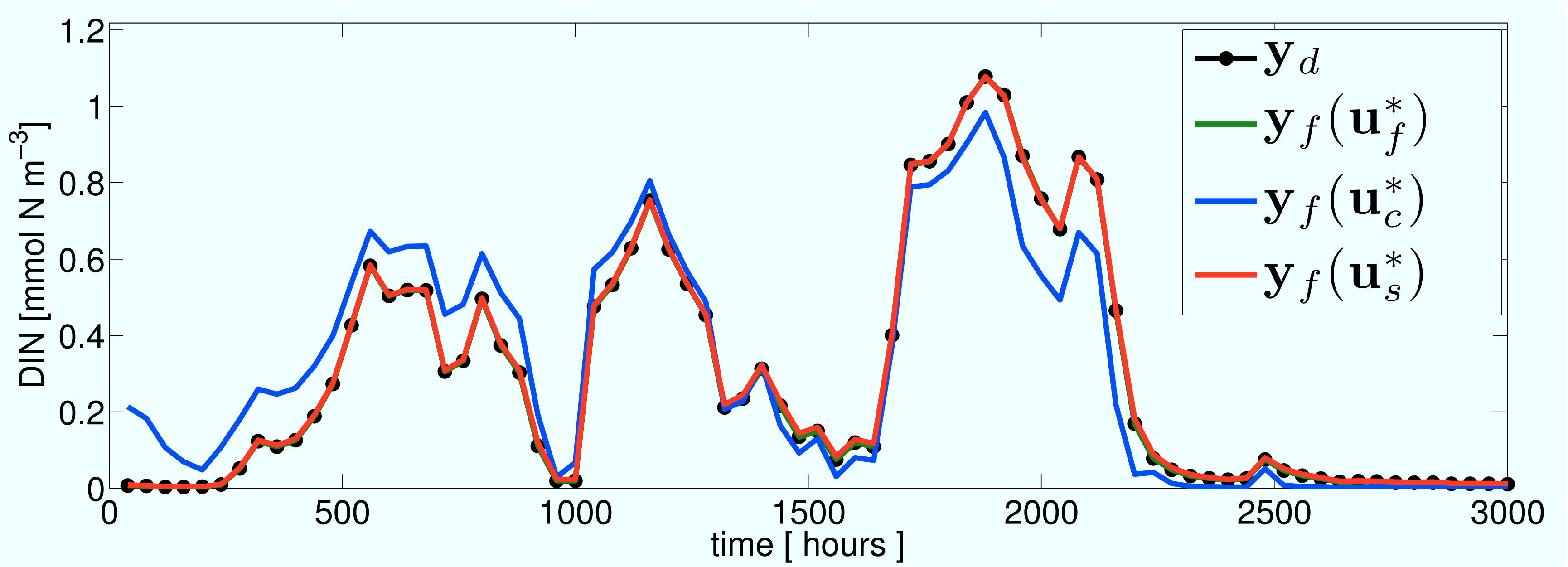

Figure: Fine, coarse model and surrogate optimization: Optimal solutions.

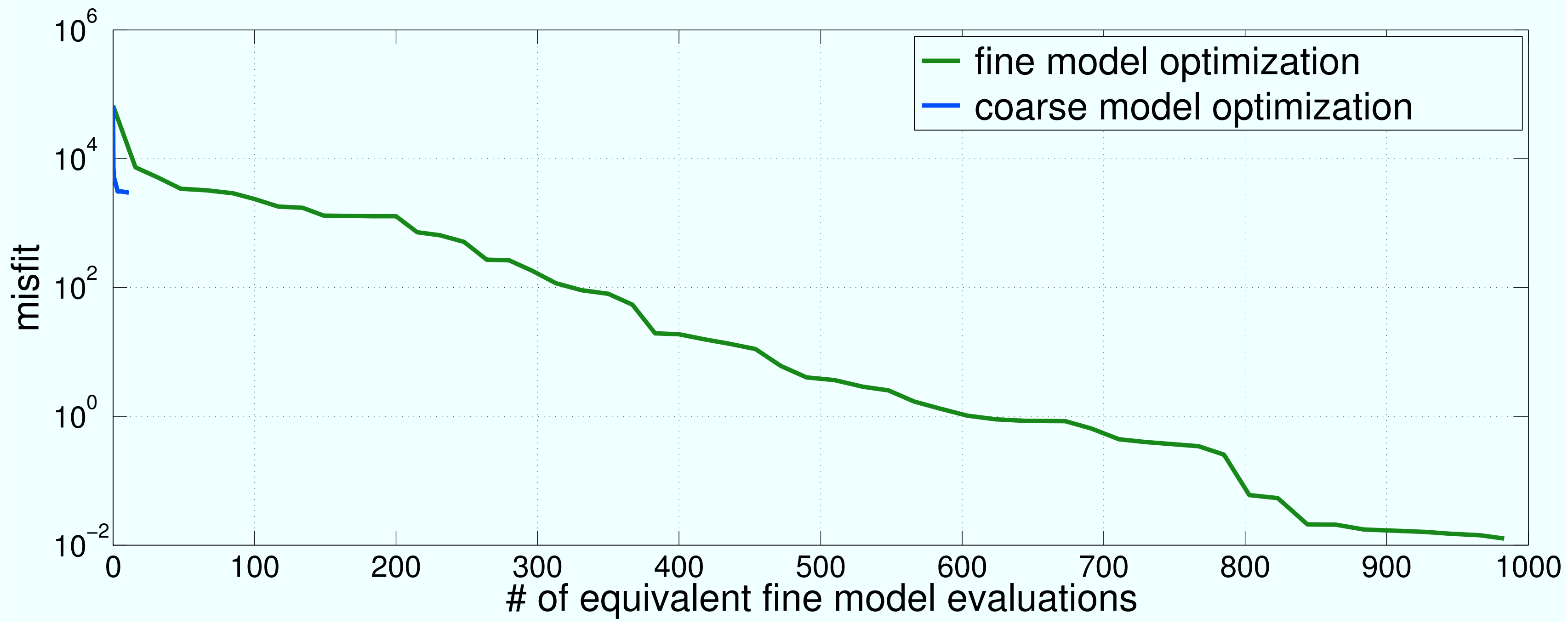

Figure: Convergence history of cost function.

1D NPZD model: Numerical results

Verification by model generated data

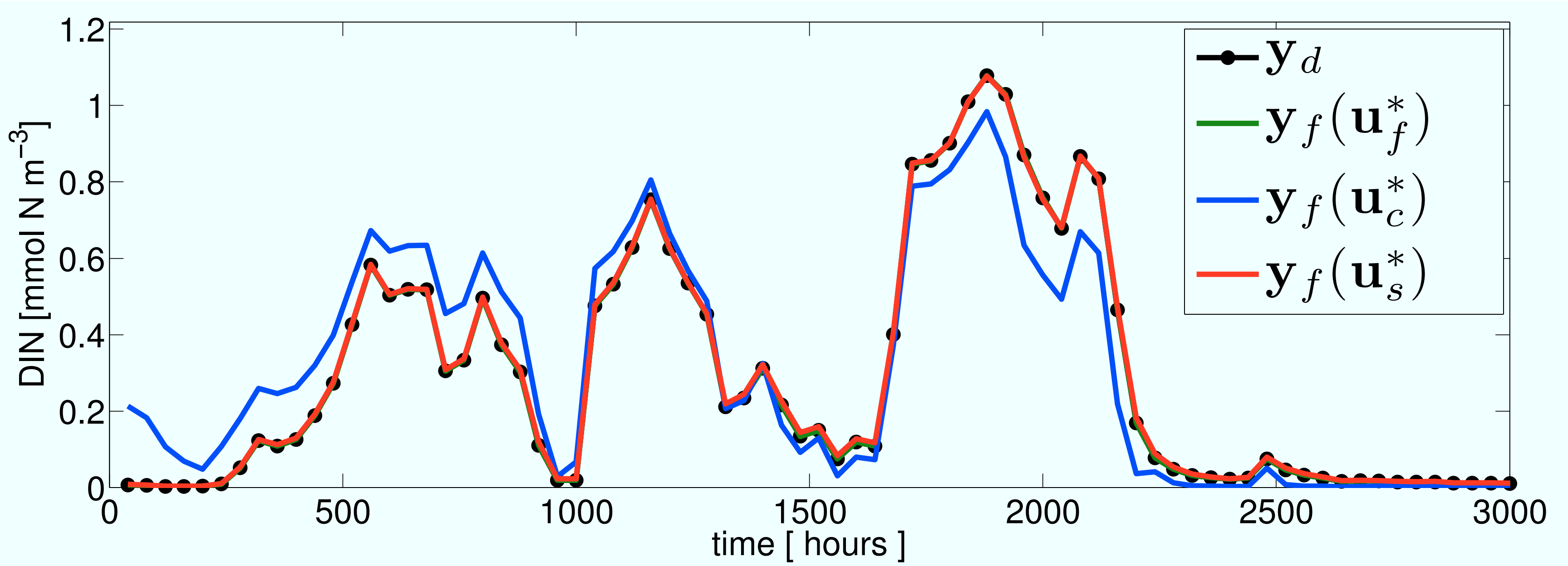

Figure: Fine, coarse model and surrogate optimization: Optimal solutions.

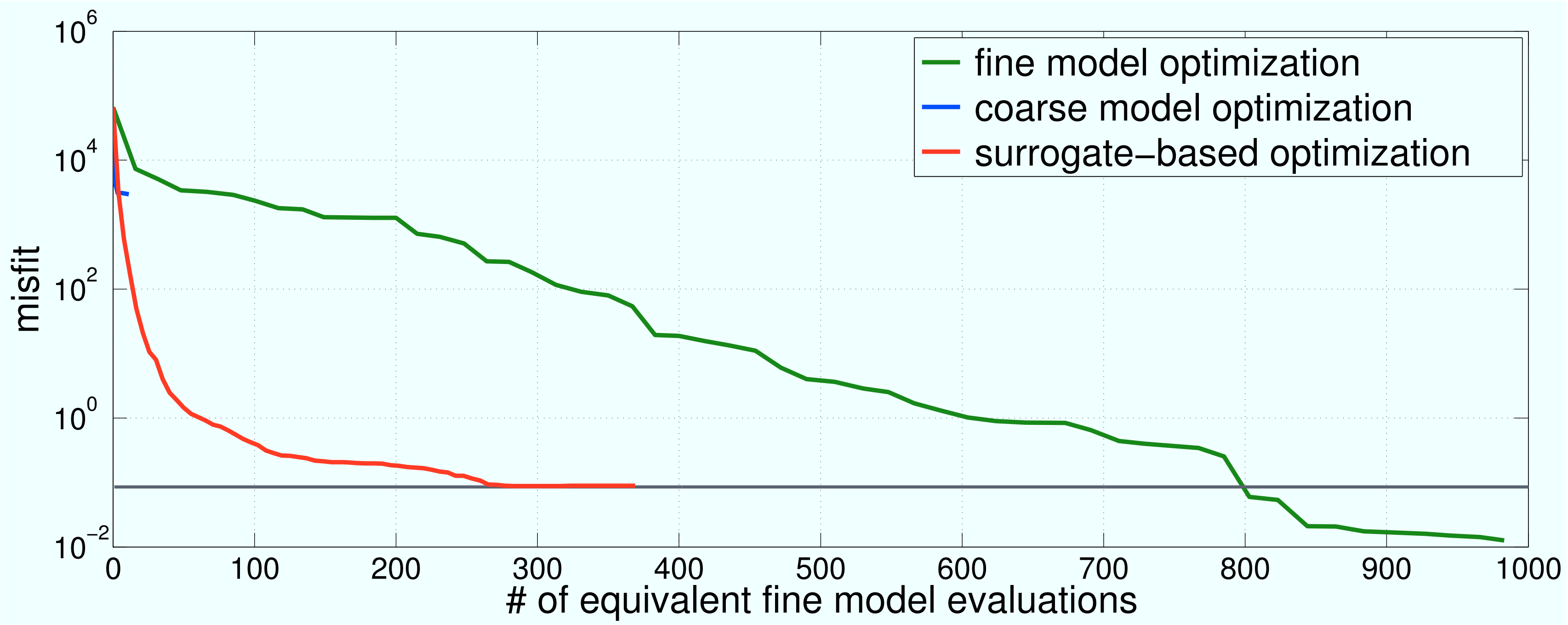

Figure: Convergence history of cost function.

Verification by model generated data

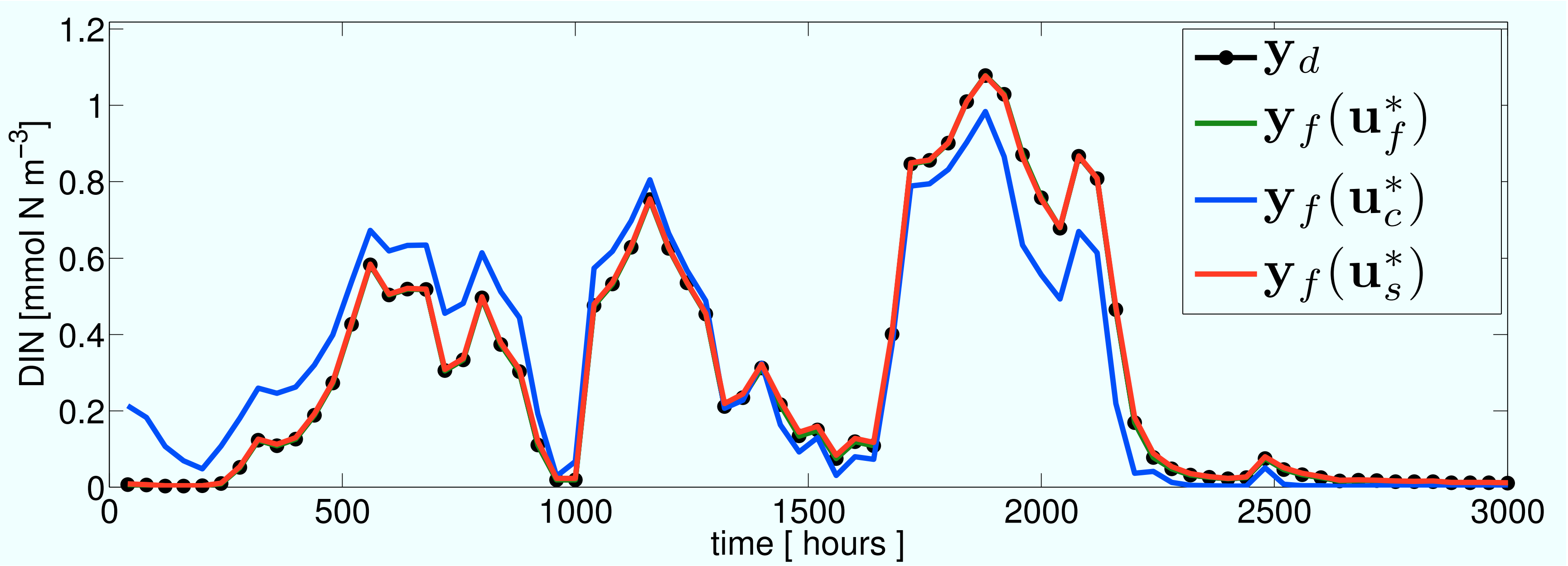

Figure: Fine, coarse model and surrogate optimization: Optimal solutions.

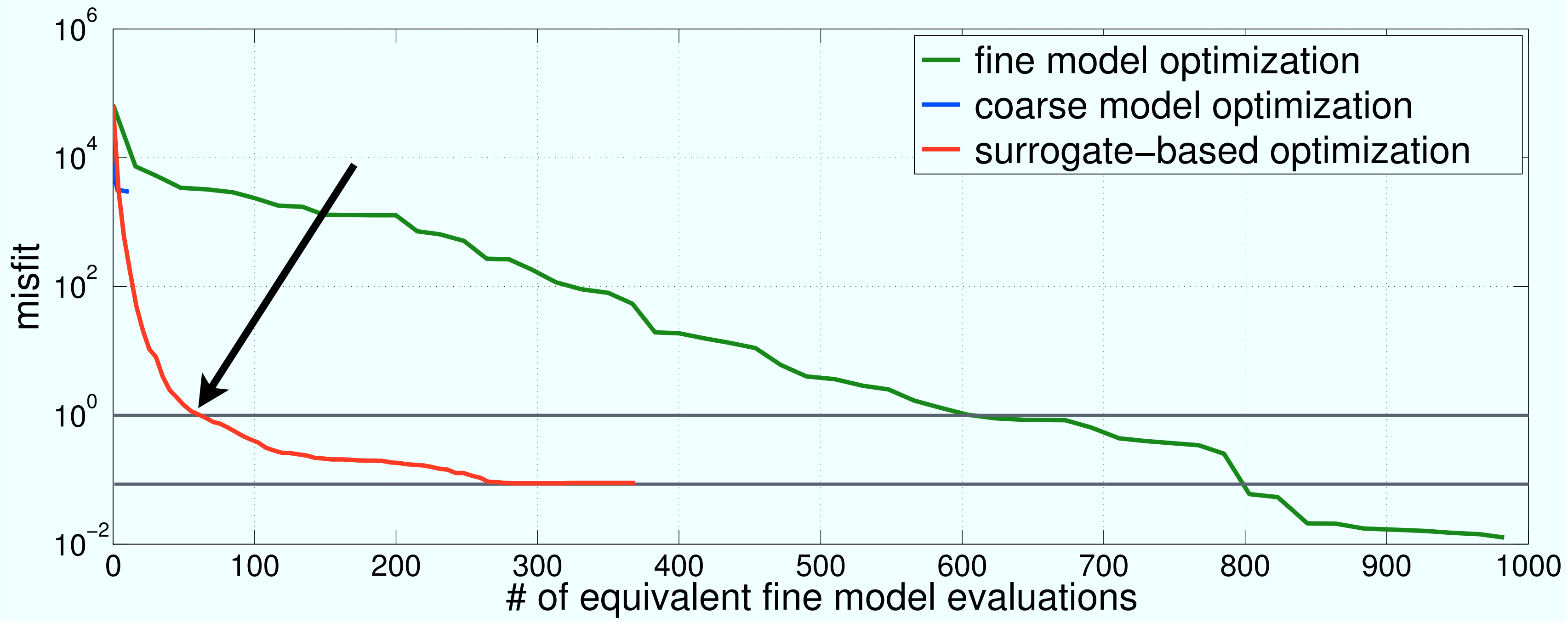

Figure: Convergence history of cost function.

1D NPZD model: Numerical results

Verification by model generated data

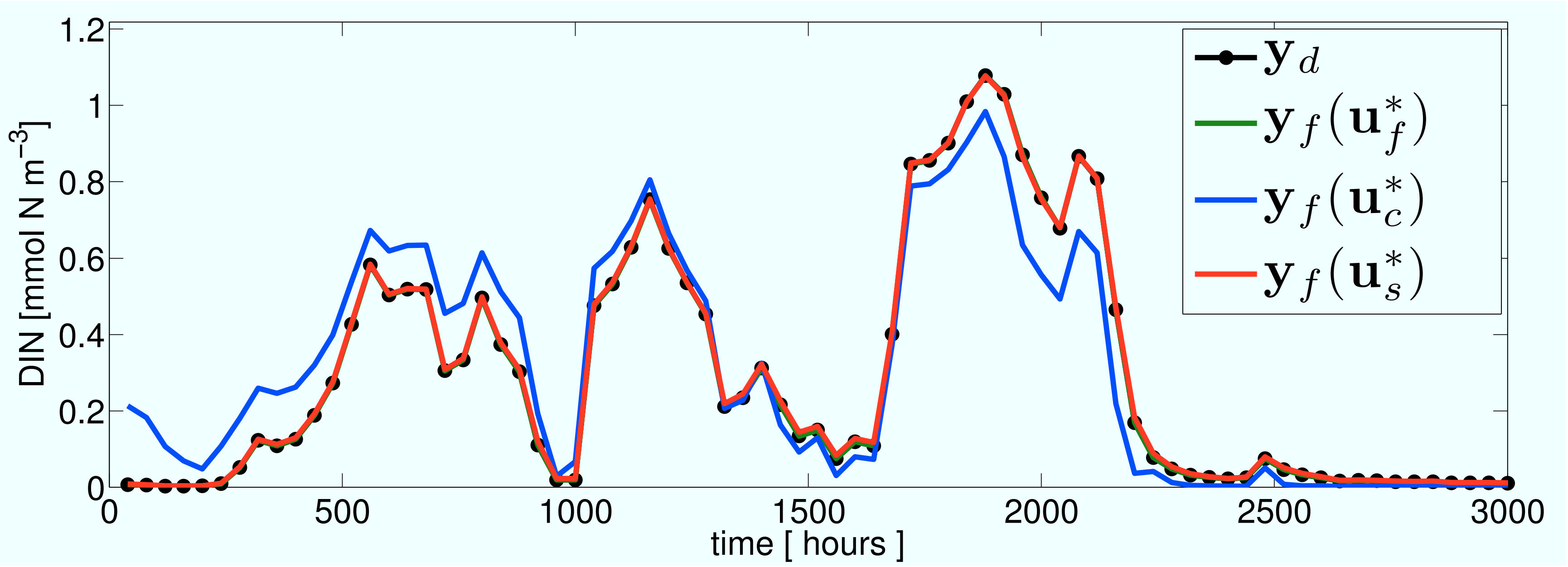

Figure: Fine, coarse model and surrogate optimization: Optimal solutions.

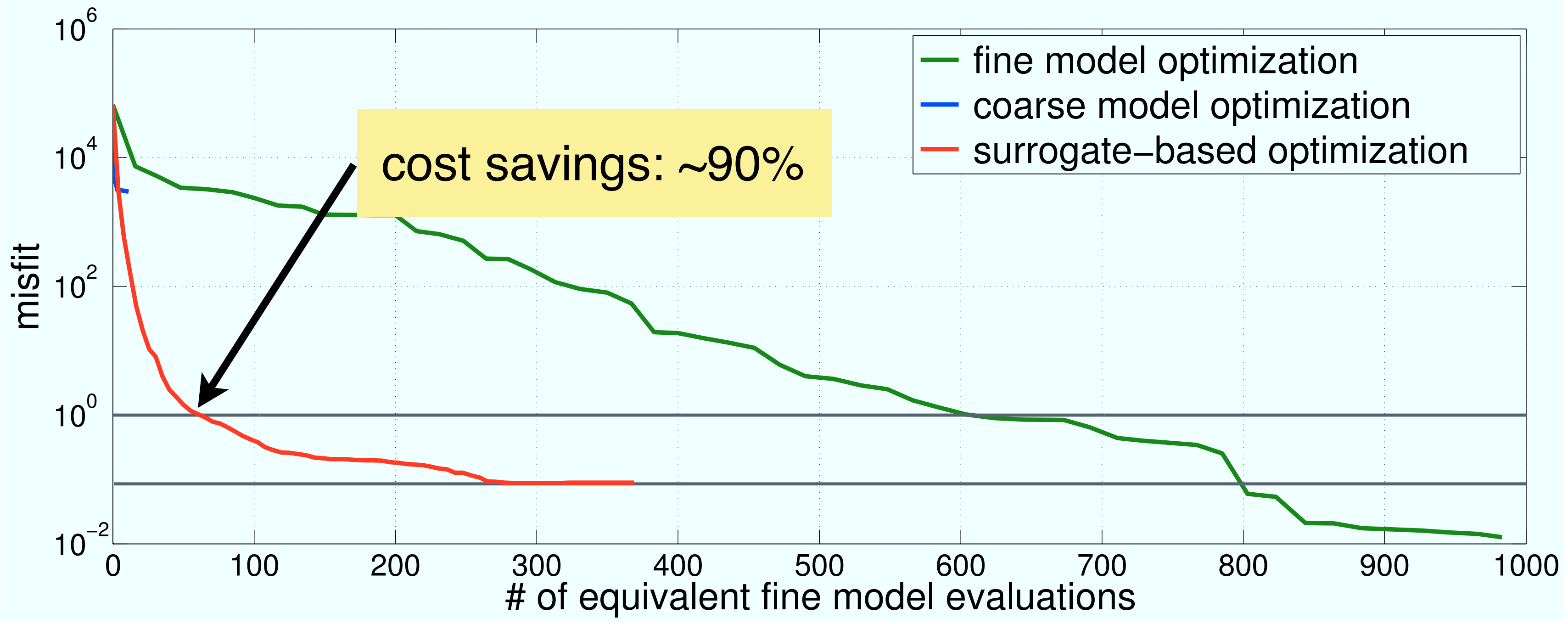

Figure: Convergence history of cost function.

- Exact first-order consistency important

- Extensive optimization runs performed:

  Local, gradient-based + global, genetic algorithms ➔ no suitable fit of the target [1]

- However: Similar performance of surrogate-based optimization

[1] Schartau, Oschlies (2003); Schartau (2001); Rückelt et al. (2010)

Institut für Informatik

future ocean KIEL MARINE SCIENCES

- Exact first-order consistency important

- Extensive optimization runs performed:

  Local, gradient-based + global, genetic algorithms ➔ no suitable fit of the target [1]

- However: Similar performance of surrogate-based optimization

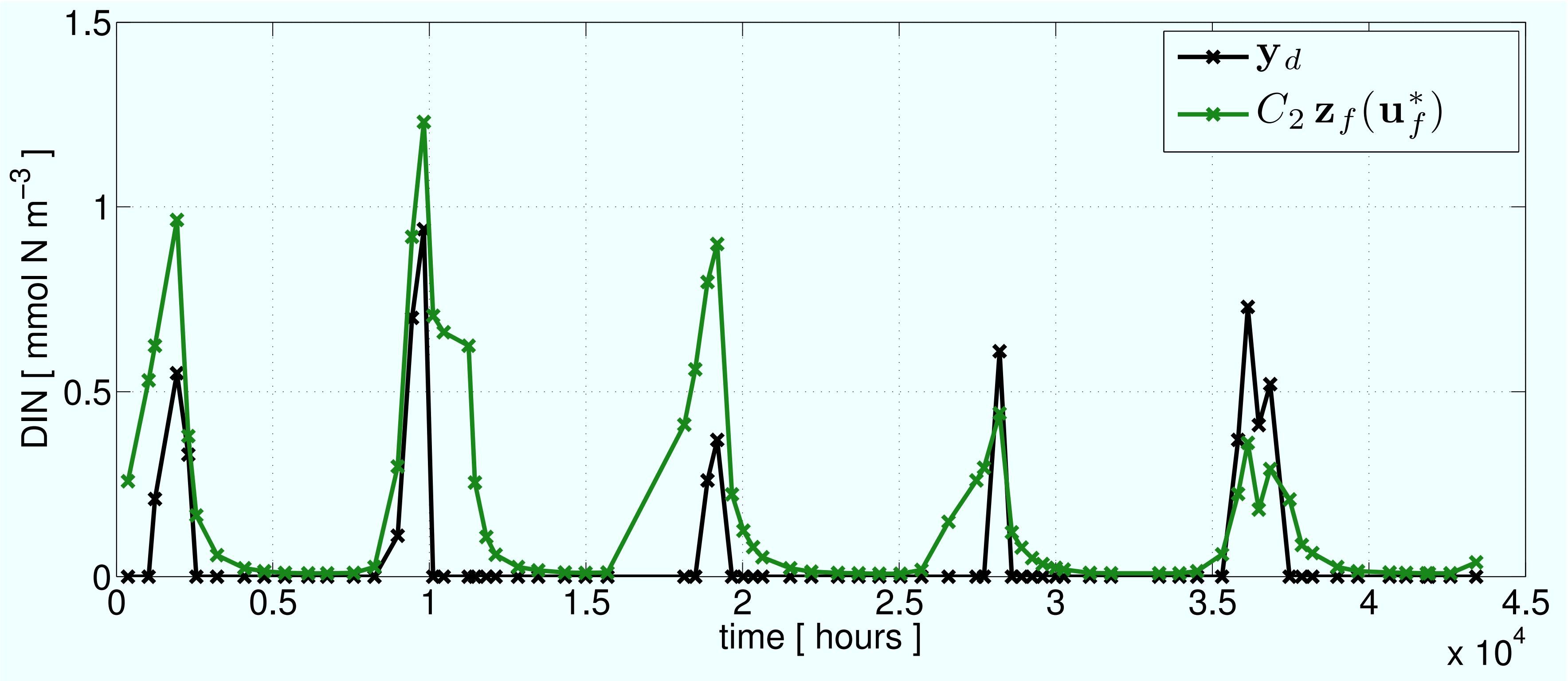

Figure: Fine, coarse model and surrogate optimization: Optimal solutions.

[1] Schartau, Oschlies (2003); Schartau (2001); Rückelt et al. (2010)

- Exact first-order consistency important

- Extensive optimization runs performed:

  Local, gradient-based + global, genetic algorithms ➔ no suitable fit of the target [1]

- However: Similar performance of surrogate-based optimization

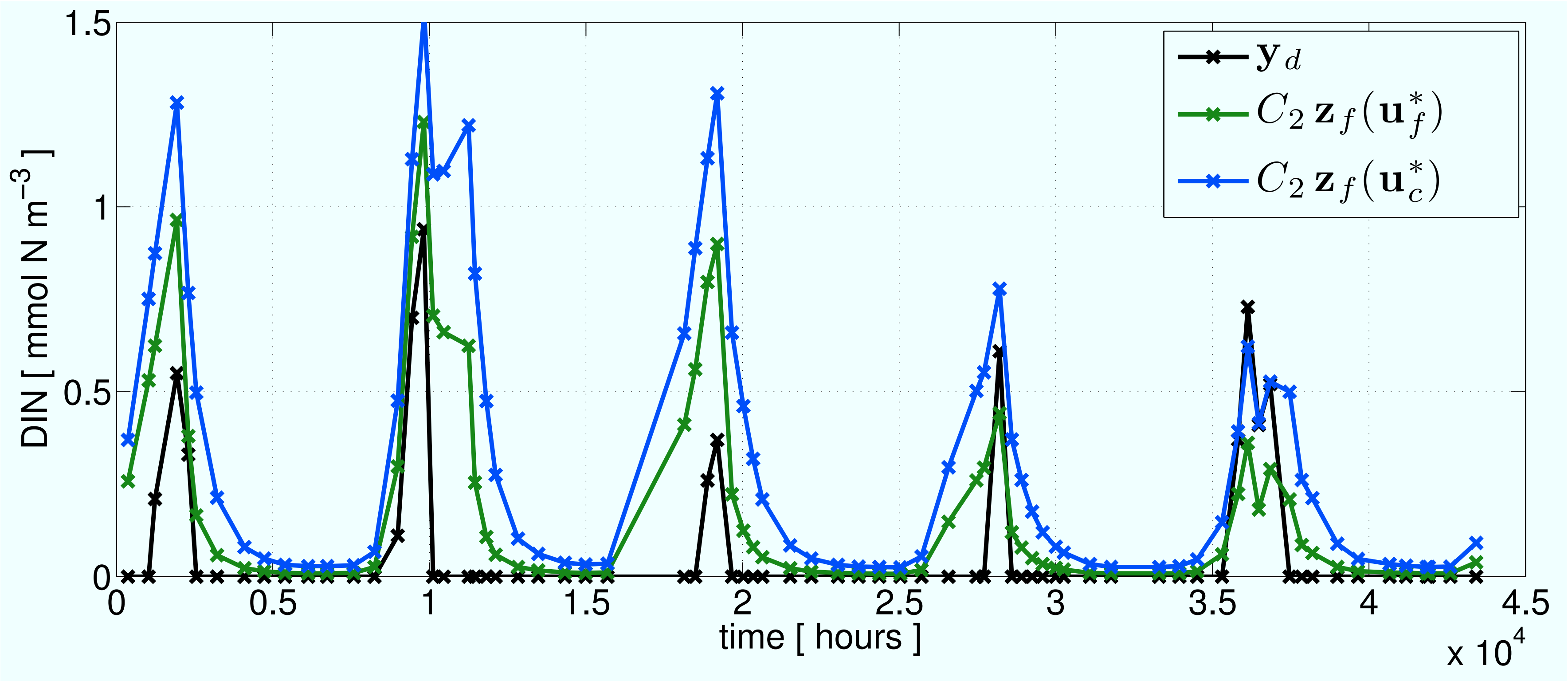

Figure: Fine, coarse model and surrogate optimization: Optimal solutions.

[1] Schartau, Oschlies (2003); Schartau (2001); Rückelt et al. (2010)

- Exact first-order consistency important

- Extensive optimization runs performed:

  Local, gradient-based + global, genetic algorithms ➔ no suitable fit of the target [1]

- However: Similar performance of surrogate-based optimization

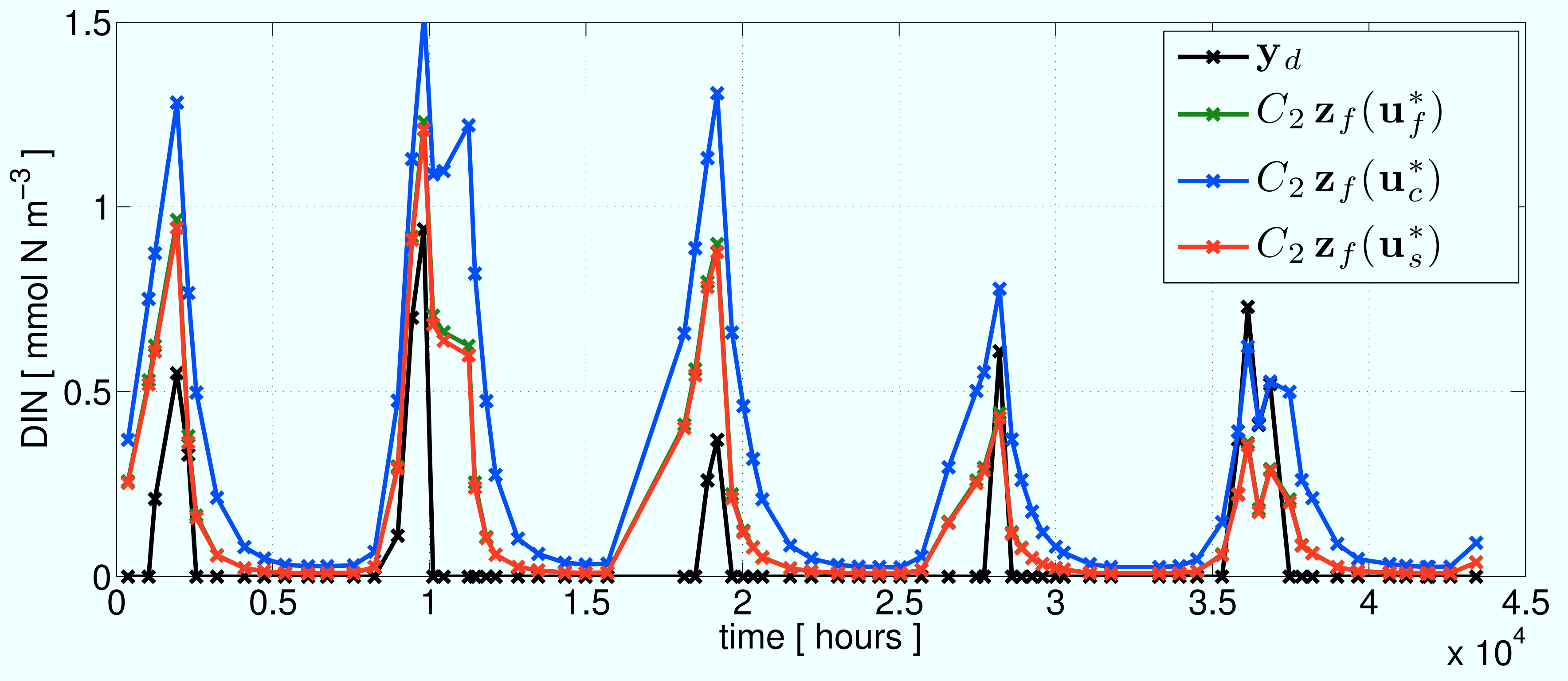

Figure: Fine, coarse model and surrogate optimization: Optimal solutions.

[1] Schartau, Oschlies (2003); Schartau (2001); Rückelt et al. (2010)

- Exact first-order consistency important

- Extensive optimization runs performed:

  Local, gradient-based + global, genetic algorithms ➔ no suitable fit of the target [1]

- However: Similar performance of surrogate-based optimization

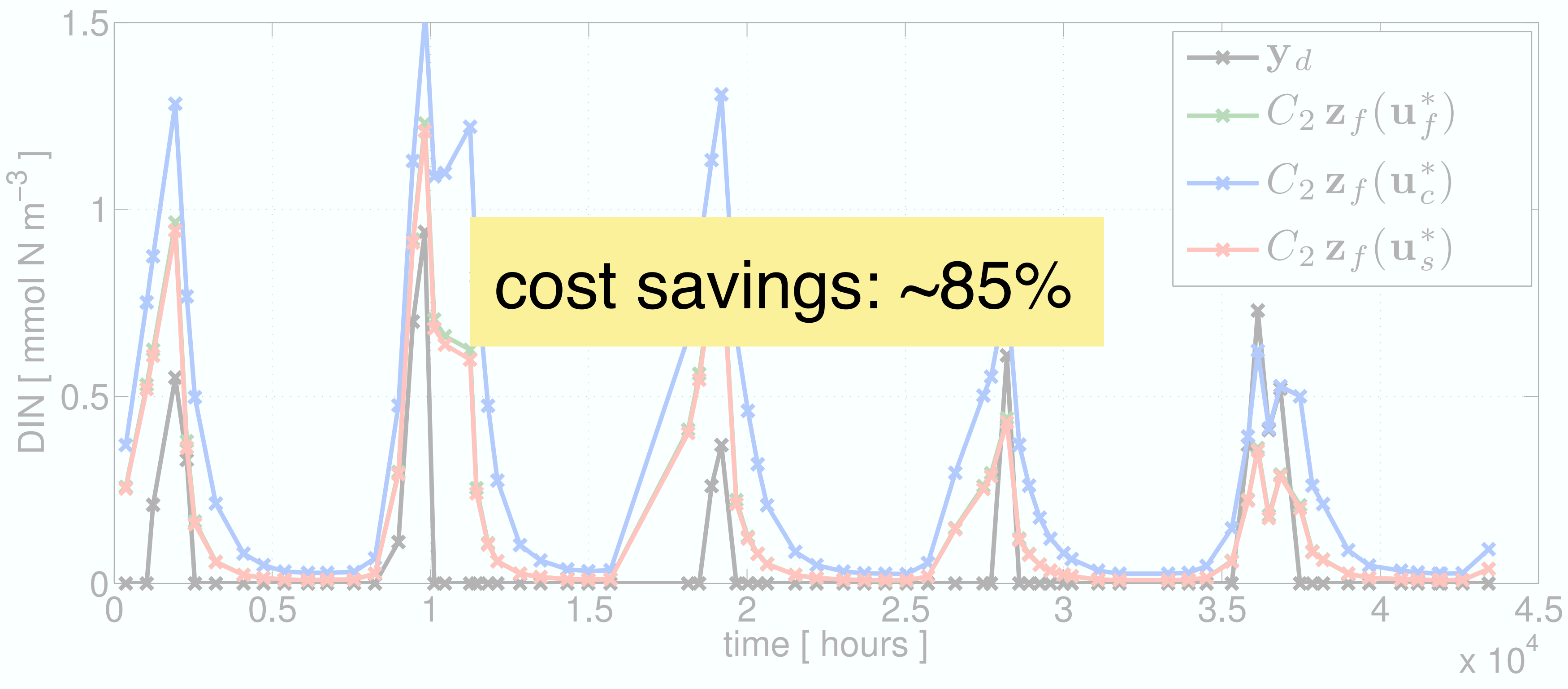

Figure: Fine, coarse model and surrogate optimization: Optimal solutions.

[1] Schartau, Oschlies (2003); Schartau (2001); Rückelt et al. (2010)

- „Reference“ fine model: 3000 fixed-point iteration steps
- Coarse model: Reduced number of fixed point iteration steps

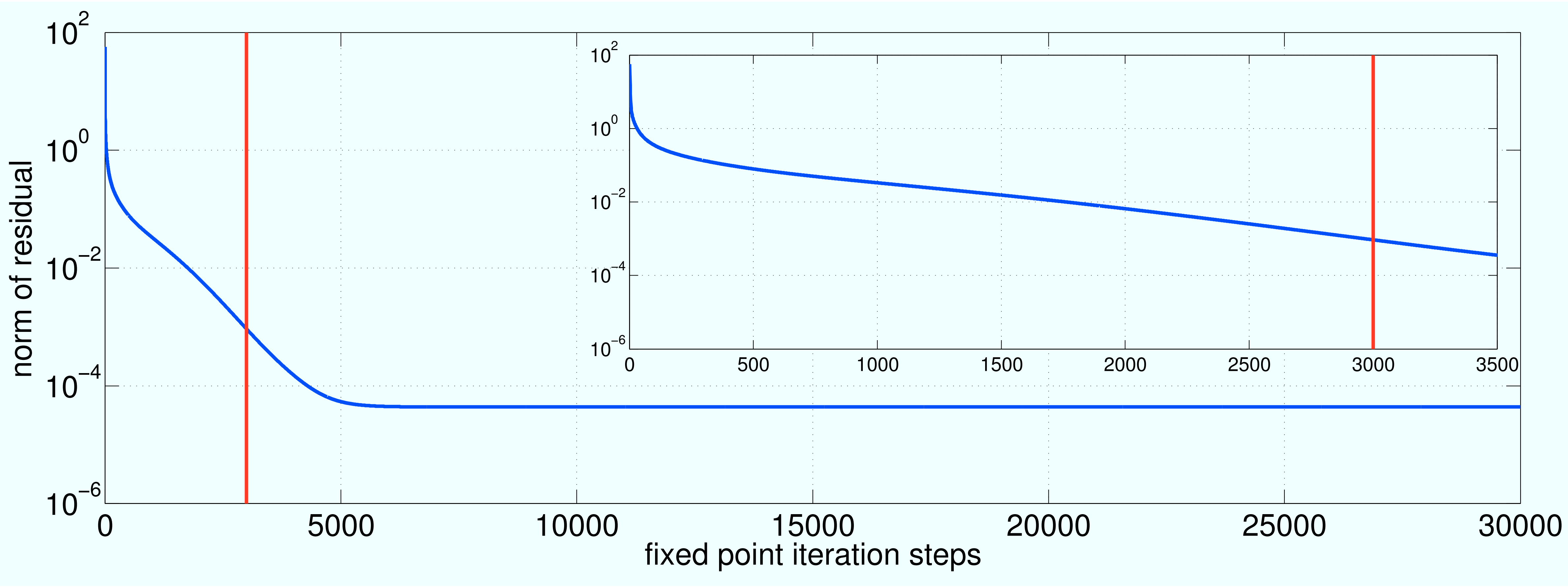

Figure: Convergence of the fixed point iteration towards a steady annual cycle.

- „Reference“ fine model: 3000 fixed-point iteration steps
- Coarse model: Reduced number of fixed point iteration steps

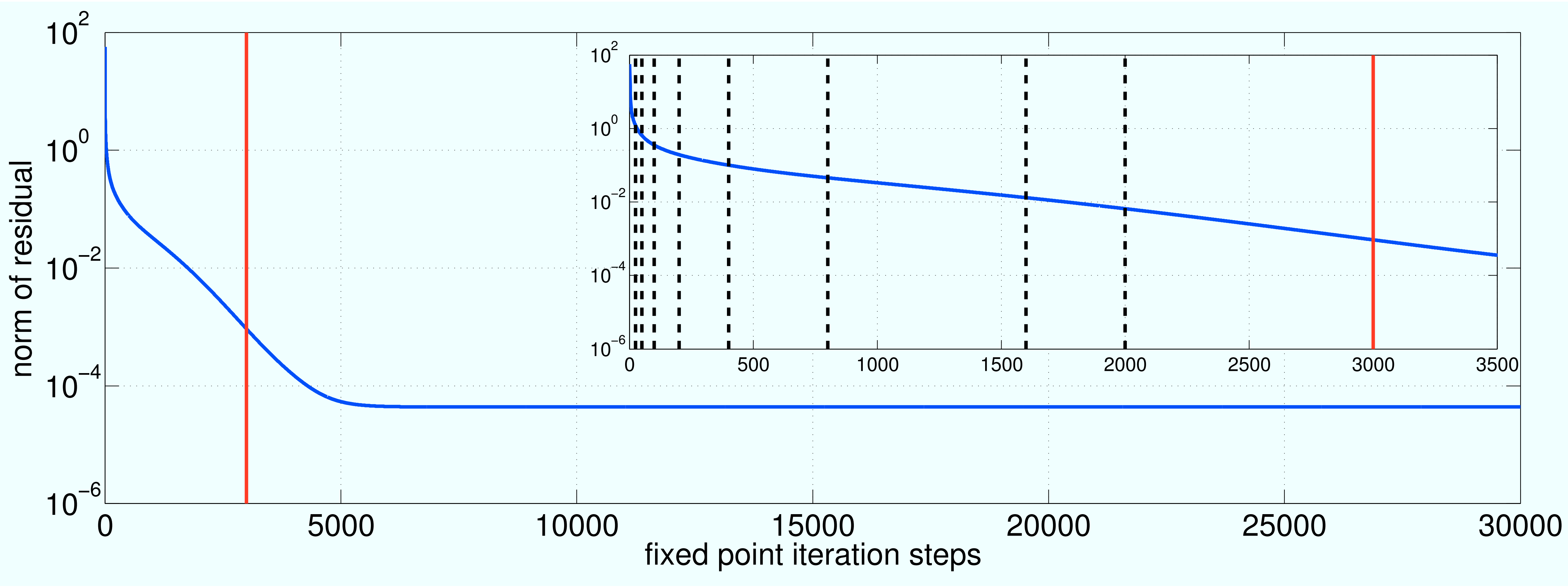

Figure: Convergence of the fixed point iteration towards a steady annual cycle.

- „Reference“ fine model: 3000 fixed-point iteration steps
- Coarse model: Reduced number of fixed point iteration steps

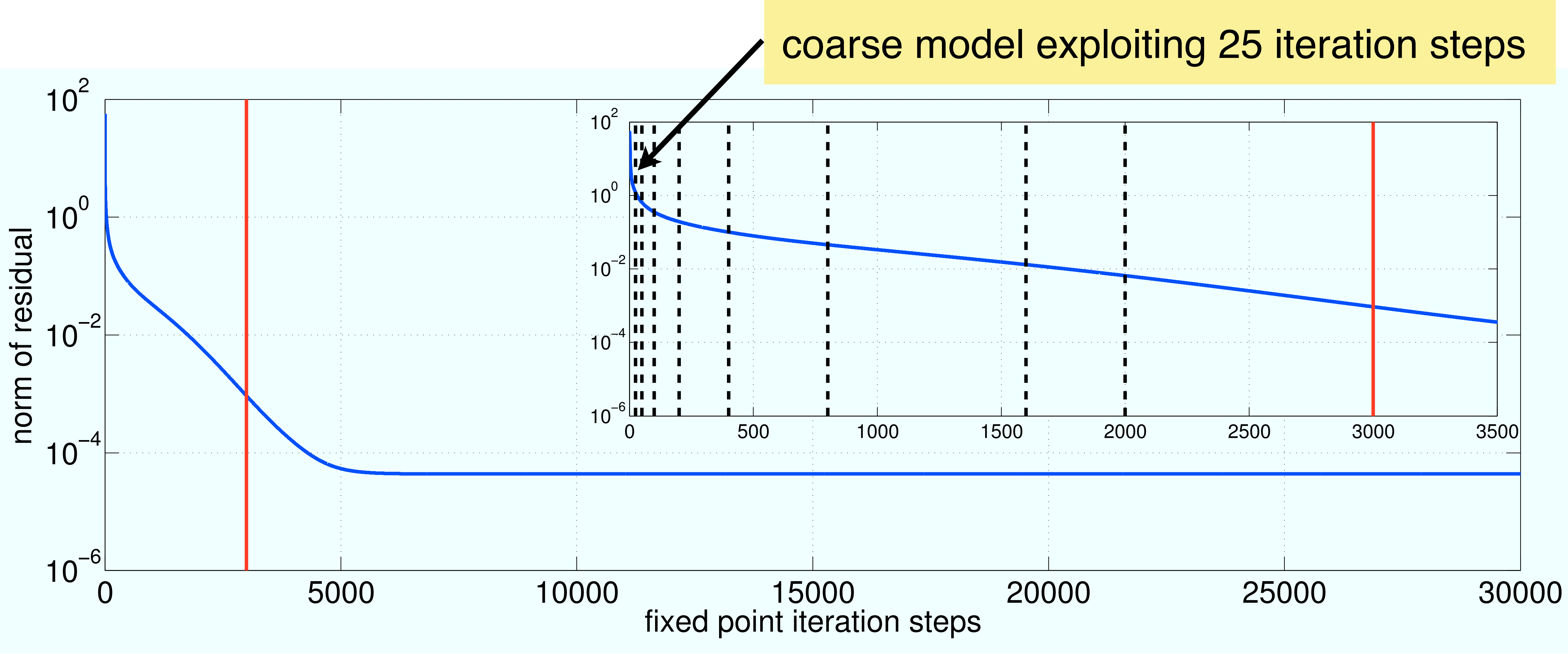

Figure: Convergence of the fixed point iteration towards a steady annual cycle.

3D N-DOP model: Multiplicative response correction

Generalization capability

- Again: Quality of approximation in neighborhood of „construction point“

  ➔ important for algorithm‘s performance

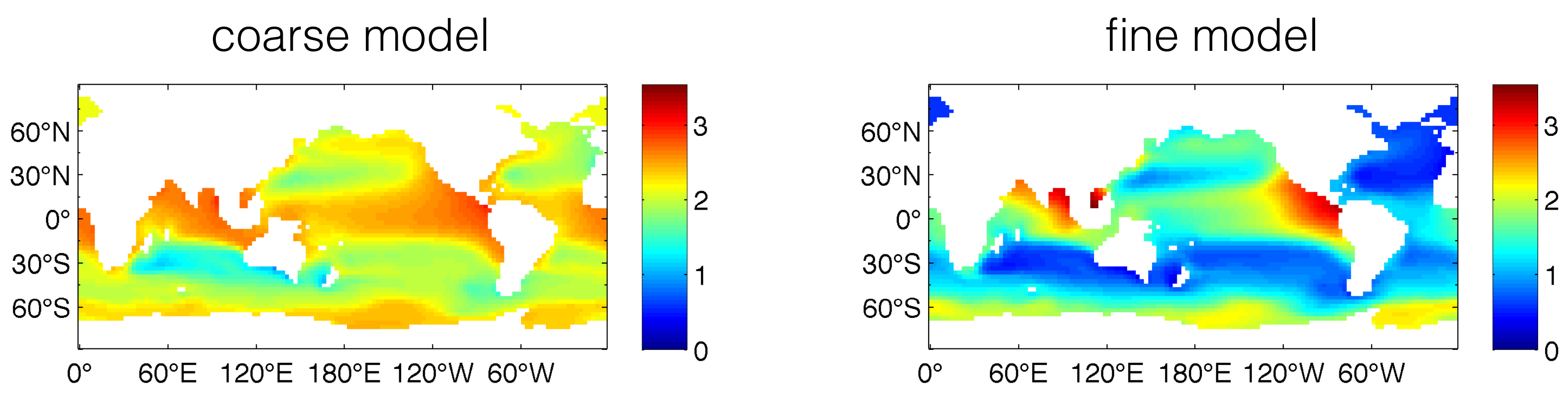

Figure: Distribution of tracer concentration (phosphorus) at ~455m depth at some neighboring parameter.

3D N-DOP model: Multiplicative response correction

Generalization capability

- Again: Quality of approximation in neighborhood of „construction point“

  ➔ important for algorithm‘s performance

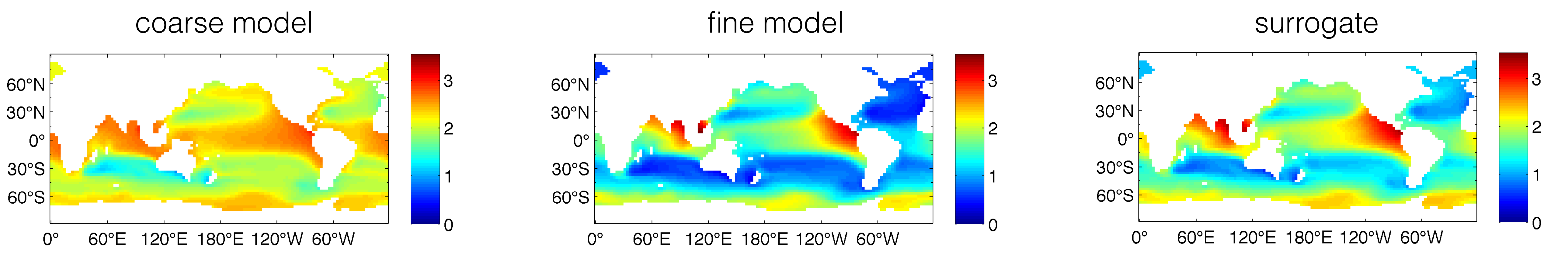

Figure: Distribution of tracer concentration (phosphorus) at ~455m depth at some neighboring parameter.

3D N-DOP model: Multiplicative response correction

Generalization capability

- Again: Quality of approximation in neighborhood of „construction point“

  ➔ important for algorithm‘s performance

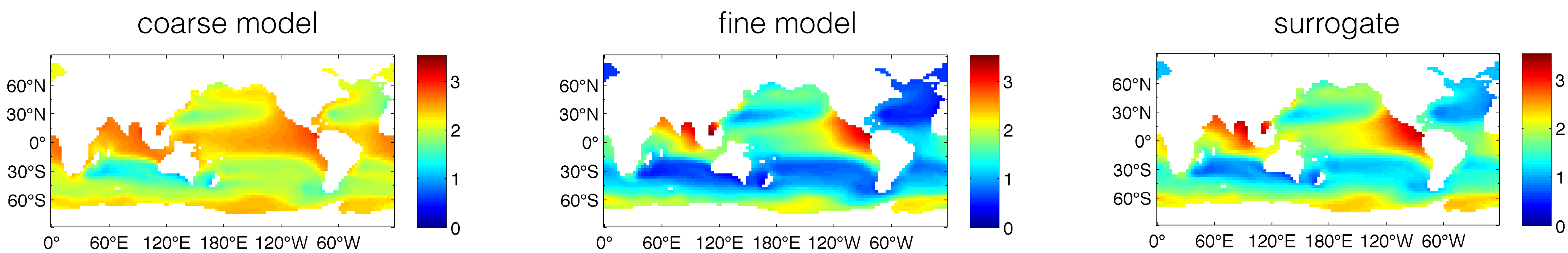

Figure: Distribution of tracer concentration (phosphorus) at ~455m depth at some neighboring parameter.

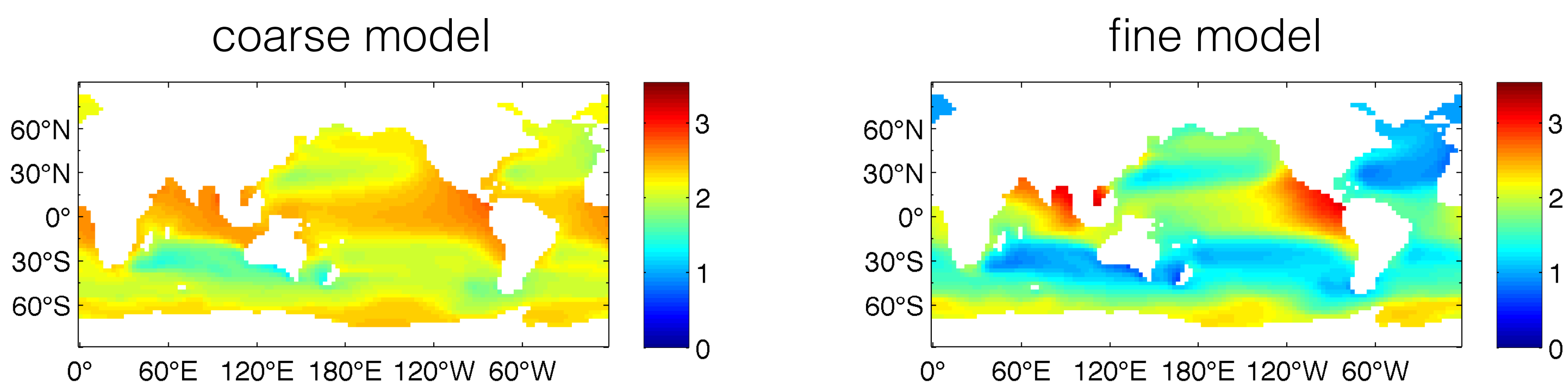

Figure: ... and in a closer vicinity.

3D N-DOP model: Multiplicative response correction

Generalization capability

- Again: Quality of approximation in neighborhood of „construction point“

  ➔ important for algorithm‘s performance

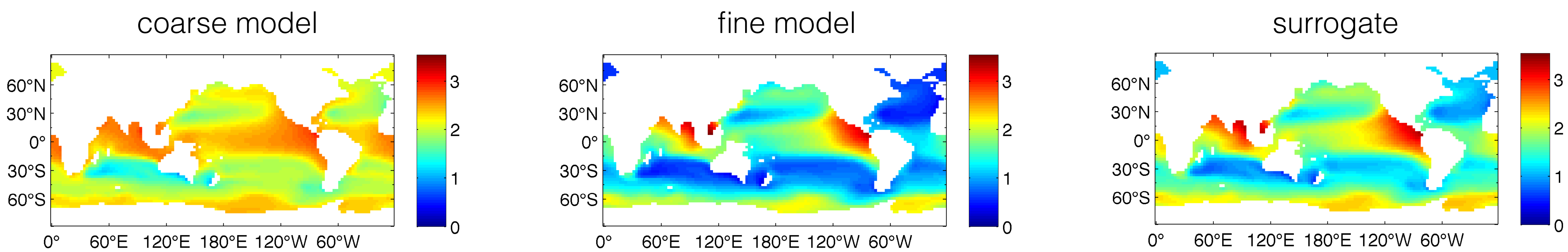

Figure: Distribution of tracer concentration (phosphorus) at ~455m depth at some neighboring parameter.

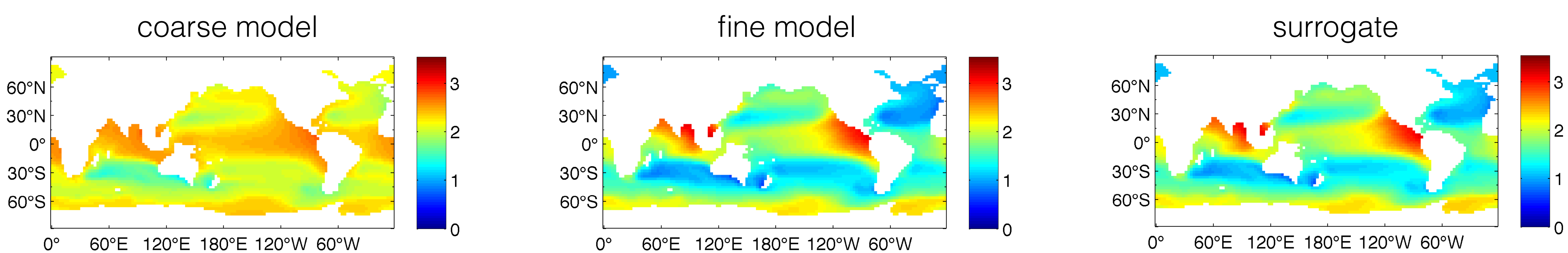

Figure: ... and in a closer vicinity.

3D N-DOP model: Numerical results

Verification by model generated data

Figure: Distribution of tracer concentration (phosphorus) at ~25m depth and some point in time.

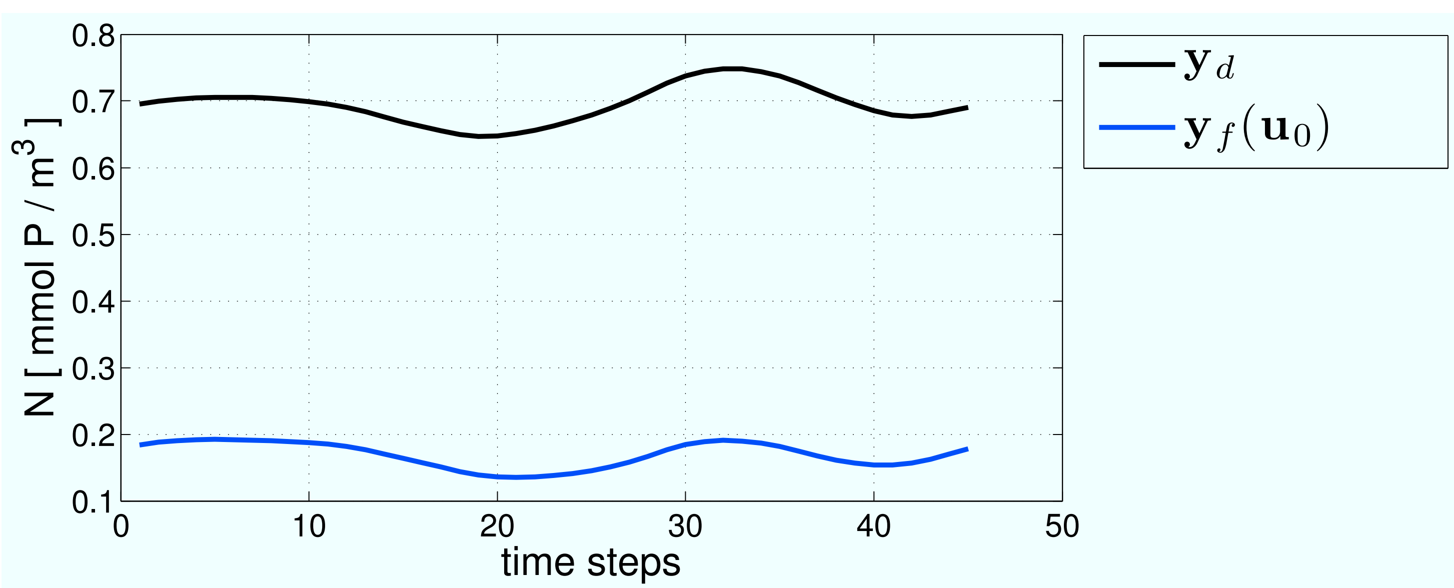

Figure: Trajectory of tracer concentration at one selected location: x=90°E, y=0°.

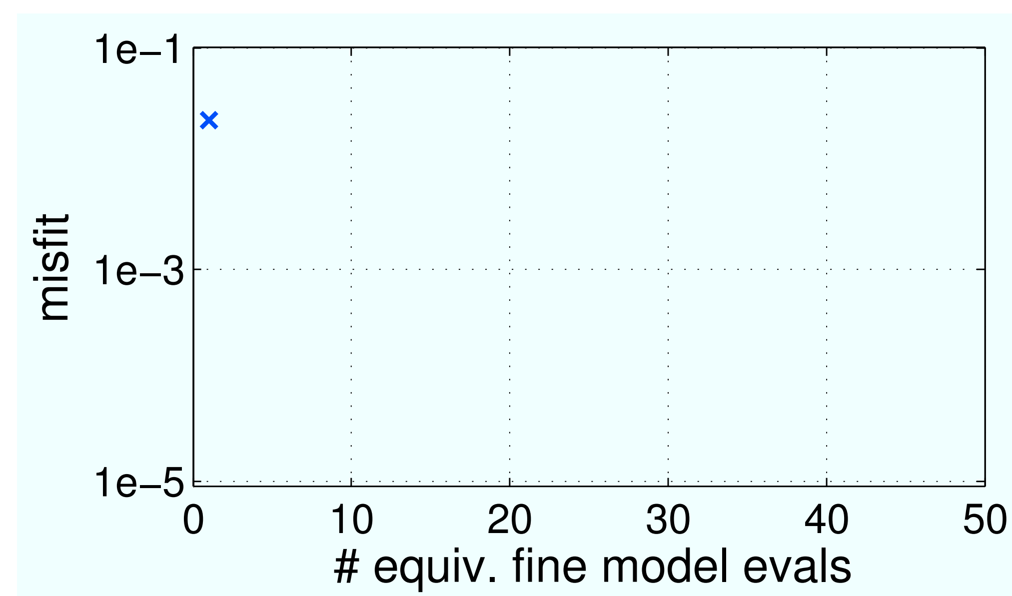

Figure: Convergence history of cost function.

3D N-DOP model: Numerical results

Verification by model generated data

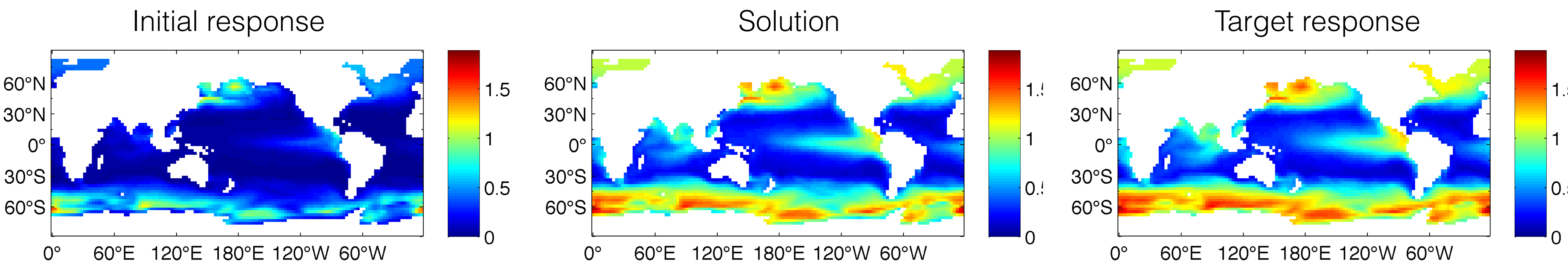

Figure: Distribution of tracer concentration (phosphorus) at ~25m depth and some point in time.

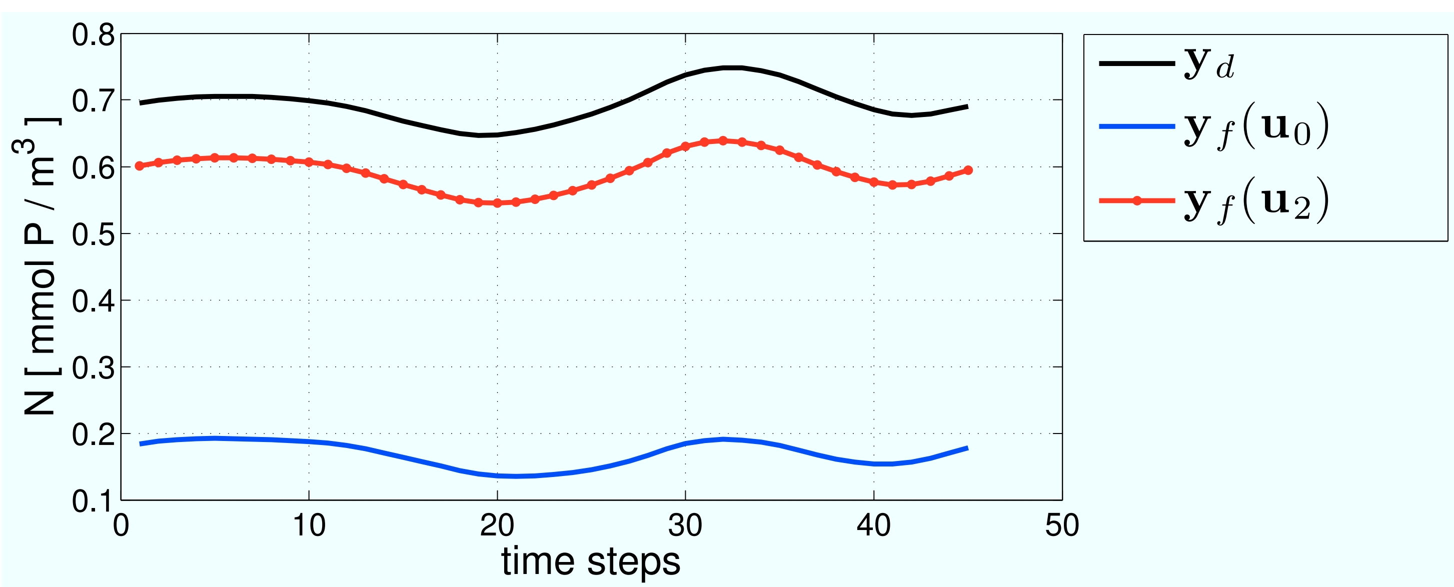

Figure: Trajectory of tracer concentration at one selected location: x=90°E, y=0°.

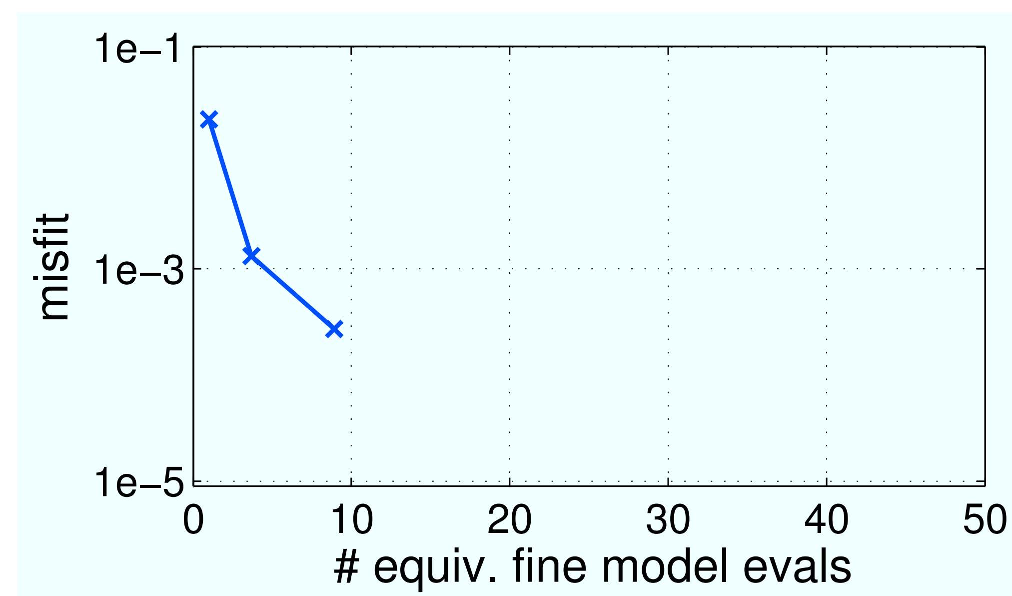

Figure: Convergence history of cost function.

3D N-DOP model: Numerical results

Verification by model generated data

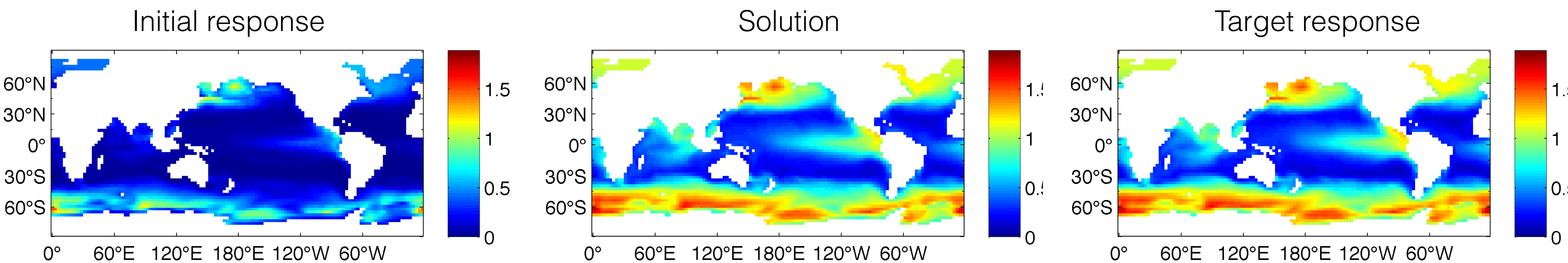

Figure: Distribution of tracer concentration (phosphorus) at ~25m depth and some point in time.

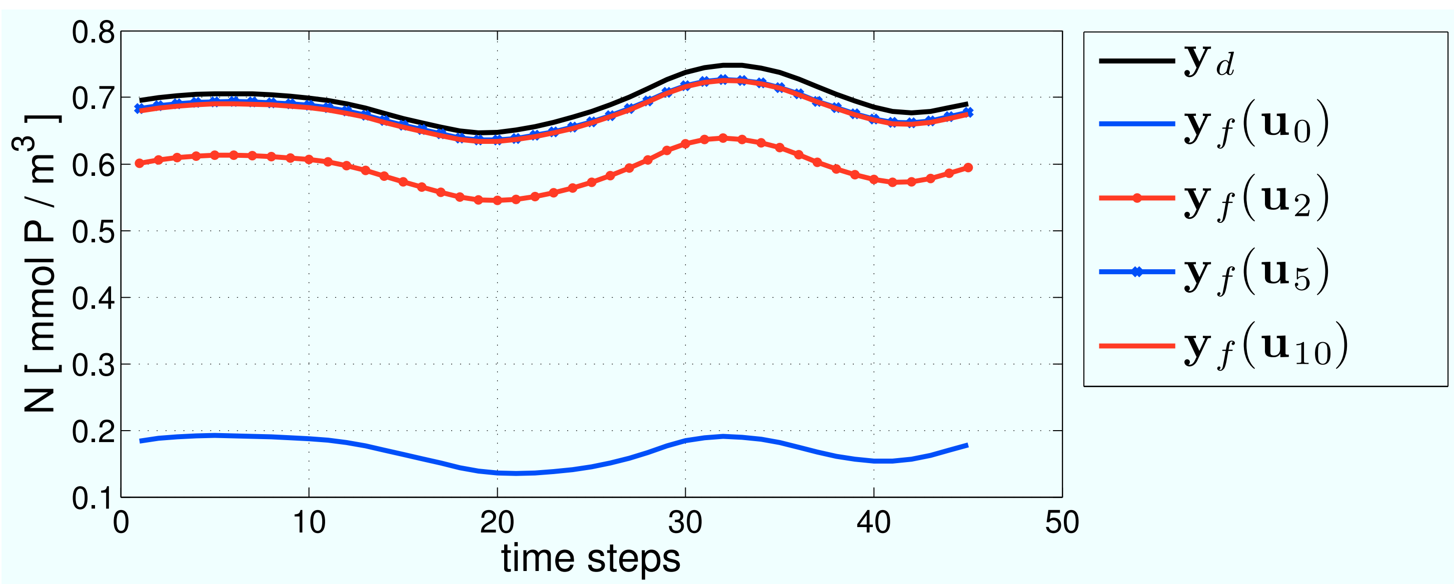

Figure: Trajectory of tracer concentration at one selected location: x=90°E, y=0°.

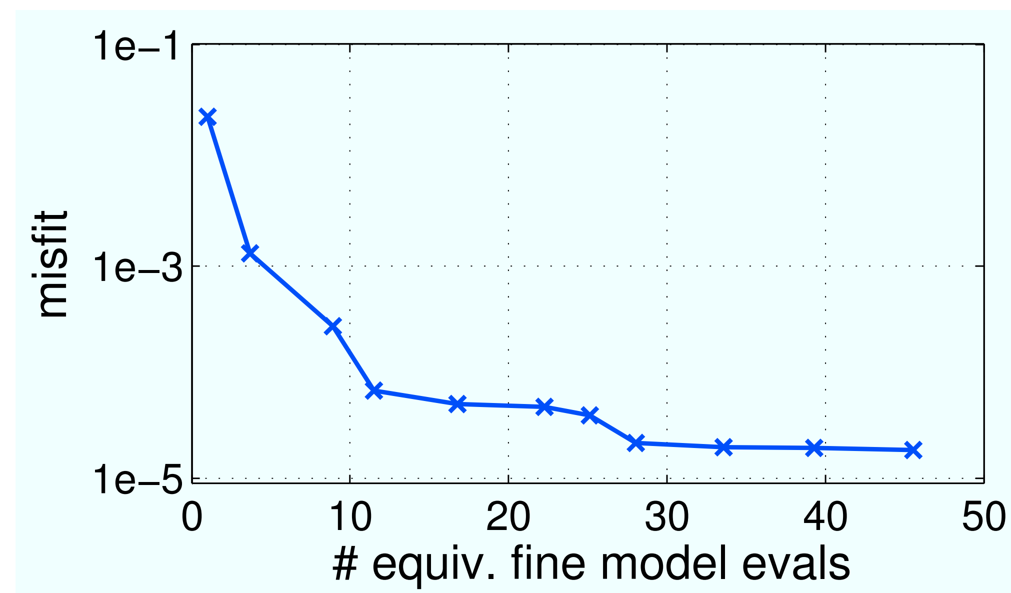

Figure: Convergence history of cost function.

Surrogate-based optimization:

- Accurate solution already after 9 - 46 equivalent fine model evaluations
- Whole optimization in the range of hours

Direct fine model optimization:

- Prospectively: 500 - 1000 fine model evaluations
- Whole optimization in the range of several days up to weeks

3D N-DOP model: Numerical results

Verification by model generated data

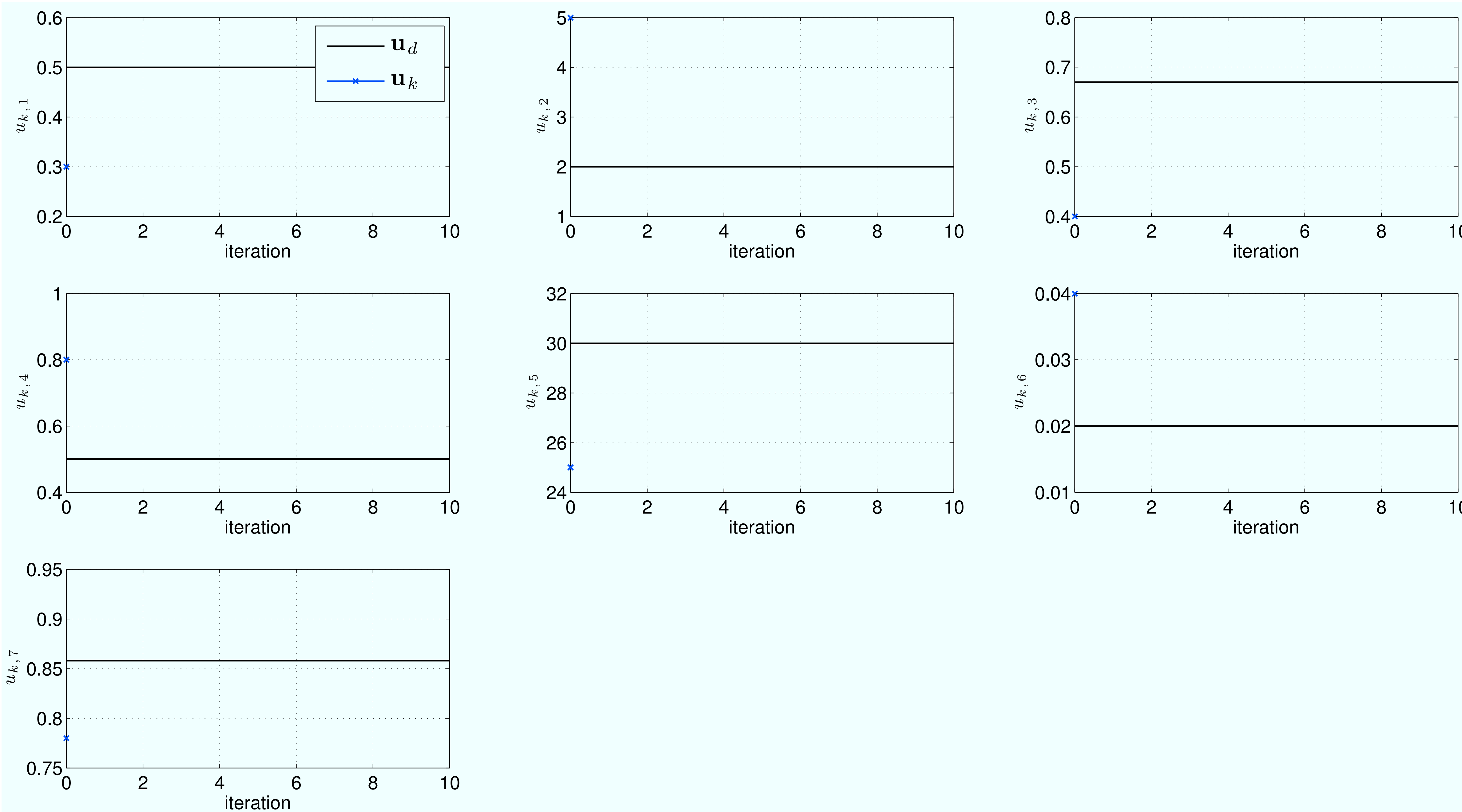

Figure: Convergence history of parameters.

3D N-DOP model: Numerical results

Verification by model generated data

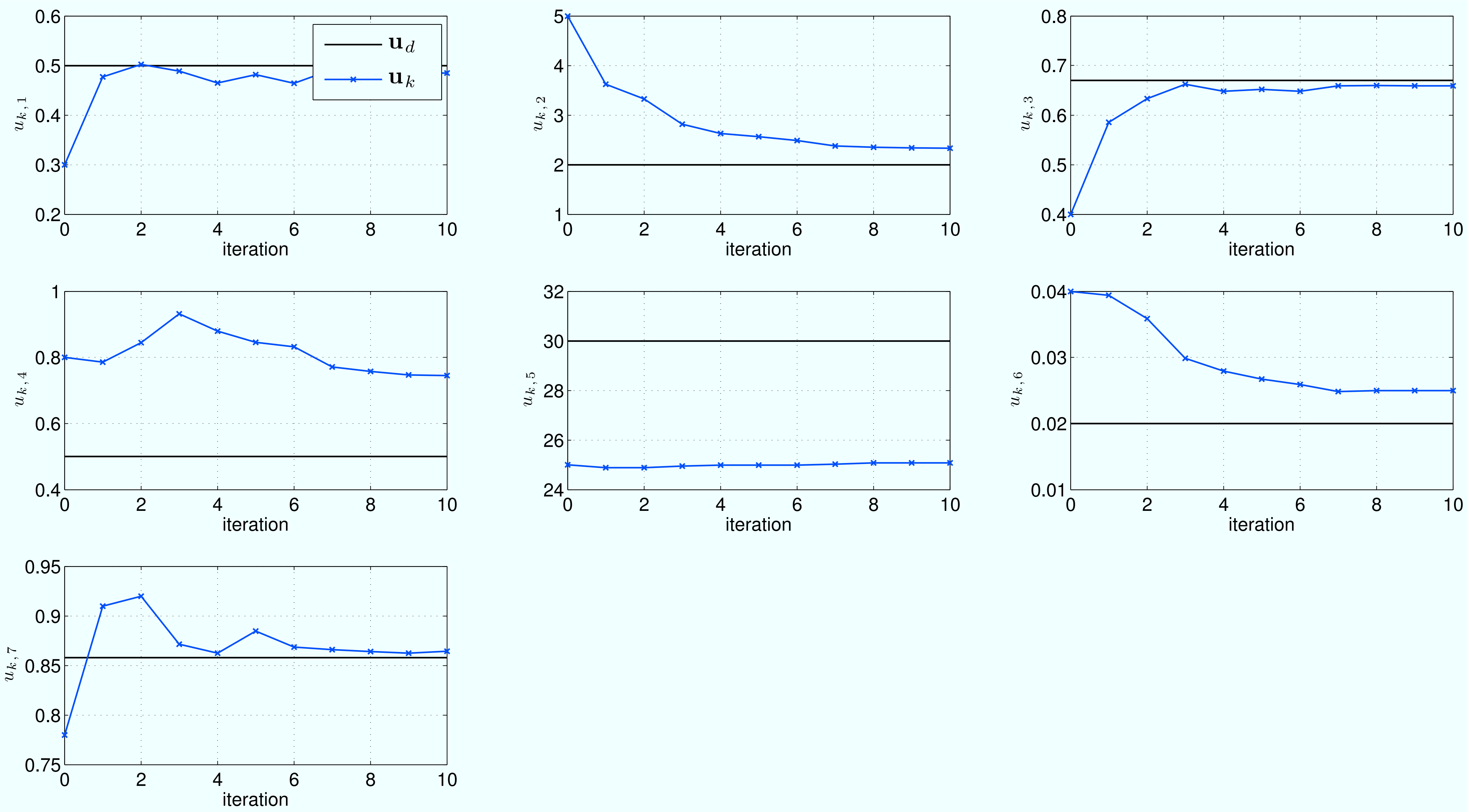

Figure: Convergence history of parameters.

Summary

- Fundamental aim: Computationally efficient calibration of marine ecosystem models

- Surrogate-based optimization employing physics-based coarse models

- Coarse models:
  - Coarser mesh discretization (1D NPZD model)
  - Relaxed convergence criterion (3D N-DOP model)

- Coarse model accuracy is not sufficient for direct use

- A multiplicative response correction

  ➔ yields sufficiently accurate corrected coarse model (surrogate)

- Surrogate-based optimization

  ➔ solution at low computational costs

Acknowledgements

Prof. Dr. Thomas Slawig

Professor at the Institute for Computer Science, Christian-Albrechts-Universität Kiel, Germany

Prof. Dr. Andreas Oschlies

Professor of Marine Biogeochemical Modelling at the Helmholtz Centre for Ocean Research Kiel, Germany

Prof. Slawomir Koziel, Ph.D.

Associate Professor at the Engineering Optimization & Modeling Center, School of Science and Engineering, Reykjavik University, Iceland

Summary

- Fundamental aim: Computationally efficient calibration of marine ecosystem models
- Surrogate-based optimization employing physics-based coarse models
- Coarse models:
  - Coarser mesh discretization (1D NPZD model)
  - Relaxed convergence criterion (3D N-DOP model)
- Coarse model accuracy is not sufficient for direct use
- A multiplicative response correction

  ➔ yields sufficiently accurate corrected coarse model (surrogate)
- Surrogate-based optimization

  ➔ solution at low computational costs

Outlook

- Enhancements of current algorithms

  ➔ improvements of performance + decrease in computational costs

- 3D optimization with real measurement data

- Yet other approaches (e.g., Space Mapping) might have great potential

- Other physics-based coarse models (e.g., simplified physics)

- Coarser discretization ➔ analysis of numerical stability

- Application for exhaustive model-data comparison studies

  ➔ essential to reveal full potential in practice

1D NPZD model: Numerical results

Verification by model generated data

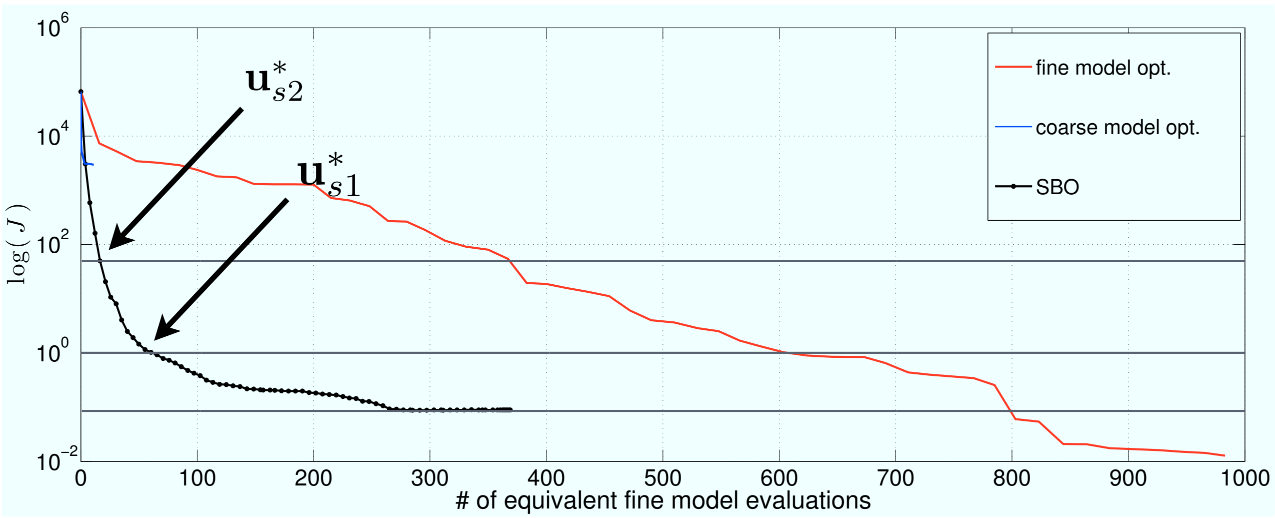

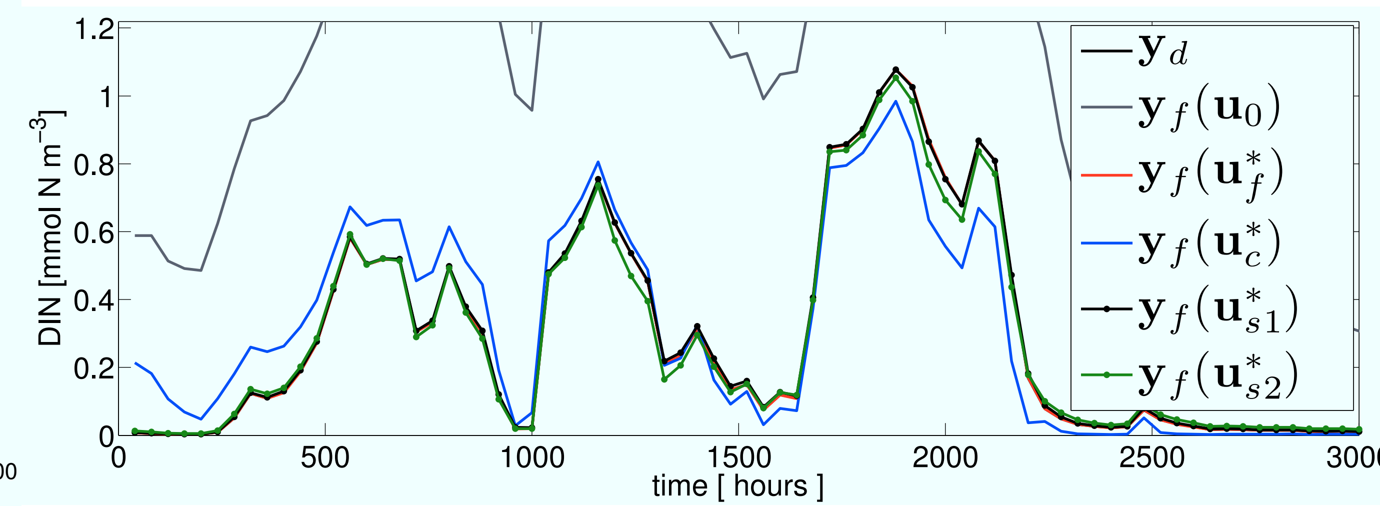

iterate	u_1	u_2	$\dots$									u_{12}
	SBO (original and improved scheme)											
$\mathbf{u}^*_{s1}$	0.705	0.626	0.044	0.015	0.060	0.937	1.908	0.016	0.147	0.020	0.629	4.237
$\mathbf{u}^*_{s2}$	0.738	0.604	0.028	0.010	0.036	1.024	1.678	0.010	0.206	0.020	0.541	4.318
	Coarse model optimization											
$\mathbf{u}^*_c$	0.300	1.066	0.036	0.065	0.064	0.025	0.040	0.065	0.010	0.012	0.730	3.448
	Fine model optimization											
$\mathbf{u}^*_f$	0.747	0.596	0.025	0.010	0.030	0.999	2.046	0.010	0.203	0.020	0.493	4.310
$\mathbf{u}_d$	0.750	0.600	0.025	0.010	0.030	1.000	2.000	0.010	0.205	0.020	0.500	4.320

$\mathbf{u}_i$	Description	Optimization Problem
$\mathbf{u}_0$	Randomly chosen initial parameter vector	
$\mathbf{u}^*_{f1}$	Result of an *original* fine model optimization	$\mathbf{u}^*_{f1} := \underset{\mathbf{u}\in U_{ad}}{\text{argmin}}\ J_1(\mathbf{y}_f(\mathbf{u}))$ (O.1)
$\mathbf{u}^*_{f2}$	Result of a *reference* fine model optimization	$\mathbf{u}^*_{f2} := \underset{\mathbf{u}\in U_{ad}}{\text{argmin}}\ J_2(\mathbf{z}_f(\mathbf{u}))$ (O.2)
$\mathbf{u}^*_c$	Result of a coarse model optimization	$\mathbf{u}^*_c := \underset{\mathbf{u}\in U_{ad}}{\text{argmin}}\ J_2(\mathbf{z}_c(\mathbf{u}))$ (O.3)
$\mathbf{u}^*_s$	Result of a SBO run using $\mathbf{u}^*_c$ as initial parameter vector	$\mathbf{u}_{k+1} = \underset{\mathbf{u}\in U_{ad}, \Vert \mathbf{u}-\mathbf{u}_k \Vert^2 \leq \delta_k}{\text{argmin}}\ J_2(\mathbf{s}_k(\mathbf{u})),\ k = 0, 1, \ldots,\ \mathbf{u}_0 := \mathbf{u}^*_c$ (O.4)

$$J_1(\mathbf{y}_f) := \Vert C_1\,\mathbf{y}_f - \mathbf{y}_d \Vert^2_\sigma,$$

$$J_2(\mathbf{z}) := \Vert C_2\,\mathbf{z} - \mathbf{y}_d \Vert^2_\sigma,$$

$$\mathbf{z} = \begin{cases} \text{reference fine model response}, & \mathbf{z} = \mathbf{z}_f \\ \text{smoothed coarse model response}, & \mathbf{z} = \mathbf{z}_c \\ \text{surrogate's response at iteration } k, & \mathbf{z} = \mathbf{s}_k \end{cases}$$

1D NPZD model: Numerical results

Model calibration with measurement data

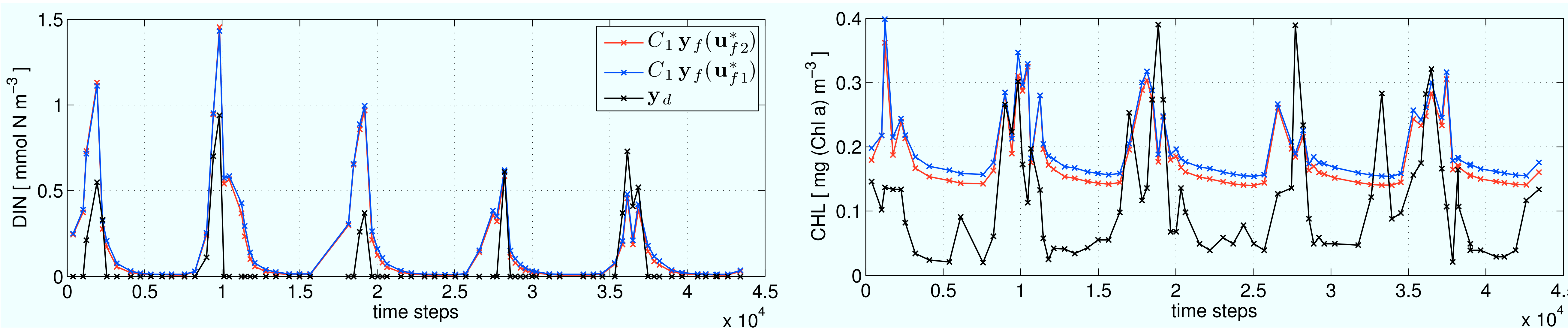

(a) Response is transformed using the operator C_1 to make it commensurable with the measurement data $\mathbf{y}_d$.

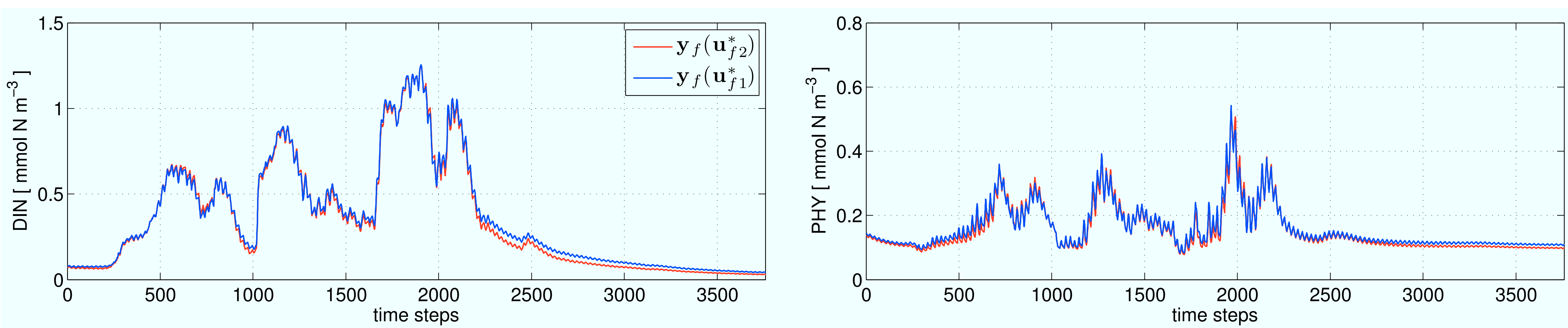

(b) Untransformed response to assess the overall quality.

Model calibration with measurement data

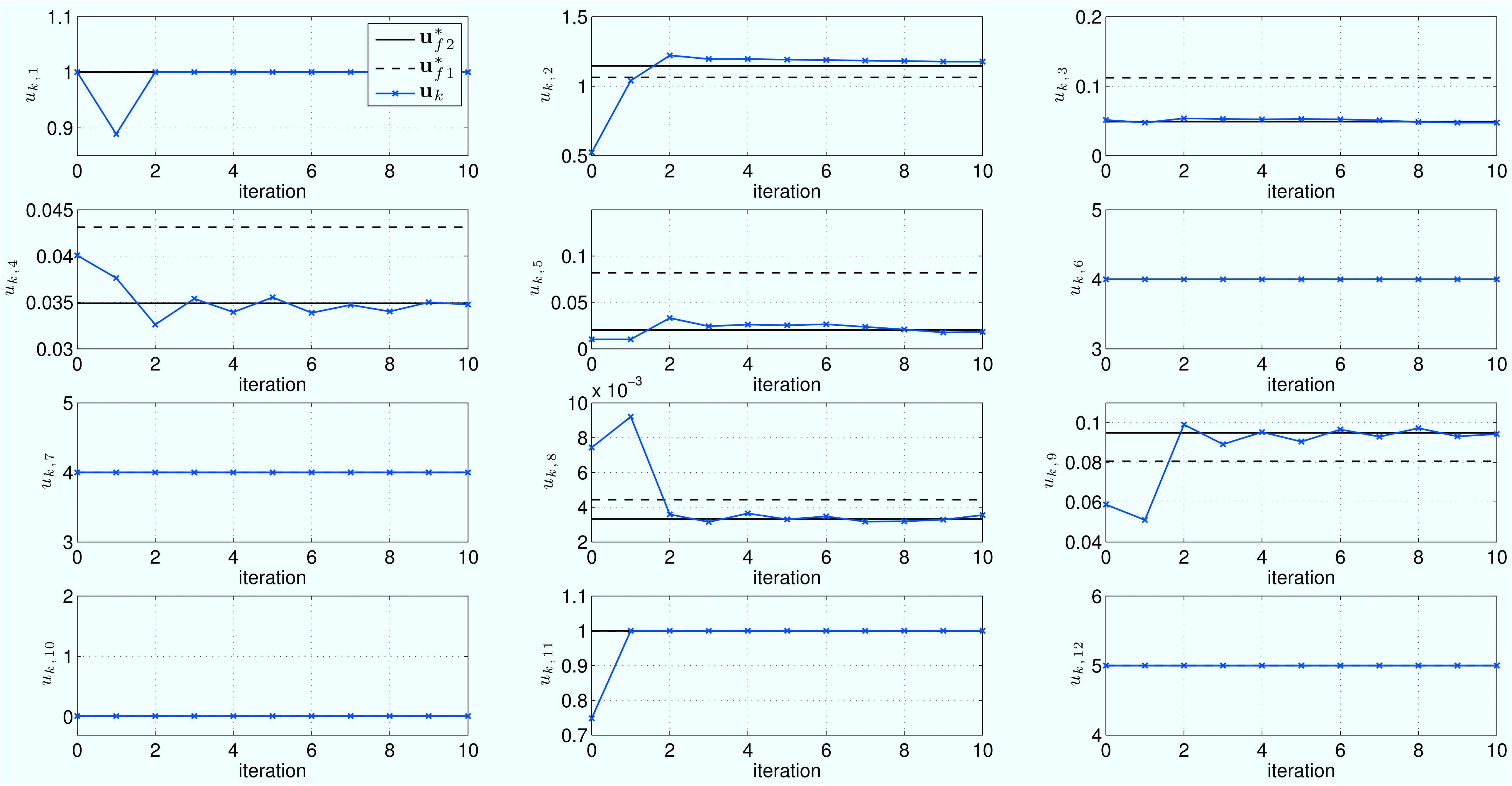

1D NPZD model: Numerical results

Model calibration with measurement data

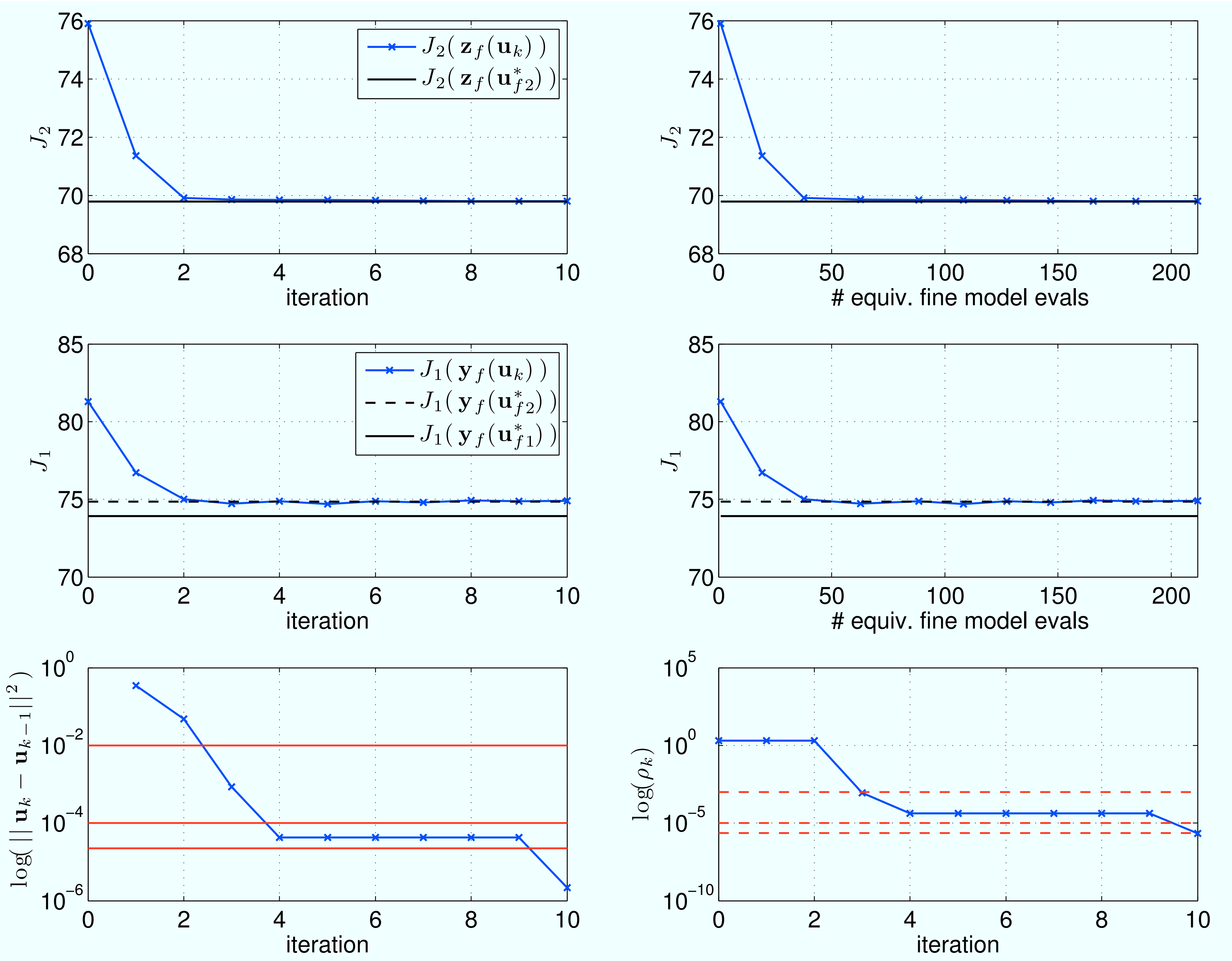

- Using TMM + fixed time step τ, the time integration scheme reads

$$\begin{aligned} \mathbf{y}_{j+1} &= \mathbf{A}_{imp,j}\,(\mathbf{A}_{exp,j}\,\mathbf{y}_j + \tau\,\mathbf{q}_j(\mathbf{y}_j,\mathbf{u})) \\ &=: \varphi_j(\mathbf{y}_j,\mathbf{u}), \qquad\qquad j = 0,\ldots,n_\tau - 1 \end{aligned}$$

- Here n_τ is the total number of time steps and $\boldsymbol{A}_{imp,j}$, $\boldsymbol{A}_{exp,j}$ are the implicit and explicit transport matrices at time step j

- Steady annual cycle: we are looking for a fixed point of the mapping

$$\mathbf{y}_{n_\tau} = \Phi(\mathbf{y}_0,\mathbf{u}) = \mathbf{y}_0 \qquad \Phi := \varphi_{n_\tau-1}\circ\cdots\circ\varphi_0$$

- One application of the mapping Φ corresponds to the computation of one year model time

- The whole fixed point iteration now consists of a repeated application of the mapping Φ:

$$\mathbf{y}^{l+1} = \Phi(\mathbf{y}^l,\mathbf{u}), \quad l = 0,\ldots,n_l - 1$$

- n_l: the total number of iterations (model years) necessary
- y^l: denotes the vector of discretized tracer after l years, i.e., $y^l := y_{l\cdot n_\tau}$

u_i	Name	Description	Unit
u_1	λ	remineralization rate of DOP	$1/d$
u_2	α	maximum community production rate	$1/d$
u_3	σ	fraction of DOP, $\bar{\sigma} = (1 - \sigma)$	$-$
u_4	K_N	half saturation constant of N	$m\,molP/m^3$
u_5	K_I	half saturation constant of light	W/m^2
u_6	K_{H2O}	attenuation of water	$1/m$
u_7	b	sinking velocity exponent	$-$

What has been done so far?

- Transport matrix approach for passive tracers (Transport Matrix Method) [1]

- Another approach: exploit a coarse resolution model initially
  - ➔ seek a model state already close to the desired periodic solution
  - ➔ utilized as initial condition for a subsequent high-resolution (fine) model simulation [1]

- Yet another, common strategy to obtain a computationally cheaper coarse model: Direct optimization of a temporally/ spatially coarser resolution model

- However:
  - Such coarse models are usually not sufficiently accurate to directly exploit them in a classical optimization loop in lieu of the original fine model
  - Optimized solution: rather inaccurate approximation of the desired fine one only
  - Most likely, a subsequent and usually expensive fine model optimization is required
  - Therefore, the overall optimization costs can be still comparably high

[1] Khatiwala et al. (2005)

- Suitable approximations of sampled fine model data (e.g., polynomial regression, kriging, support-vector regression, ...)

$$y = a_0 + a_1 x + a_2 x^2 + a_3 x^3 + \cdots + a_m x^m + \varepsilon.$$

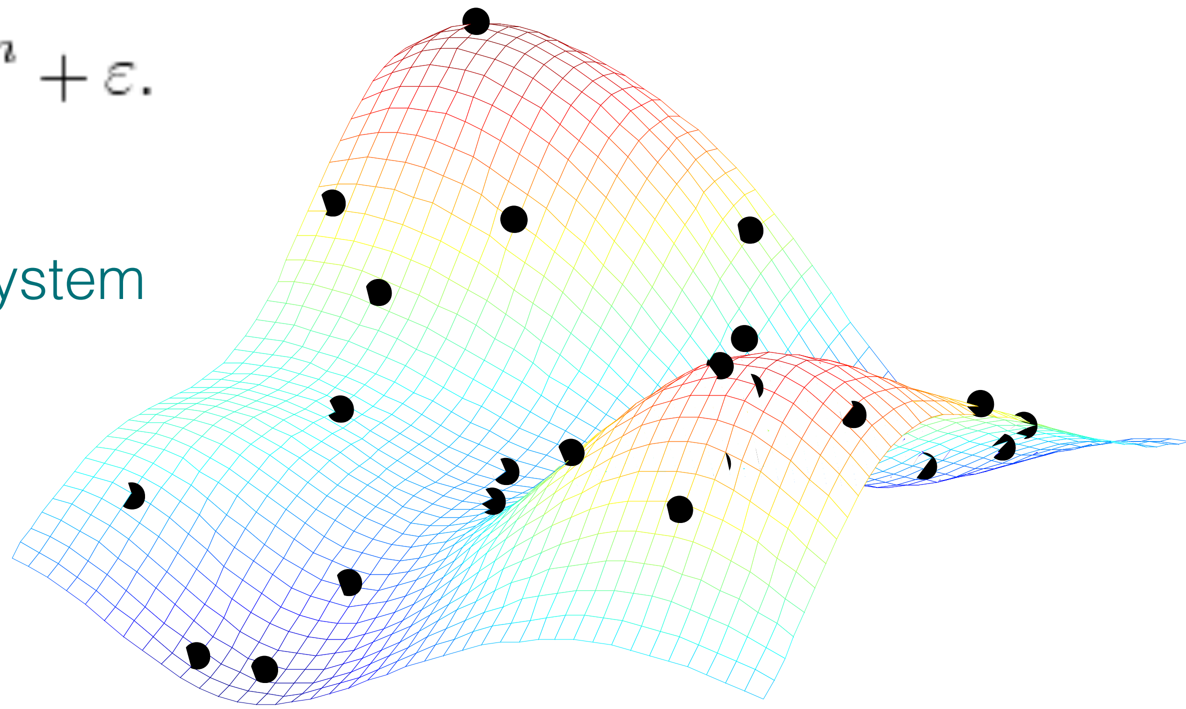

- Constructed without previous knowledge of the system
- Do not inherit any physical characteristics (generalization capability not as good)
- Cheap model evaluation
- But, typically substantial amount of fine model data samples to set up a model is required and to ensures a reasonable accuracy level
- Methodology is rather generic ➔ applicable to a wide class of problems

Picture Source: S. Koziel, Reykjavik University, Iceland

Physics-Based Surrogates

- Fundamental advantage:
  SBO schemes working with physics-based surrogates normally require small number of fine model evaluations to yield a sufficient accuracy (often, only one per iteration)

- Thus, the computational burden is shifted towards the cheap coarse model

- Key prerequisites:
  - Quality of the coarse model is critical ➔ inaccurate model may result in poor algorithm performance
  - Cheap and yet reasonably accurate coarse model as well as a properly selected and low-cost alignment procedure
  - Agreement of function and derivative information (not necessarily exact)
  - Globalization: Some standard trust-region/ line-search approaches

- Underlying coarse model, correction approach is problem specific
  ➔ their reuse across different problems is rare

Surrogate-based optimization: State-of-the-art

Space Mapping

- One of the most recognized SBO techniques exploiting physics-based coarse models
- A mapping relating the fine and coarse model parameters is proposed to calibrate a physics-based coarse model
- This mapping using so-called parameter extraction (PE) is a nonlinear opt. problem itself

$$\mathbf{s}_k(\mathbf{u}) = \bar{\mathbf{y}}_c(\mathbf{u}, \mathbf{p}_k), \quad \mathbf{p}_k = \underset{\mathbf{p}}{\operatorname{argmin}} \left(\sum_{i=0}^{k} \| \mathbf{y}_f(\mathbf{u}_k) - \bar{\mathbf{y}}_c(\mathbf{u}_k, \mathbf{p}) \| \right)$$

(Generic SM surrogate model, i.e., coarse model y_C with auxiliary mapping p_k)

Domain distortion (input SM)

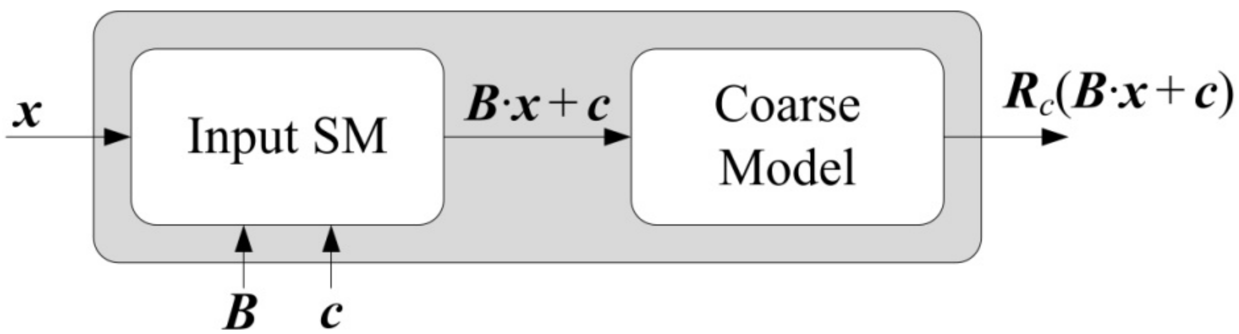

Response distortion (output SM)

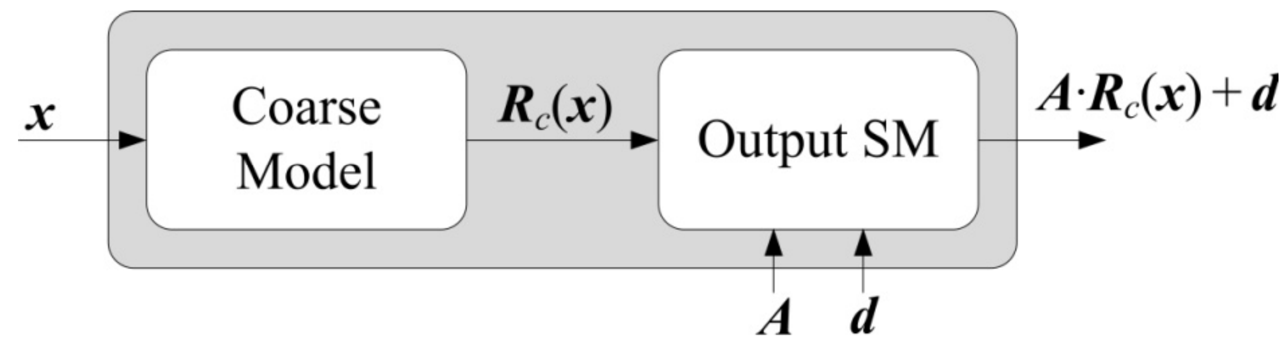

Picture Source: S. Koziel, Reykjavik University, Iceland

Institut für Informatik · future ocean KIEL MARINE SCIENCES

- Aggressive Space Mapping [1] (firstly developed by John W. Bandler et al. in 1994):

$$\mathbf{s}_k(\mathbf{u}) := \hat{\mathbf{y}}\left(\mathbf{p}_k(\mathbf{u})\right), \quad \mathbf{p}_k(\mathbf{u}) = \mathbf{p}(\mathbf{u}_k) + \mathbf{p}'(\mathbf{u}_k)\left(\mathbf{u} - \mathbf{u}_k\right),$$

$$\hat{\mathbf{u}}_k = \mathbf{p}(\mathbf{u}_k) := \operatorname*{argmin}_{\mathbf{u}\in U} ||\,\hat{\mathbf{y}}(\mathbf{u}) - \mathbf{y}(\mathbf{u}_k)\,||_Y^2 \,.$$

- If either the fine model nearly matches the data in an optimum or if both models are similar near their respective optima we obtain so-called perfect mapping [2]

$$\mathbf{p}(\mathbf{u}^*) = \operatorname*{argmin}_{\mathbf{u}\in U} \;||\,\hat{\mathbf{y}}(\mathbf{u}) - \mathbf{y}(\mathbf{u}^*)\,||_Y^2 \;\approx\; \operatorname*{argmin}_{\mathbf{u}\in U} \;||\,\hat{\mathbf{y}}(\mathbf{u}) - \mathbf{y}_d\,||_Y^2 = \hat{\mathbf{u}}^*.$$

- This motivates to solve for

$$\mathbf{F}(\bar{\mathbf{u}}) := \mathbf{p}(\bar{\mathbf{u}}) - \hat{\mathbf{u}}^* = 0 \qquad \hat{\mathbf{u}}^* := \operatorname*{argmin}_{\mathbf{u}\in U} \; J\left(\,\hat{\mathbf{y}}(\mathbf{u})\,\right)$$

- Under certain conditions, ASM is equivalent to use the surrogate in a SBO algorithm [12]

$$\bar{\mathbf{u}}_s = \operatorname*{argmin}_{\mathbf{u}\in U} \; J\left(\,\hat{\mathbf{y}}(\mathbf{p}(\mathbf{u}))\,\right)$$

[1] John W. Bandler et al. (1994); [2] Echeverría and Hemker (2005)

- Aggressive Space Mapping [1] (firstly developed by John W. Bandler et al. in 1994)
  ➔ based on a parameter mapping from the fine to the coarse model parameters

$$\mathbf{p}(\mathbf{u}) = \hat{\mathbf{u}},$$

- such that the mapped coarse model – the surrogate – provides an approximation of the fine model y, i.e.,

$$\mathbf{y}(\mathbf{u}) \approx \hat{\mathbf{y}}\left(\mathbf{p}(\mathbf{u})\right) \qquad (*)$$

- Original Space Mapping approach:

$$\mathbf{F}(\bar{\mathbf{u}}) := \mathbf{p}(\bar{\mathbf{u}}) - \hat{\mathbf{u}}^* = 0 \quad (**) \qquad \hat{\mathbf{u}}^* := \underset{\mathbf{u}\in U}{\operatorname{argmin}}\ J\left(\hat{\mathbf{y}}(\mathbf{u})\right)$$

- or equivalently, using (*):

$$\mathbf{y}(\bar{\mathbf{u}}) \approx \hat{\mathbf{y}}(\hat{\mathbf{u}}^*)$$

- Aggressive Space Mapping ➔ solves for a solution of (**), using

$$\mathbf{p}_k(\mathbf{u}) := \mathbf{p}(\mathbf{u}_k) + \mathbf{p}'(\mathbf{u}_k)(\mathbf{u} - \mathbf{u}_k)$$

$$\hat{\mathbf{u}}_k = \mathbf{p}(\mathbf{u}_k) := \operatorname{argmin}_{\mathbf{u}\in U}\ ||\,\hat{\mathbf{y}}(\mathbf{u}) - \mathbf{y}(\mathbf{u}_k)\,||_Y^2$$

- ... and exploiting a Quasi-Newton iteration + Broyden rank-one approximation for ***p*'(*u*$_k$)**

[1] John W. Bandler et al. (1994); Echeverría and Hemker (2005)

Surrogate‘s Quality

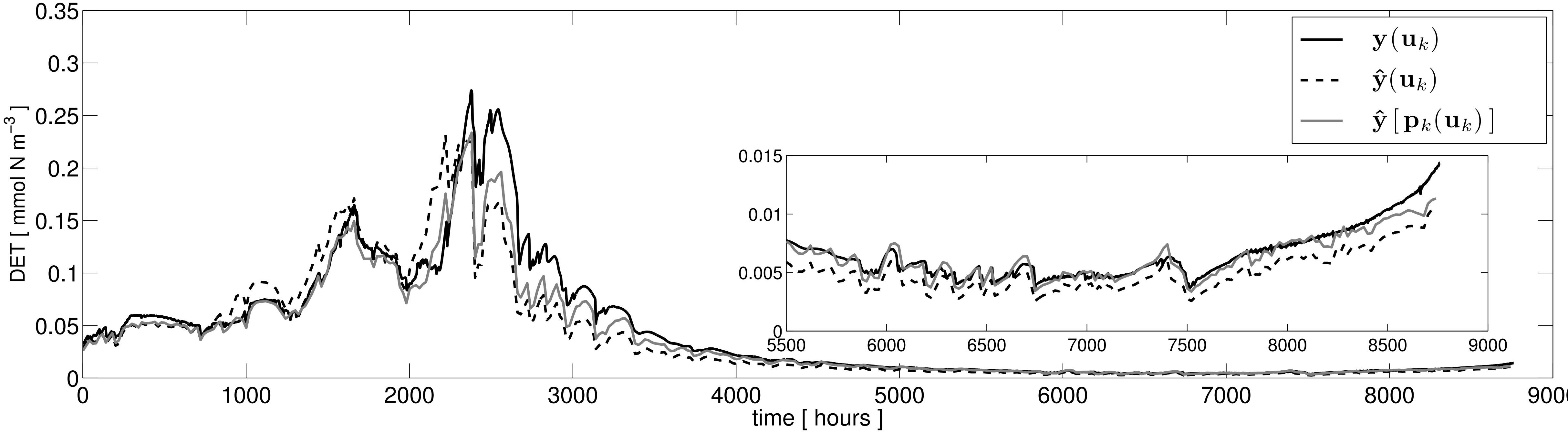

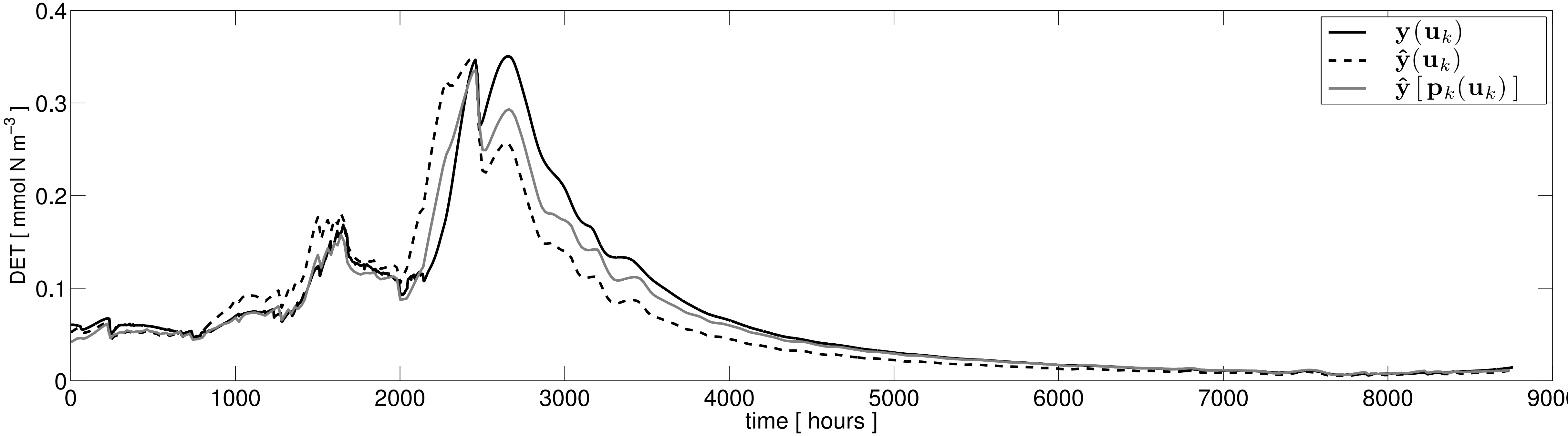

Figure: Fine and coarse model output y, $\hat{\mathbf{y}}$ as well as the aligned surrogate $s_k(u_k) = \hat{\mathbf{y}}(p_k(u_k))$ for the state detritus, at the same randomly chosen parameter vector u_k, at depths z ≈ 25m (top) and z ≈ 60 m (bottom).

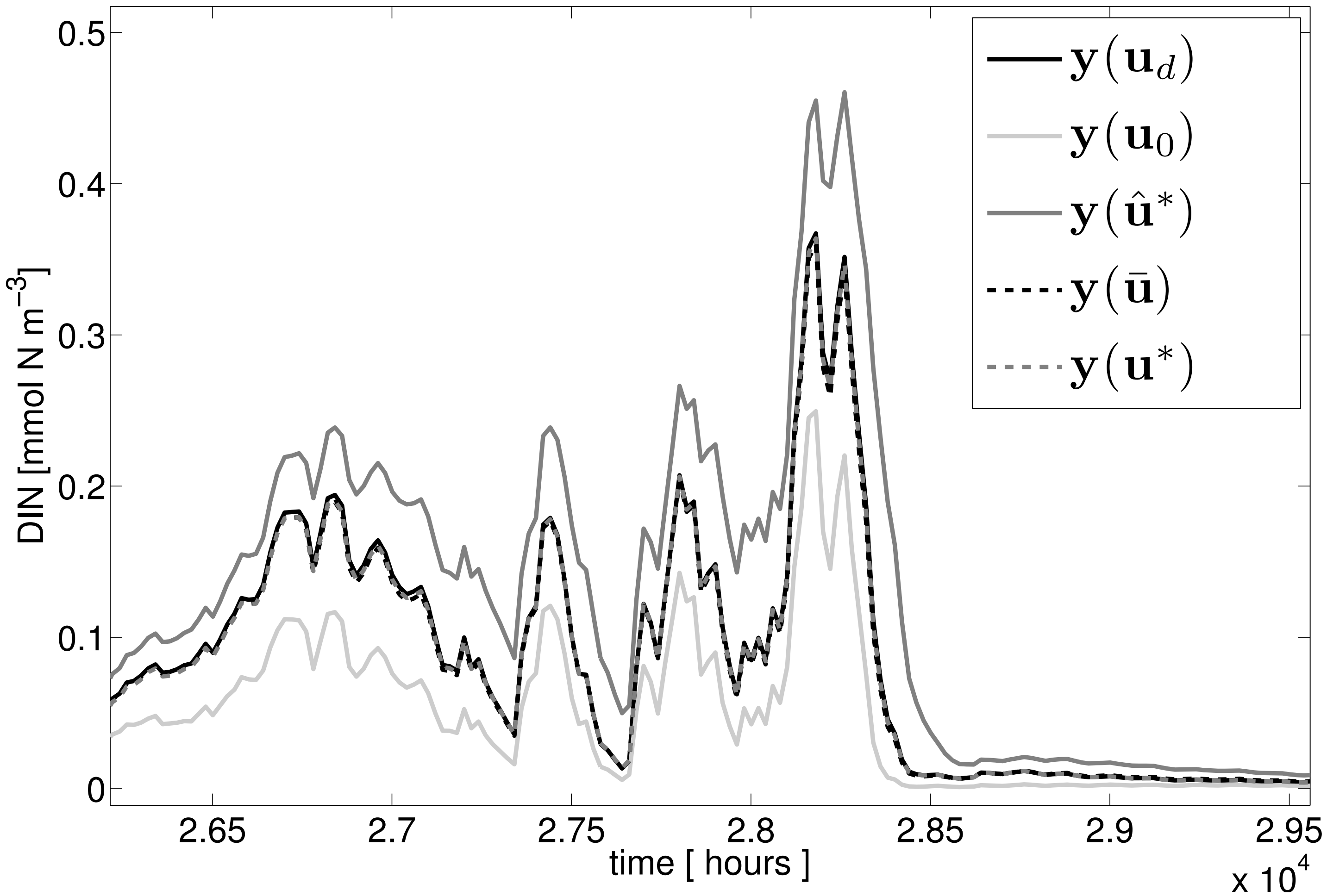

	J	C_i
$\mathbf{u}_0$	5.9e-03	
$\mathbf{u}^*$	1.6e-05	281
$\hat{\mathbf{u}}^*$	1.8e-03	19.95
$\bar{\mathbf{u}}$	5.0e-05	80.25
$\mathbf{u}_d$	57.54% reduction	

Figure:

(left) Fine model output y^β for dissolved inorganic nitrogen at depth $z \approx 2.68$ m. Shown are (from top to bottom):

(i) Synthetic target data, i.e., fine model output at randomly chosen parameters u_d,

(ii) fine model output at the initial value u_0,

(iii) at the coarse model optimum $\hat{u}^*$

(iv) at the result of the ASM algorithm $\bar{\mathbf{u}}$

(v) at the result of the direct fine model optimization u^*,

(right) Values of the cost function J, computational costs C_i (in terms of number of equivalent fine model evaluations)

Cost savings, when using ASM algorithm, are about 57% when compared to the direct fine model optimization.

- Coarse model response might be close to zero (and maybe even negative due to approximation errors) and a few magnitudes smaller than the fine one
- This leads to large (possibly negative) entries in the corresponding correction tensor A_k
- Such a correction tensor still ensures zero-order consistency
- But it may lead to (locally) poor approximation in the vicinity of u_k
- Still, the overall shape of the surrogate's response provides a reasonable approximation

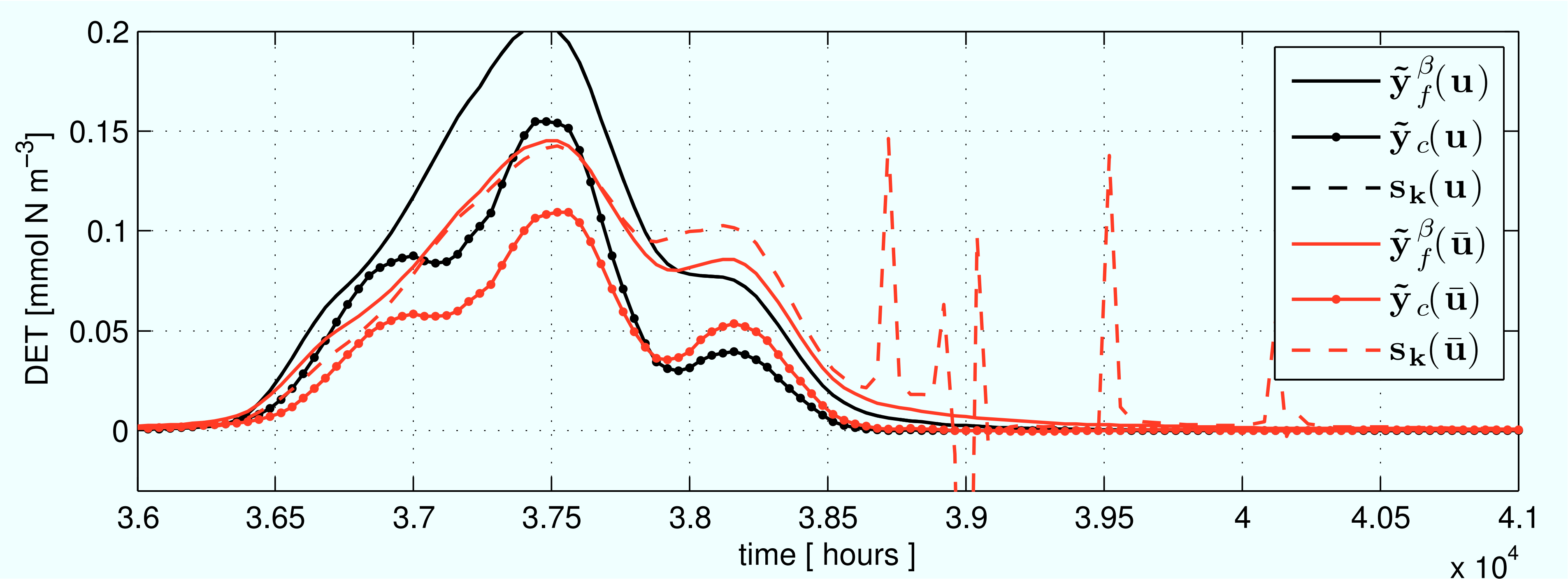

Figure: Surrogate's, fine and coarse model responses for the state detritus at depth $z \approx -2.68$ m, at one iterate u_k and in a vicinity $\bar{\mathbf{u}}_{\mathbf{k}}$.

- A few simple means can address these issues and further improve the accuracy of the surrogate's response as well as the performance of the optimization algorithm

$$(i)\ \mathbf{y}_c = \begin{cases} 0; & \text{if } \mathbf{y}_c \leq 0 \\ \mathbf{y}_c; & \text{else} \end{cases}, \quad (ii)\ \mathbf{a}_k = \begin{cases} a_{\text{ub}}; & \text{if } \mathbf{a}_k \geq a_{\text{ub}} \\ \mathbf{a}_k; & \text{else} \end{cases},$$

$$(iii)\ \mathbf{a}_k = 1 \text{ if } (\tilde{\mathbf{y}}_f^{\beta} \leq \epsilon \text{ and } \tilde{\mathbf{y}}_c \leq \epsilon),$$

- Large positive and negative peaks present in the surrogate responses using the original correction scheme are removed

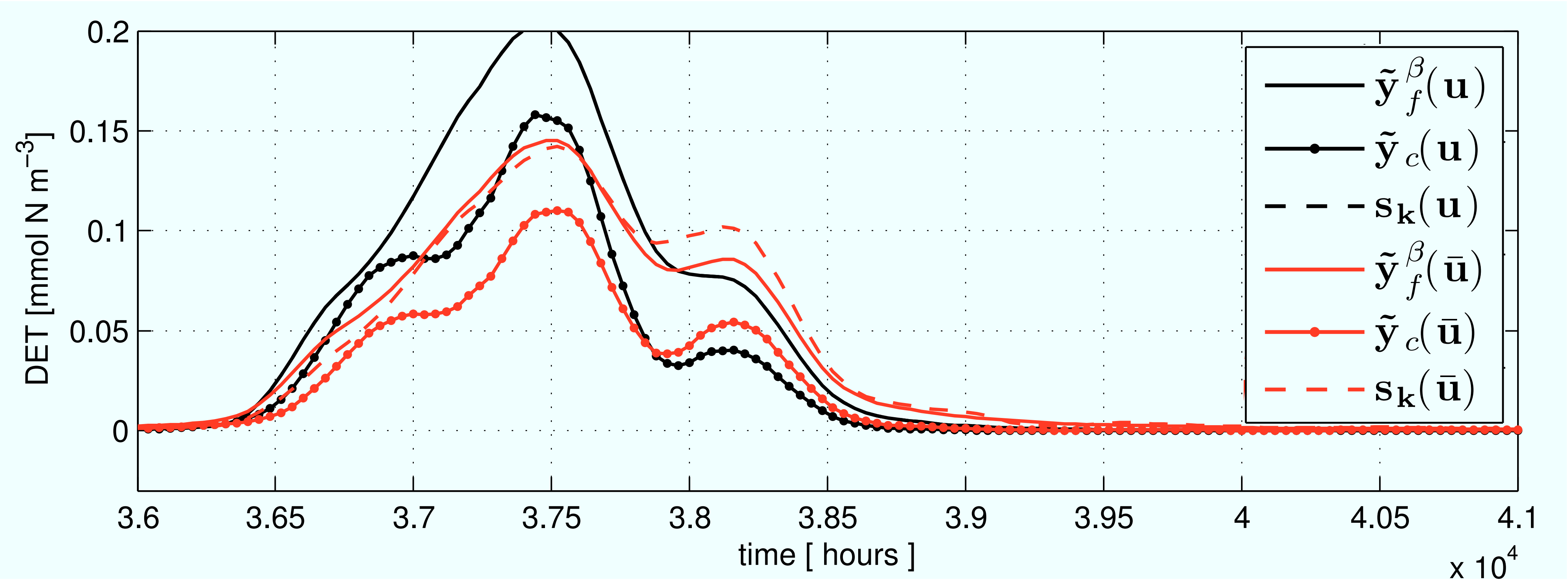

Figure: Same model responses as on previous slide.

1D NPZD Model

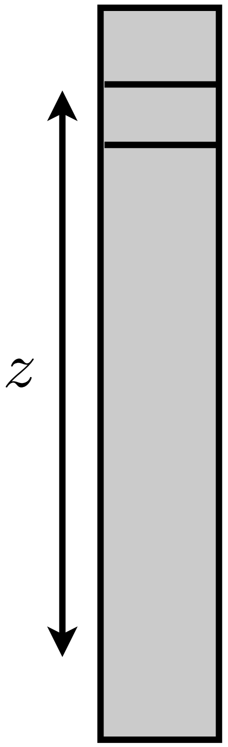

$$\frac{\partial y_i}{\partial t} = \mathrm{div}(\kappa \nabla y_i) - \mathrm{div}(v y_i) + q_i(y, \mathbf{u}), \quad i = 1, \ldots, n_t$$

$$\frac{\partial y_i}{\partial t} = \partial_z\,(\kappa\,\partial_z y_i) + q_i(y, \mathbf{u}), \quad i = 1, \ldots, 4,$$

$$\begin{aligned}
q_1(y,u) &= \Phi_m^z\, y_3 + \gamma_m\, y_4 - J(y_1, y_2, t, z)\, y_2, \\
q_2(y,u) &= J(y_1, y_2, t, z) y_2 - G(y_2, \epsilon, g)\, y_3 - \Phi_m^p\, y_2, \\
q_3(y,u) &= \beta\, G(y_2, \epsilon, g)\, y_3 - \Phi_m^z\, y_3 - \Phi_z^*\, (y_3)^2, \\
q_4(y,u) &= (1-\beta)\, G(y_2, \epsilon, g)\, y_3 + \Phi_m^p\, y_2 + \Phi_z^*\, (y_3)^2 \\
&\quad - \gamma_m\, y_4 - w_s\, \partial_z y_4.
\end{aligned}$$

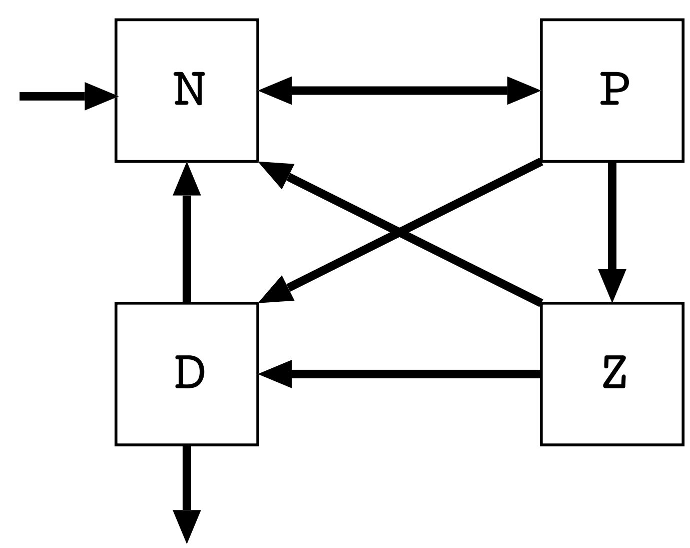

u_i	symbol	value/range	unit (d=86400 s)	parameter meaning
	C_{ref}	1.066	1	growth coefficient
	c	1	$^\circ C^{-1}$	growth coefficient
	R	6.625	1	molar carbon to nitrogen ratio (*Redfield ratio*)
	k_w	25	m^{-1}	PAR extinction length
u_1	β	[0, 1]	1	assimilation efficiency of zooplankton
u_2	μ_m	$\mathbb{R}_0^+$	d^{-1}	phytoplankton growth rate parameter
u_3	α	$\mathbb{R}_0^+$	$m^2W^{-1}d^{-1}$	slope of photosynthesis versus light intensity
u_4	Φ_m^z	$\mathbb{R}_0^+$	d^{-1}	zooplankton loss rate
u_5	κ	$\mathbb{R}_0^+$	$m^2(\text{mmol N})^{-1}$	light attenuation by phytoplankton
u_6	ϵ	$\mathbb{R}_0^+$	$m^6(\text{mmol N})^{-2}d^{-1}$	grazing encounter rate
u_7	g	$\mathbb{R}_0^+$	d^{-1}	maximum grazing rate
u_8	Φ_m^p	$\mathbb{R}_0^+$	d^{-1}	phytoplankton linear mortality
u_9	Φ_z^*	$\mathbb{R}_0^+$	$m^3(\text{mmol N})^{-1}d^{-1}$	zooplankton quadratic mortality
u_{10}	γ_m	$\mathbb{R}_0^+$	d^{-1}	detritus remineralization rate
u_{11}	k_N	$\mathbb{R}_0^+$	mmol Nm^{-3}	half saturation for NO_3 uptake
u_{12}	w_s	$\mathbb{R}_0^+$	m d^{-1}	detritus sinking velocity

- Discretized model equation of the high-fidelity model (with state variable y):

$$\underbrace{\left[I - \tau A_j^{\text{diff}}\right]}_{:=B_j^{\text{diff}}} \mathbf{y}_{j+1} = \underbrace{\left[I + \tau A^{\text{sink}}\right]}_{:=B^{\text{sink}}} B_j^Q \circ B_j^Q \circ B_j^Q \circ B_j^Q(\mathbf{y}_j),$$

$$B_j^Q(\mathbf{y}_j) \quad := \quad \left[\mathbf{y}_j + \frac{\tau}{4} Q_j(\mathbf{y}_j)\right] \qquad \mathbf{y}_j = (y_{ji})_{i=1,\dots,I}, \quad j = 1, \dots, M$$

(M = # of discrete temporal points of the fine model, I = # of discrete spatial points)

- In the original discrete model (high-fidelity model) the time step **τ** is chosen as one hour

- The low-fidelity model (with state variable ŷ) is obtained by using a coarser time discretization with

$$\hat{\tau} = \beta\tau$$

(with a coarsening factor **β** ∊ N \ {0, 1}, while keeping the spatial discretization fixed)

Institut für Informatik

future ocean KIEL MARINE SCIENCES

- Adjust/identify model parameters u such that given measurement data y_d is matched by the model output y(u)
- The mathematical task thus can be classified as a least-squares type optimization or inverse problem
- The opt. process requires a substantial number of (typically expensive) function evaluations
- Methods that aim at reducing the optimization cost (e.g. surrogate-based optimization), are highly desirable

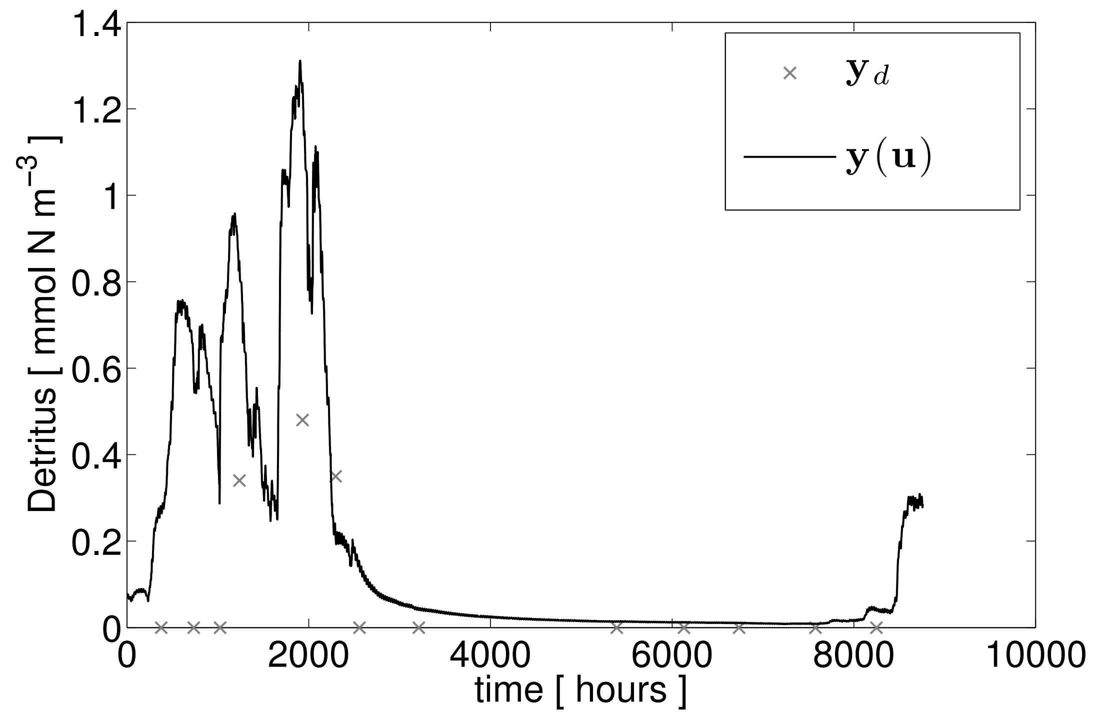

Figure: Model output $y^{(D)}$ (detritus) and target data y_d for one year at depth $z \simeq -25$ m.

$$\min_{\mathbf{u} \in U_{ad}} J(\,\mathbf{y}(\mathbf{u})\,)$$

$$J(\,\mathbf{y}\,) := \|\,\mathbf{y} - \mathbf{y}_d\,\|^2,$$

$$U_{ad} := \{\mathbf{u} \in \mathbb{R}^n : \mathbf{b}_l \le \mathbf{u} \le \mathbf{b}_u\}, \mathbf{b}_l, \mathbf{b}_u \in \mathbb{R}^n, \; \mathbf{b}_l < \mathbf{b}_u$$

- Initial boundary value problem (IBVP) for a system of time-dependent partial differential or differential algebraic equations (PDEs/DAEs) of the following form:

$$E\,\frac{\partial y}{\partial t} = f\left(y, \frac{\partial y}{\partial x_i}, \frac{\partial^2 y}{\partial x_i \partial x_j}, u\right) \quad \text{in } I \times \Omega$$

$$y(t_0, x) = y_{init} \quad \text{in } \Omega$$

$$By = 0 \quad \text{on } I \times \Gamma,$$

- Ocean circulation models (Navier-Stokes equations):
  - y may consist for example of the velocity field, pressure, temperature, salinity

- Initial boundary value problem (IBVP) for a system of time-dependent partial differential or differential algebraic equations (PDEs/DAEs) of the following form:

$$E\,\frac{\partial y}{\partial t} = f\left(y, \frac{\partial y}{\partial x_i}, \frac{\partial^2 y}{\partial x_i \partial x_j}, u\right) \quad \text{in } I \times \Omega$$

$$y(t_0, x) = y_{init} \quad \text{in } \Omega$$

$$By = 0 \quad \text{on } I \times \Gamma,$$

- Ocean circulation models (Navier-Stokes equations):
  - y may consist for example of the velocity field, pressure, temperature, salinity
- Marine ecosystem model:
  - The matrix E can be set to the identity and thus omitted
  - here, the rhs f(y, u) contains

(a) the transport (diffusion,advection) and nonlinear coupling of so-called biogeochemical tracers such as phyto-/ zooplankton etc.

(b) the ocean model data: precalculated („offline“) or obtained simultaneously („online“)

- Choosing the time step too large could lead to a numerically unstable scheme

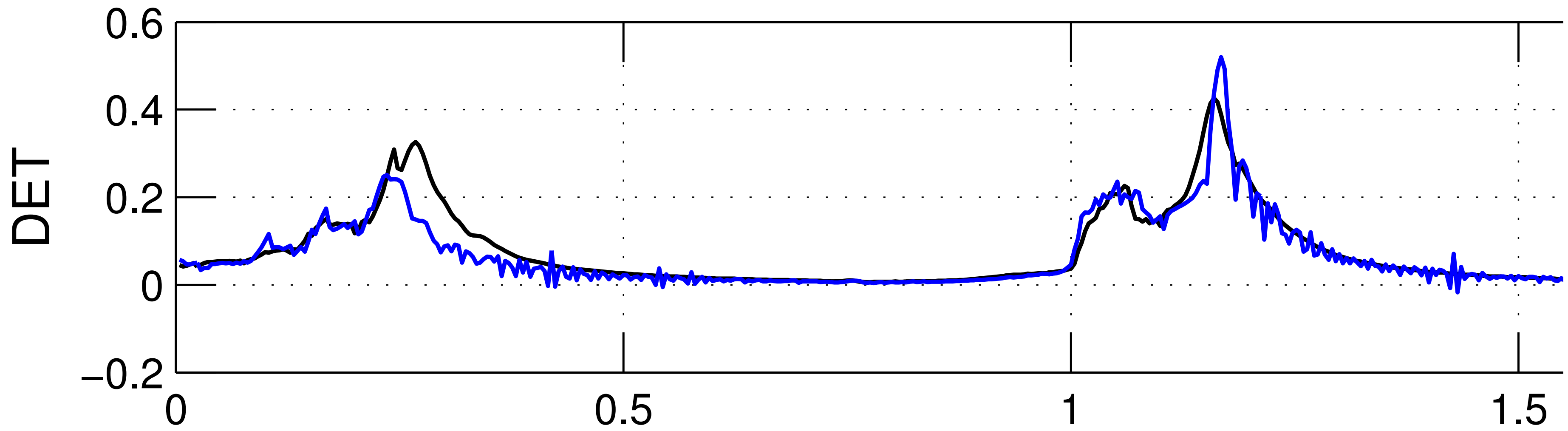

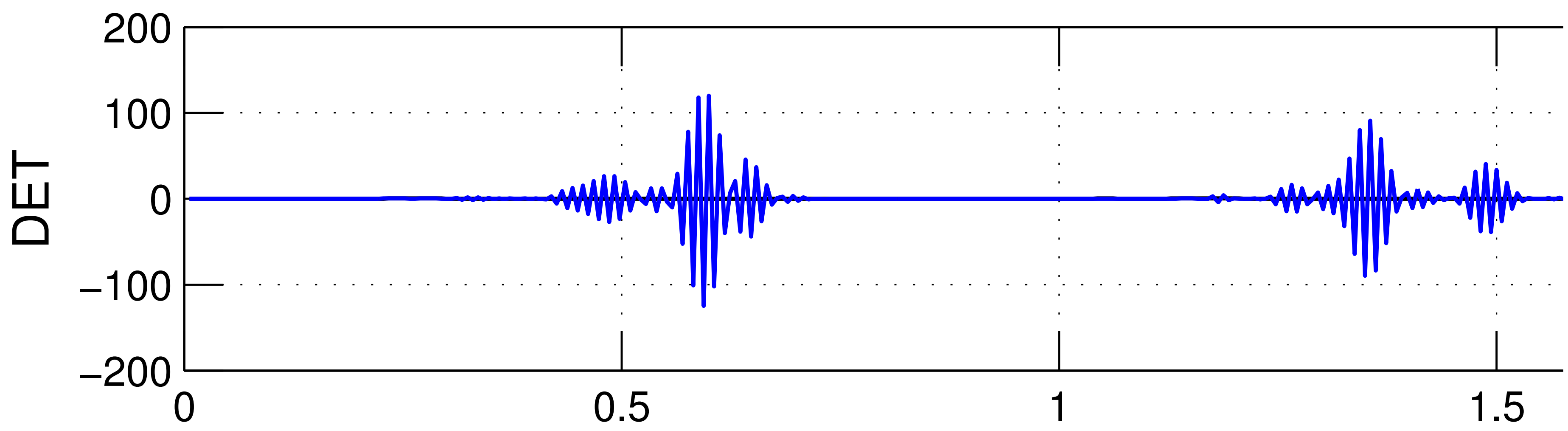

Institut für Informatik

future ocean
KIEL MARINE SCIENCES

- The condition of stability seems to be dominated by the vertical advective transport

  ➔ yielding a dependance of the time step on the ratio h / v („standard“ CFL condition)

  (h = spatial step-size, v = here, sinking velocity)

$$\underbrace{\left[I_{4n\times 4n} - \tau \tilde{A}_j^{\text{diff}}\right]}_{=:\tilde{B}_j^{\text{diff}}} \mathbf{y}_{j+1} = \underbrace{\left[I_{4n\times 4n} + \tau \tilde{A}^{\text{sink}}\right]}_{=:\tilde{B}^{\text{sink}}} \tilde{B}_j^Q \circ \tilde{B}_j^Q \circ \tilde{B}_j^Q \circ \tilde{B}_j^Q(\mathbf{y}_j),$$

$$\tilde{B}_j^Q(\mathbf{y}_j) \quad := \quad \left[\mathbf{y}_j + \frac{\tau}{4} Q_j(\mathbf{y}_j)\right]$$

- I investigate a numerical scheme of the following form

  (Grigorieff, Numerische Mathematik II für Ingenieure, St - 1)

$$\mathbf{y}_{j+1} = C_j\, \mathbf{y}_j, \quad C_j = C_j(\tau, \triangle z_i)_{i=1,\ldots,n}, \quad j = 0, 1, \ldots, m-1.$$

- One directly obtains the following description:

$$\mathbf{y}_j = \left(\prod_{l=0}^{m-1} C_l\right) \mathbf{y}_0$$

$$\curvearrowright ||\,\mathbf{y}_j\,|| \leq K\,||\,\mathbf{y}_0\,||, \quad K := \prod_{l=0}^{m-1} ||\,C_l\,||.$$

- The numerical scheme is stable if for K it holds that

$$\sup\{\,K(\tau, (\triangle z_i)_{i=1,\ldots,n}),\ \tau \to 0,\ (\triangle z_i)_{i=1,\ldots,n} \to 0\} < \infty.$$

- It follows this in turn is satisfied if

$$||\,C_j(\tau, \triangle z_i)_{i=1,\ldots,n}\,|| \leq 1, \quad j = 0, \ldots, m-1.$$

$$||\,C_j(\tau, \triangle z_i)_{i=1,\ldots,n}\,|| \leq 1 + L\tau, \quad j = 0, \ldots, m-1$$

- I linearize the nonlinear operator in the discretization scheme of the NPZD model

$$\tilde{B}_j^Q \approx \mathbf{y}_j + \frac{\tau}{4}\left[Q_j(0) + J_{Q_j}(0)\,\mathbf{y}_j\right] = \underbrace{\left[I_{4n\times 4n} + \frac{\tau}{4} J_{Q_j}(0)\right]}_{=:L_j}\mathbf{y}_j, \quad Q_j(0) = 0.$$

$$\mathbf{y}_j = \left(\prod_{l=0}^{m-1} D_l\right)\mathbf{y}_0, \quad D_l =: (\tilde{B}_l^{diff})^{-1}\,\tilde{B}^{sink}\,L_l^4$$

$$\curvearrowright ||\,\mathbf{y}_j\,|| \leq \left(\prod_{l=0}^{m-1} \left|\left|\,(\tilde{B}_l^{diff})^{-1}\,\right|\right|\right) \left|\left|\,\tilde{B}^{sink}\,\right|\right| \left(\prod_{l=0}^{m-1} ||\,L_l\,||^4\right).$$

- Accordingly, a suffiient criterion for stability of the linearized scheme in the NPZD model is

$$\left|\left|\,(\tilde{B}_j^{diff})^{-1}\,\right|\right| \leq 1, \quad \left|\left|\,\tilde{B}^{sink}\,\right|\right| \leq 1, \quad ||\,L_j\,|| \leq 1, \quad j = 0,\ldots,m-1,$$

- Independence of the numerical stability of quantities in the numerical model such as the mesh discretization is clearly desirable
- Most importantly in the context of surrogate-based optimization, this would allow to exploit an even coarser resolution to create a physically yet reasonable coarse model
- I furthermore investigated a modification of the originally exploited explicit time integration approach for the vertical advection by exploiting an implicit Euler scheme instead
- It turned out that this enhancement allows to obtain a numerically stable solution without restrictions to the mesh discretization and the vertical velocity

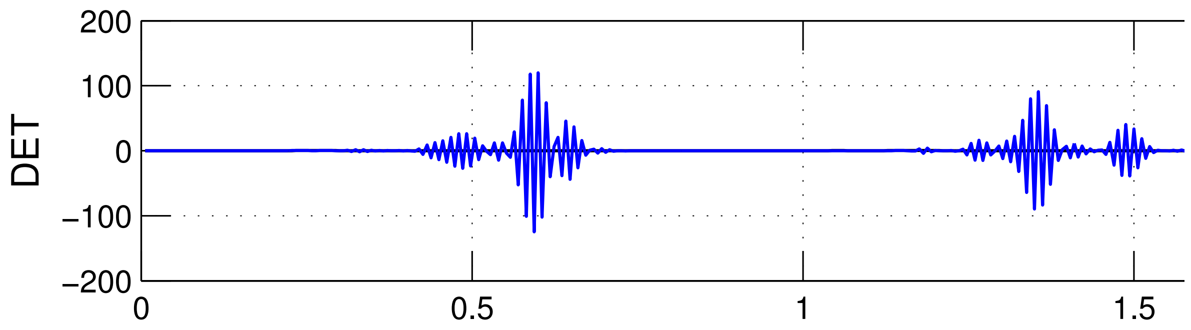

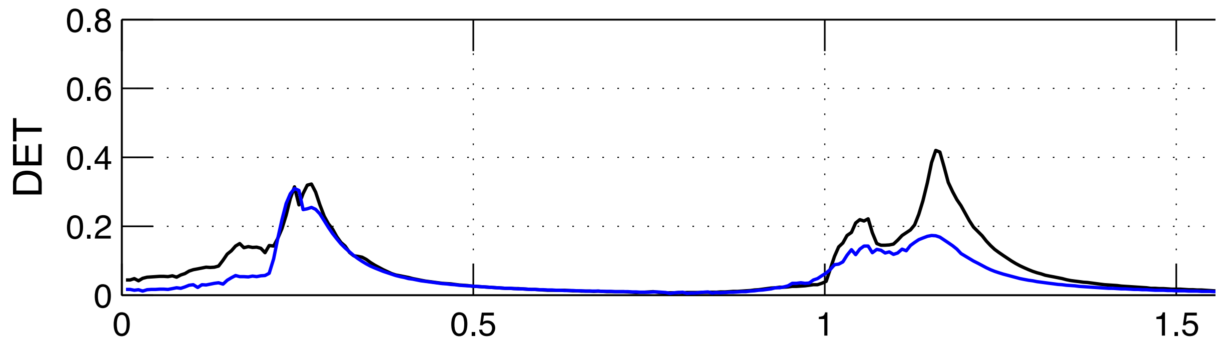

- Explicit vs. implicit Euler time-stepping scheme

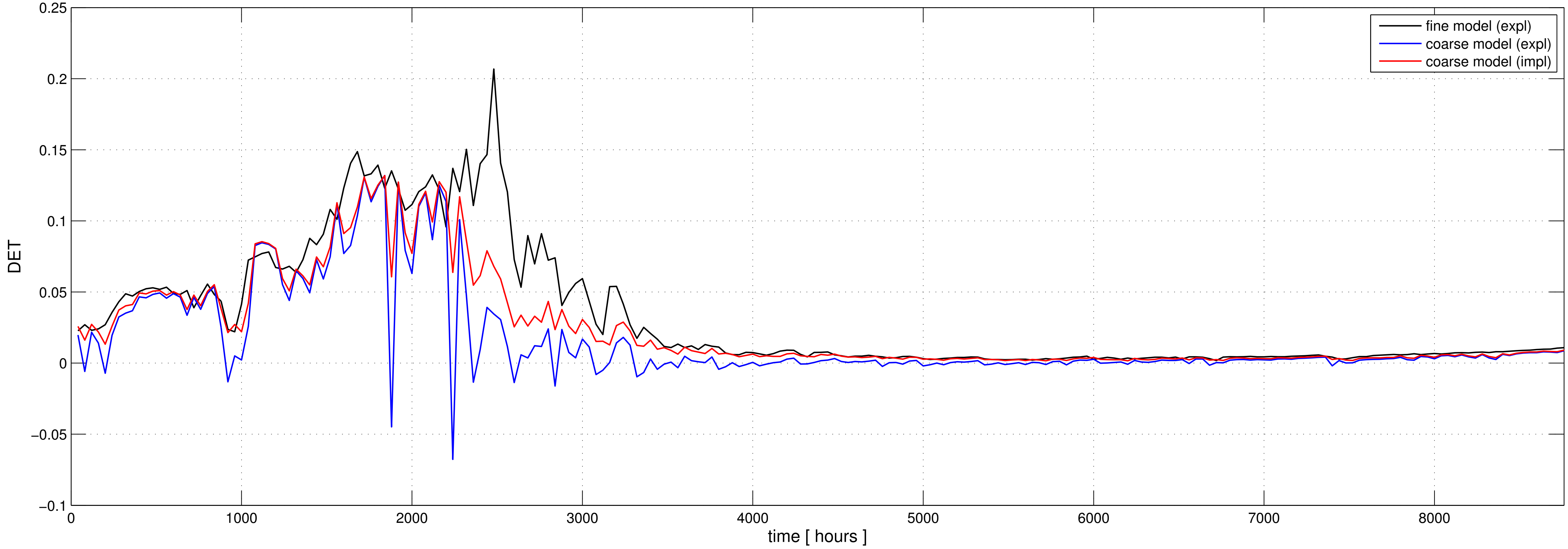

References

- N. V. Queipo, R. T. Haftka, W. Shyy, T. Goel, R. Vaidyanathan, and P. K. Tucker, “Surrogate-based analysis and optimization,” Prog. Aerosp. Sci., vol. 41, no. 1, pp. 1 – 28, 2005
- A. I. Forrester and A. J. Keane, “Recent advances in surrogate-based optimization,” Prog. Aerosp. Sci., vol. 45, no. 1-3, pp. 50 – 79, 2009
- J. W. B, Q. S. Cheng, S. A. Dakroury, A. S. Mohamed, M. H. Bakr, K. Madsen, and J. Søndergaard, “Space mapping: The state of the art,” IEEE T. Microw. Theory., vol. 52, no. 1, 2004
- S. Koziel, J. Bandler, and Q. Cheng, “Robust trust-region space-mapping algorithms for microwave design optimization,” IEEE T. Microw. Theory., vol. 58, pp. 2166 –2174, Aug. 2010.
- Kriest, I., Khatiwala, S., Oschlies, A., 2010. Towards an assessment of simple global marine biogeochemical models of different complexity. Progress In Oceanography 86, 337–360.
- Parekh, P., Follows, M.J., Boyle, E.A., 2005. Decoupling iron and phosphate in the global ocean. Global Biogeochemical Cycles 19.
- A. Oschlies and V. Garcon, “An eddy-permitting coupled physical-biological model of the north atlantic. 1. sensitivity to advection numerics and mixed layer physics,” Global Biogeochem. Cy., vol. 13, pp. 135– 160, 1999.
- Prieß M., Koziel S., Slawig T.: Improved Surrogate-Based Optimization of Climate Model Parameters Using Response Correction. Conference Proceedings, Int. Conf. Simulation and Modeling Methodologies, Technologies and Appl., SIMULTECH 2011, Noordwijkerhout, The Netherlands, July 29–31, pp. 449–457 (2011)
- Prieß, M., Koziel, S., Slawig, T., 2011b. Improved surrogate-based optimization of climate model parameters using response correction, Int. Conf. Simu- lation and Modeling Methodologies, Technologies and Appl., SIMULTECH 2011, Noordwijkerhout, The Netherlands. pp. 449–457.
- Prieß, M., Koziel, S., Slawig, T., 2011c. Surrogate-based optimization of climate model parameters using response correction. Journal of Computational Science , 1877–7503.
- Piwonski, J., Slawig, T., 2011. Metos3d: A Marine Ecosystem Toolkit for Optimization and Simulation. CAU Kiel, Institut für Informatik. http: //www.informatik.uni-kiel.de/co2/software/meteos3d.
- Prieß M., Slawig T.: Aggressive Space Mapping for the Optimization of a Marine Ecosystem Model. International Journal of Mathematical Modeling and Numerical Optimization 3, 98-116 (2012)

1D NPZD model: Numerical results

Verification by model generated data

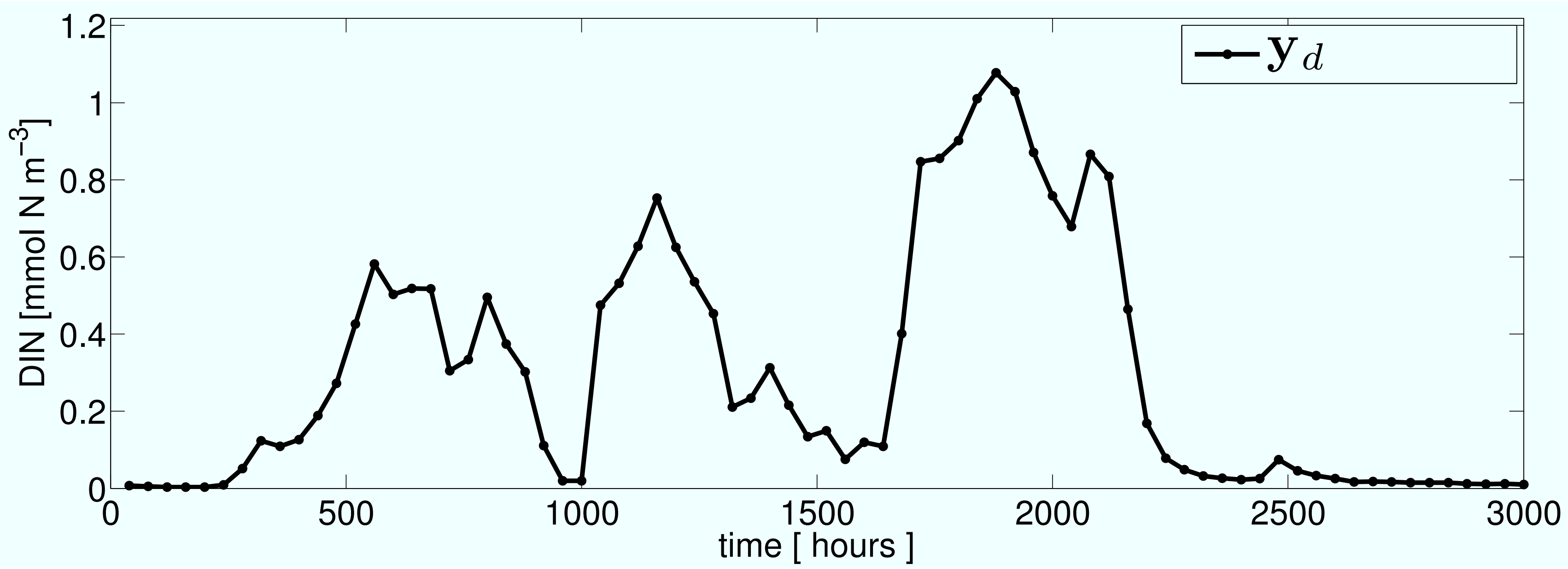

Figure: Fine, coarse model and surrogate optimization: Optimal solutions.

Verification by model generated data

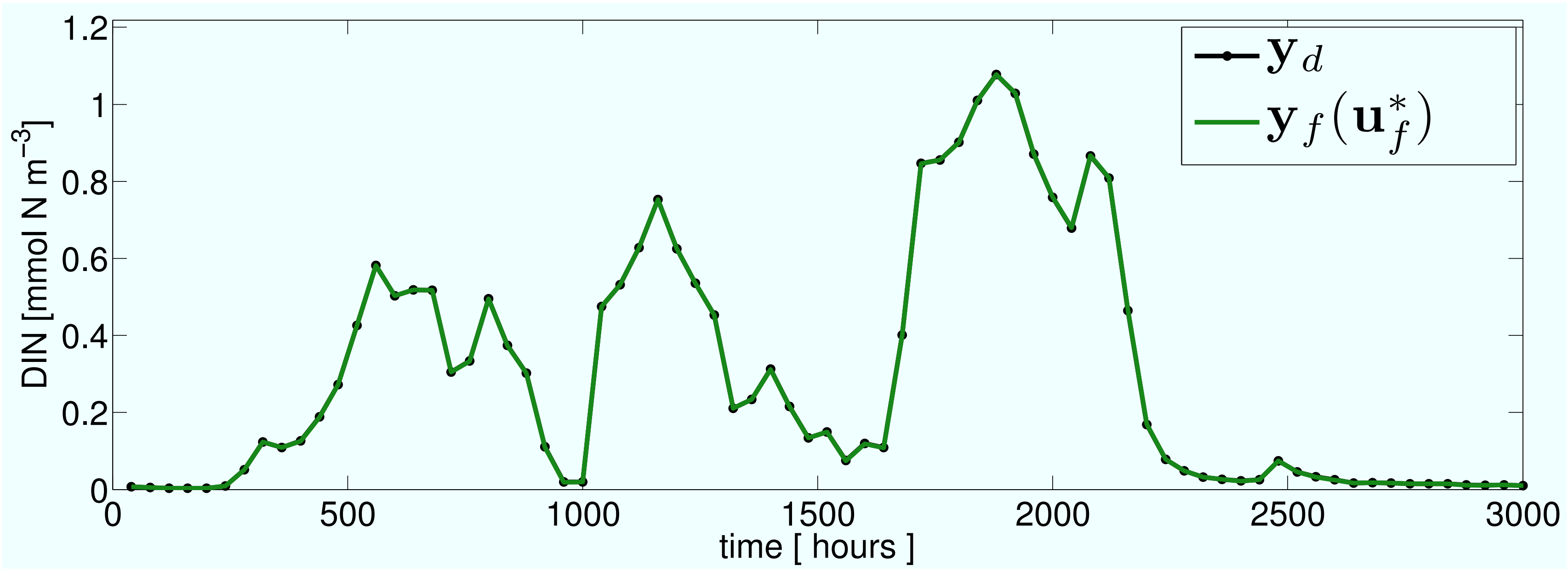

Figure: Fine, coarse model and surrogate optimization: Optimal solutions.

Institut für Informatik

future ocean
KIEL MARINE SCIENCES

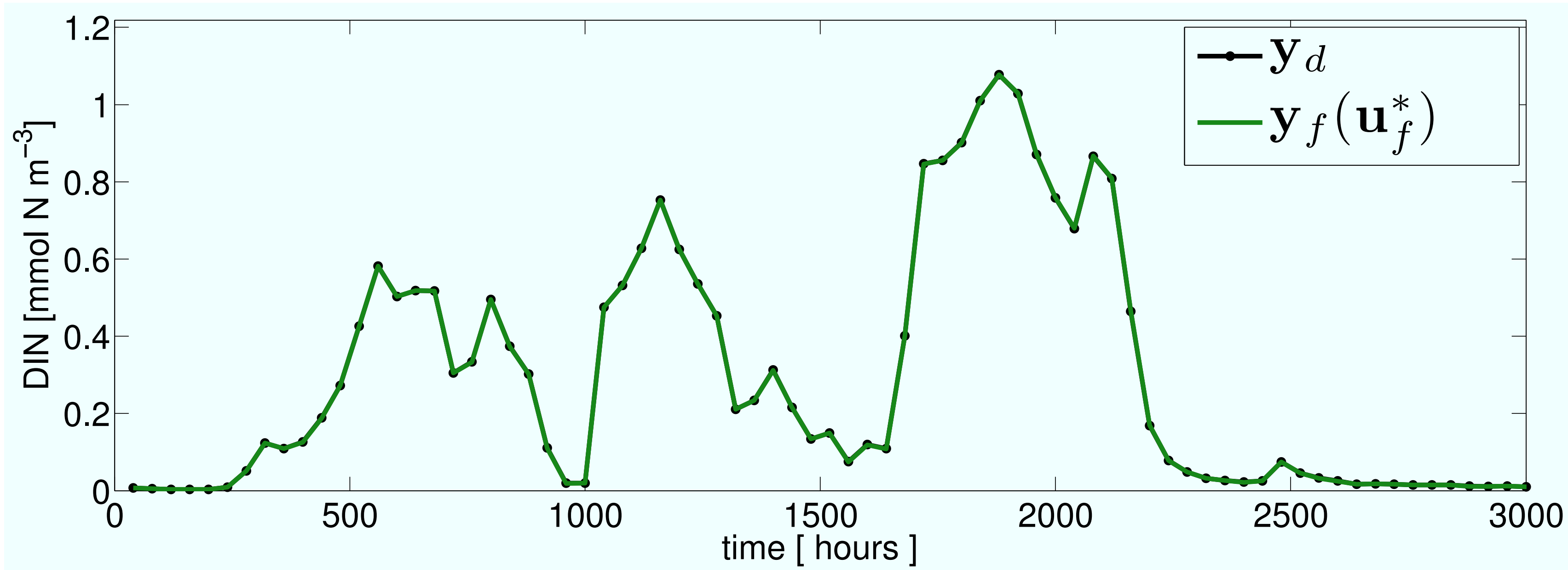

Figure: Fine, coarse model and surrogate optimization: Optimal solutions.

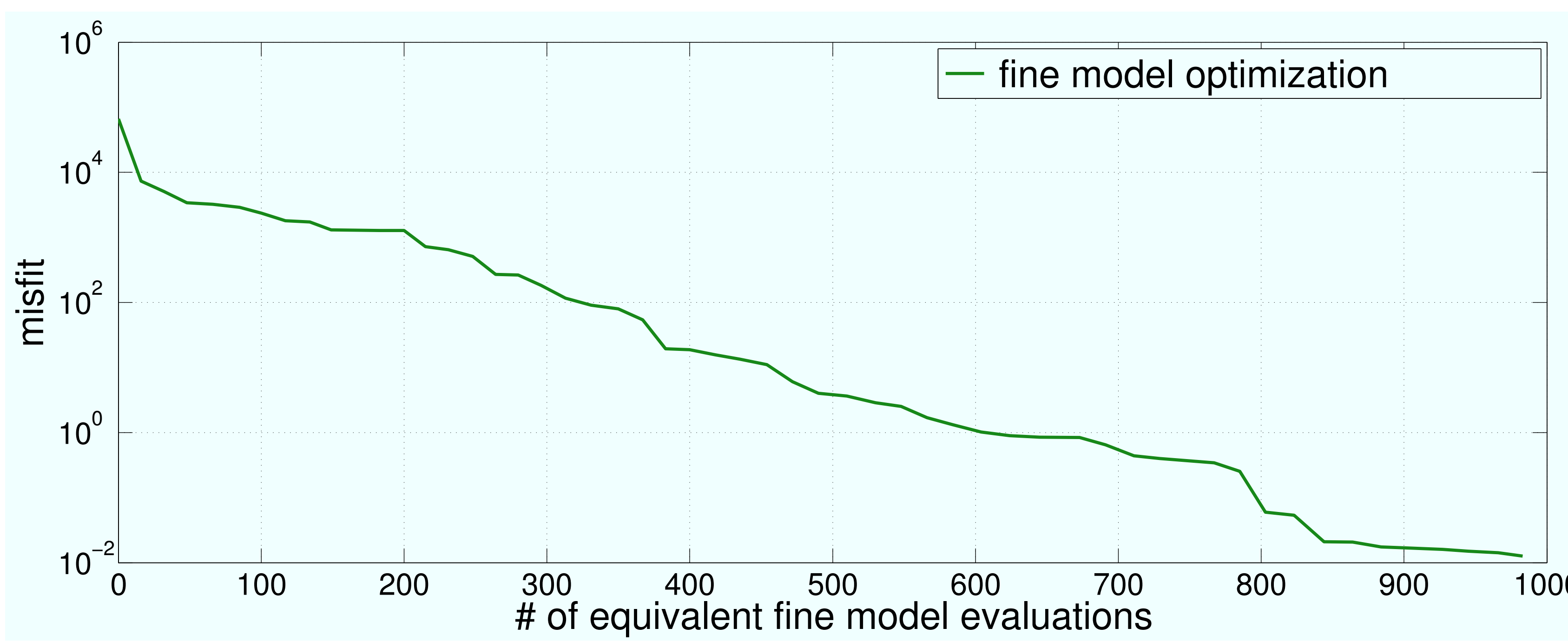

Figure: Convergence history of cost function.

1D NPZD model: Numerical results

Verification by model generated data

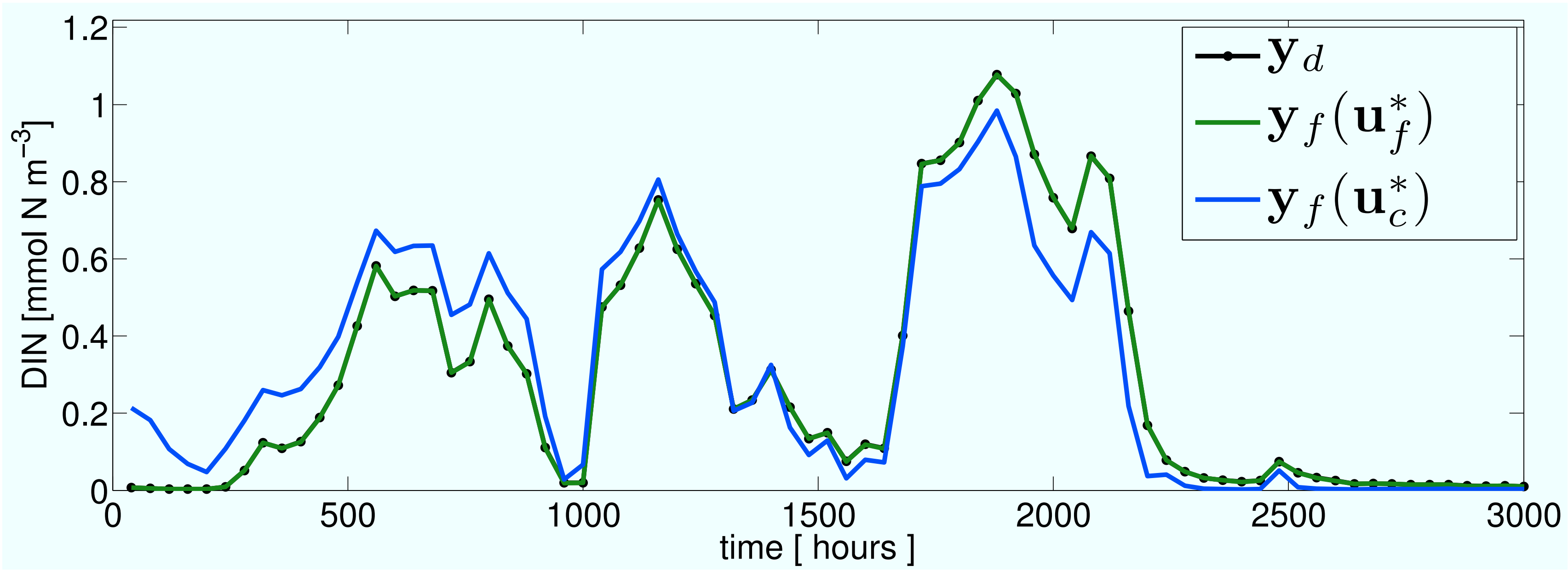

Figure: Fine, coarse model and surrogate optimization: Optimal solutions.

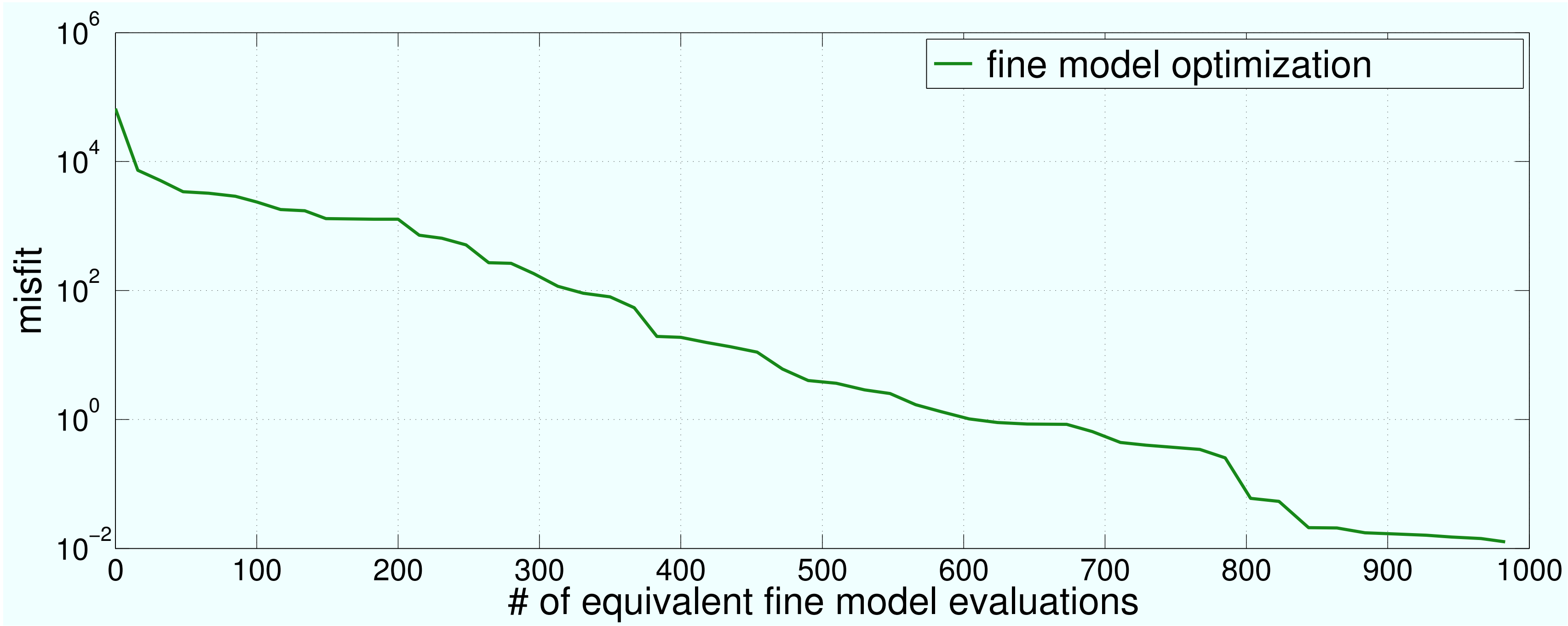

Figure: Convergence history of cost function.

1D NPZD model: Numerical results

Verification by model generated data

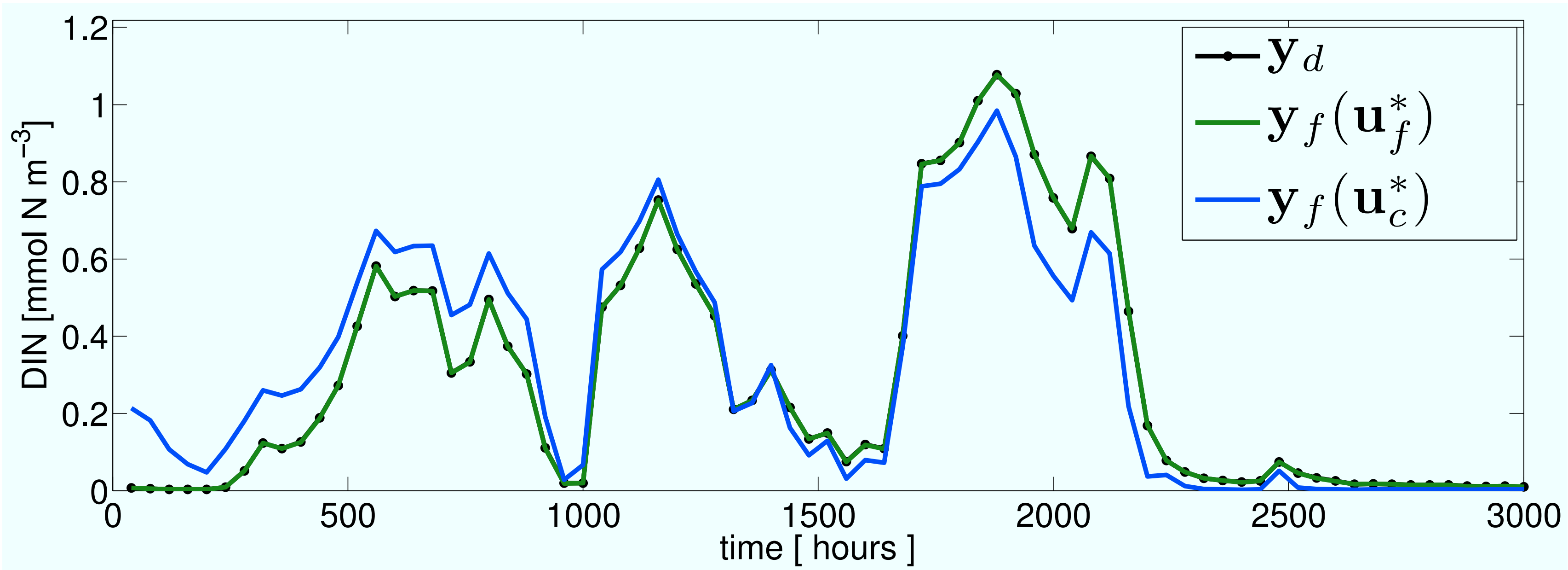

Figure: Fine, coarse model and surrogate optimization: Optimal solutions.

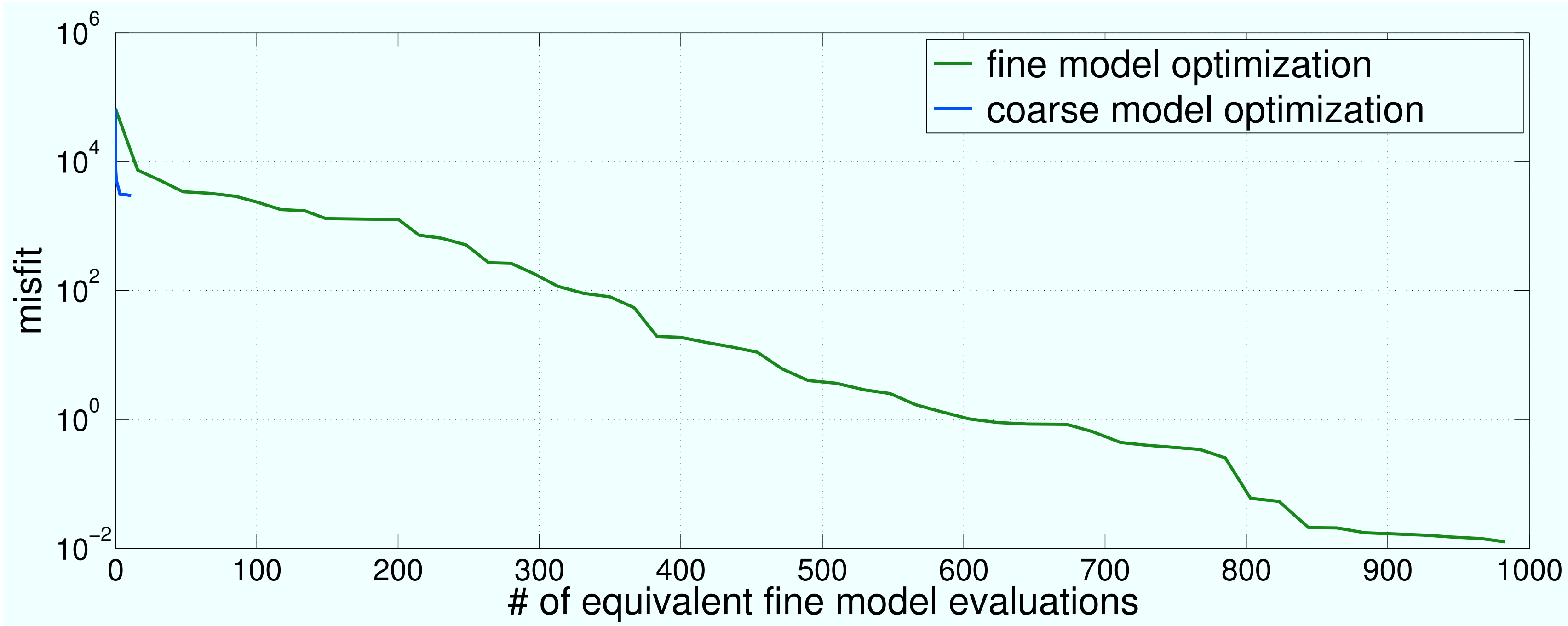

Figure: Convergence history of cost function.

1D NPZD model: Numerical results

Verification by model generated data

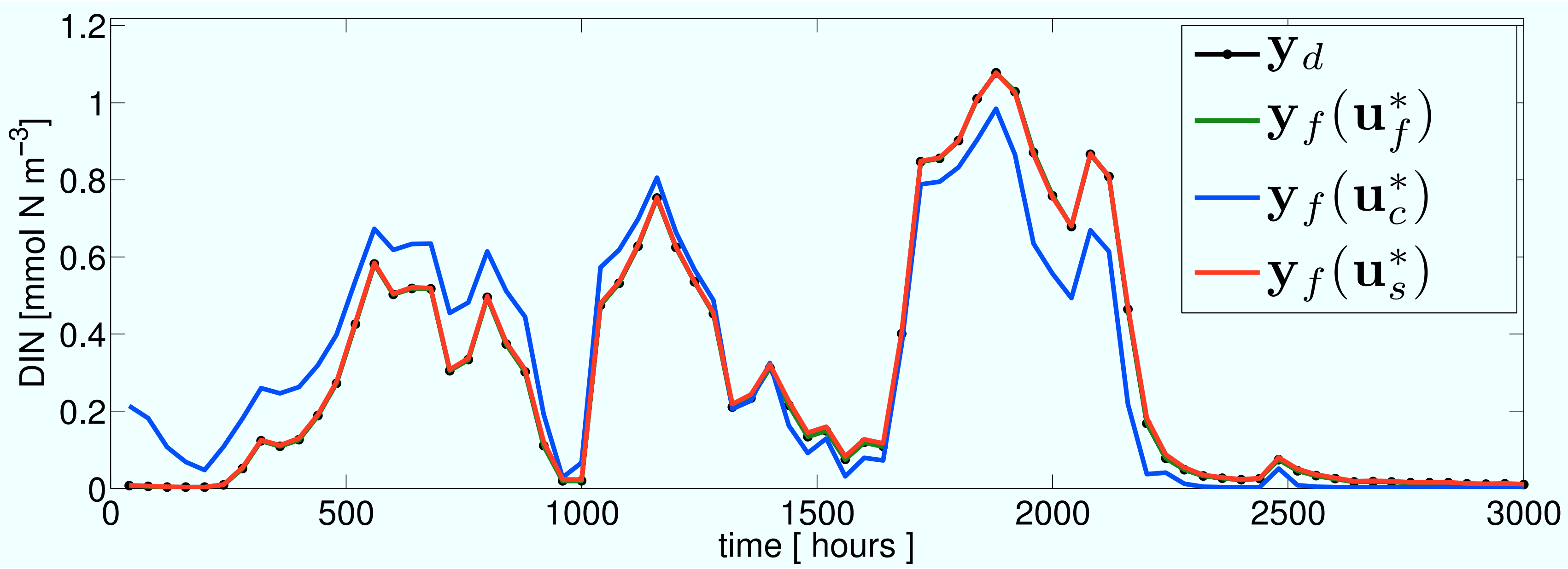

Figure: Fine, coarse model and surrogate optimization: Optimal solutions.

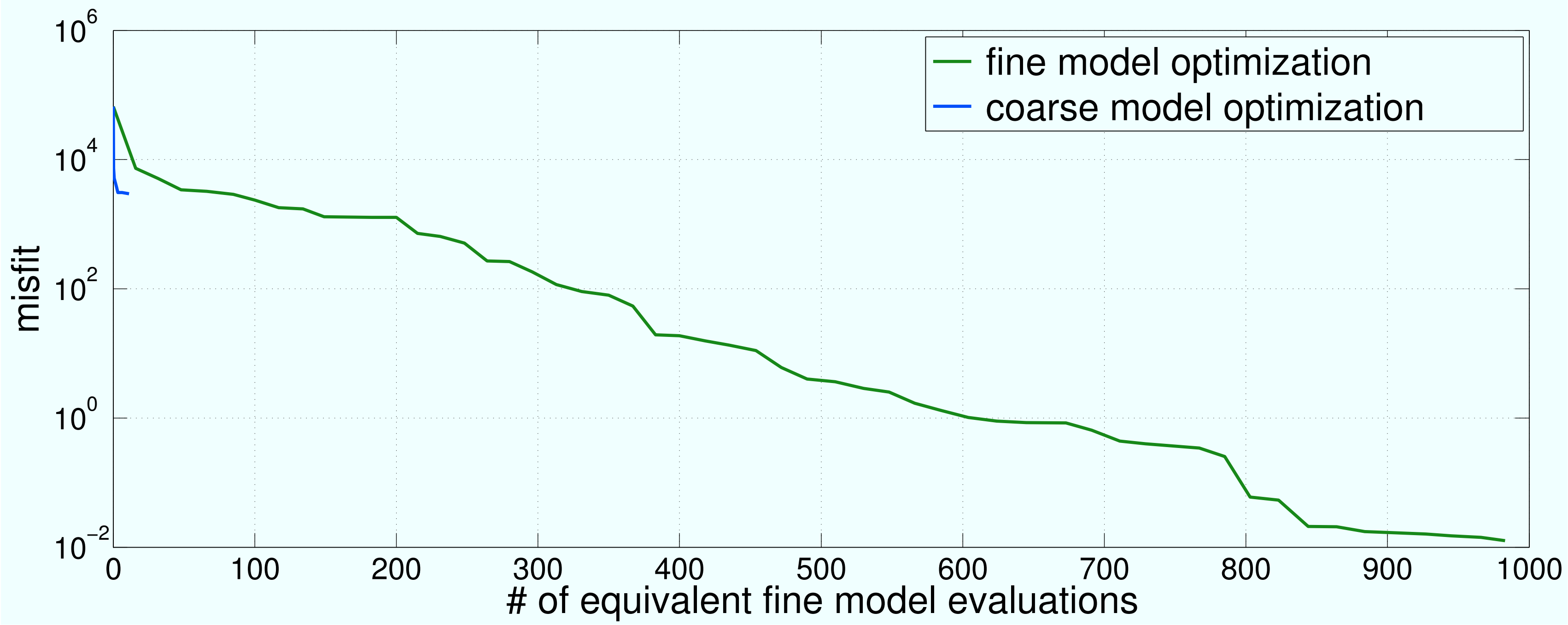

Figure: Convergence history of cost function.

1D NPZD model: Numerical results

Verification by model generated data

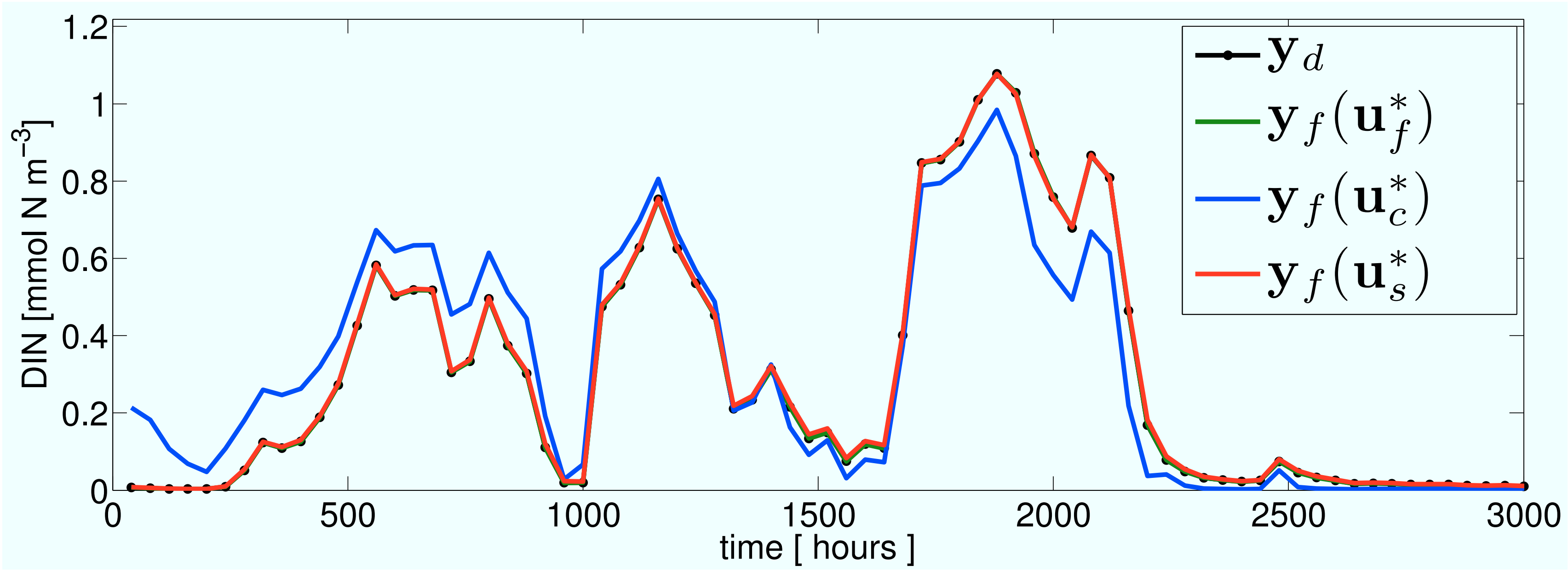

Figure: Fine, coarse model and surrogate optimization: Optimal solutions.

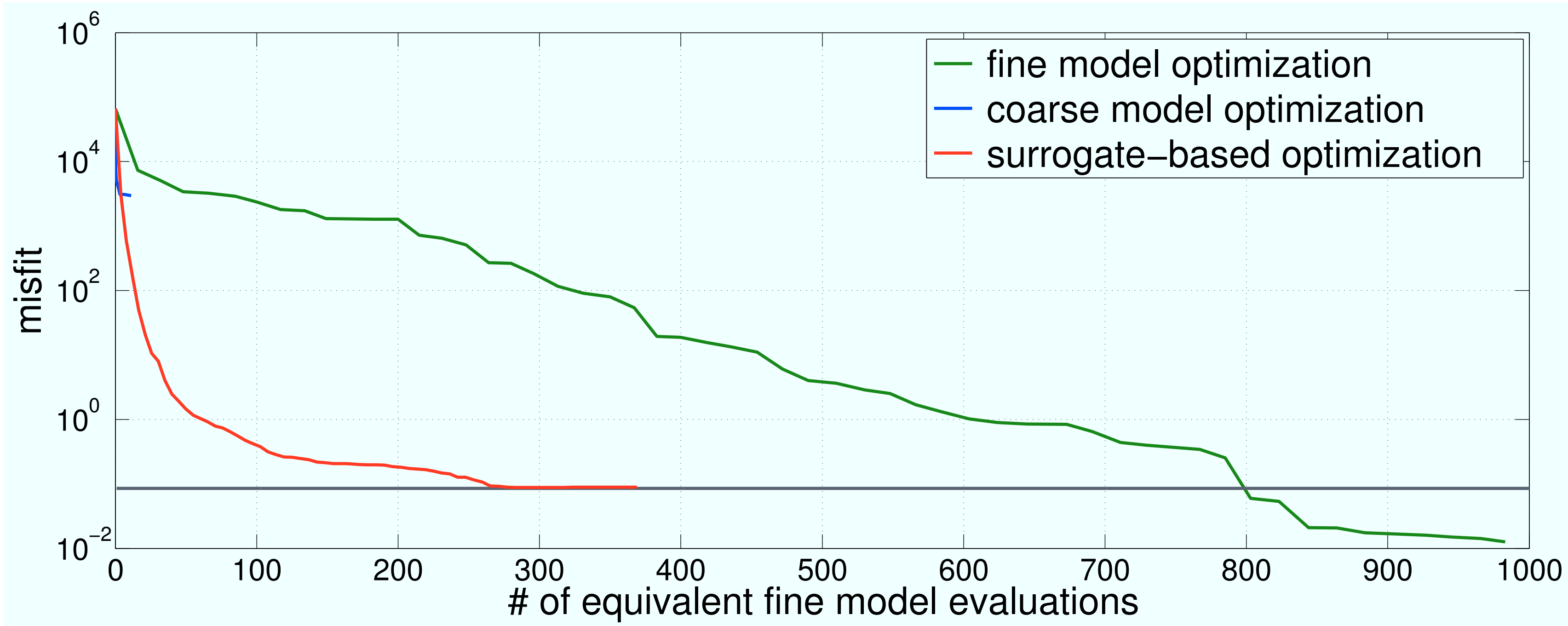

Figure: Convergence history of cost function.

1D NPZD model: Numerical results

Verification by model generated data

Institut für Informatik

future ocean
KIEL MARINE SCIENCES

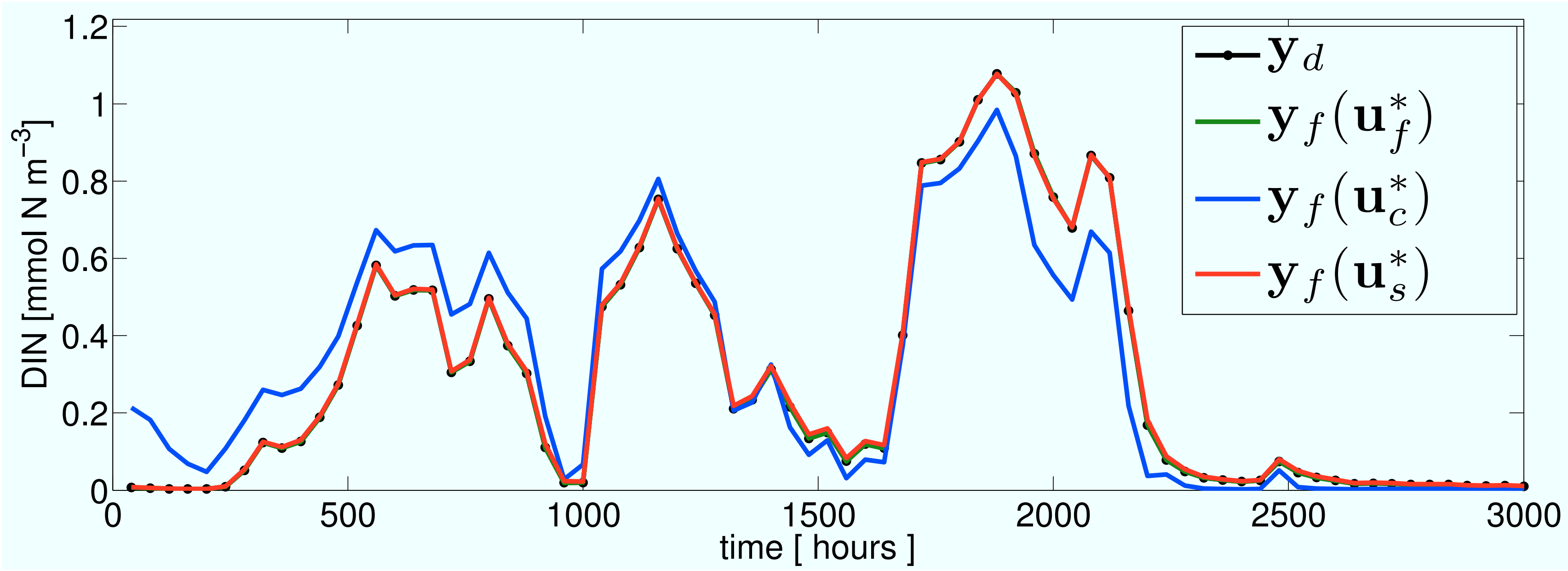

Figure: Fine, coarse model and surrogate optimization: Optimal solutions.

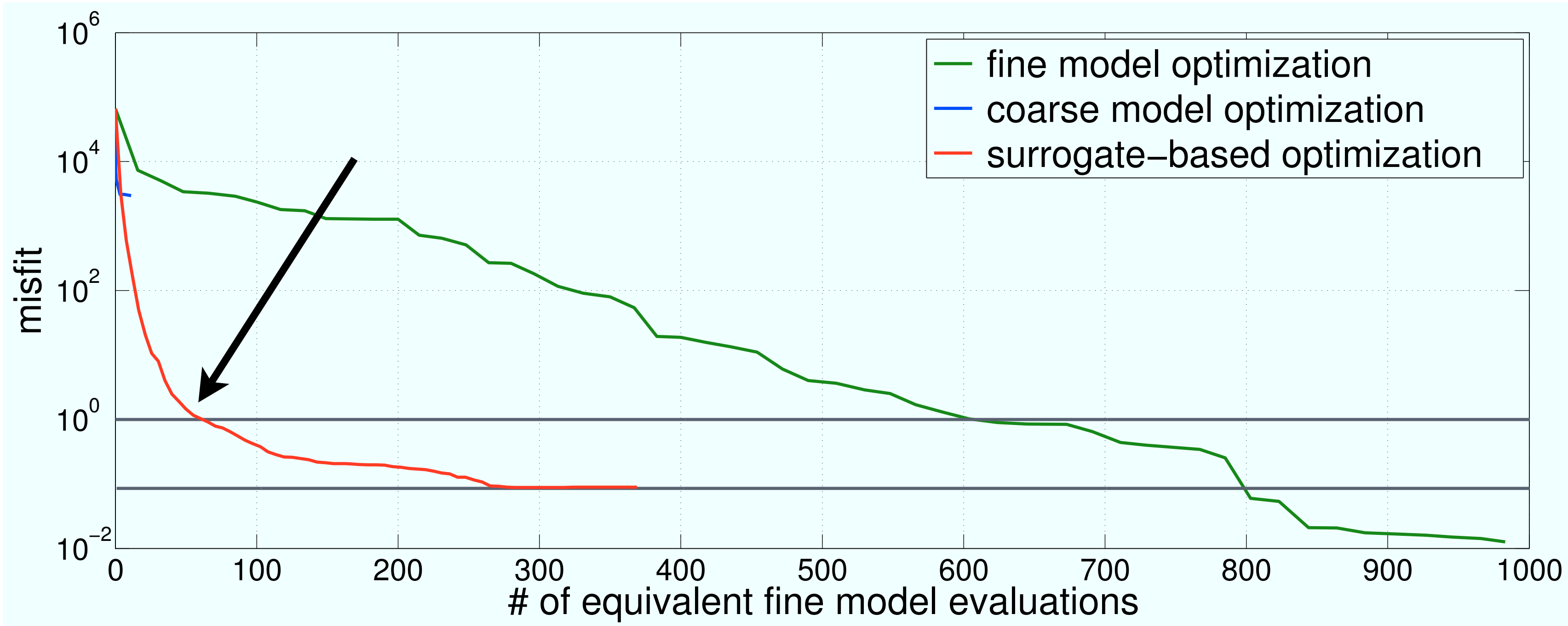

Figure: Convergence history of cost function.

1D NPZD model: Numerical results

Verification by model generated data

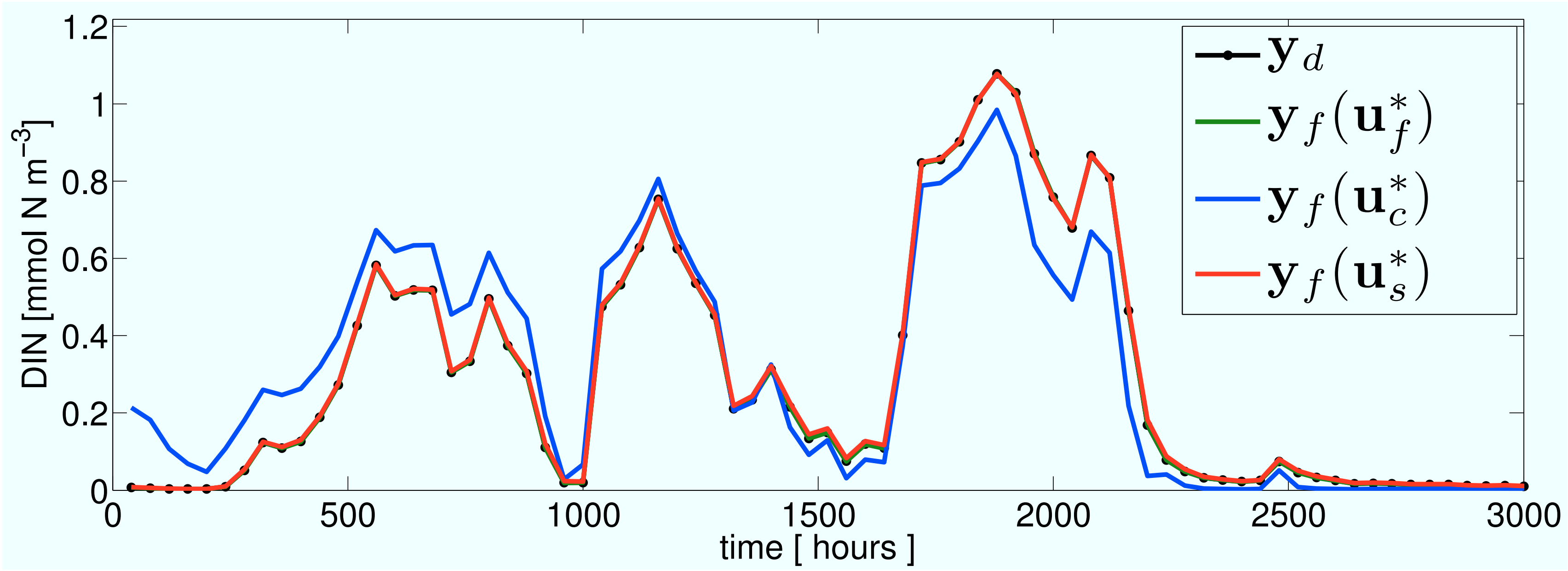

Figure: Fine, coarse model and surrogate optimization: Optimal solutions.

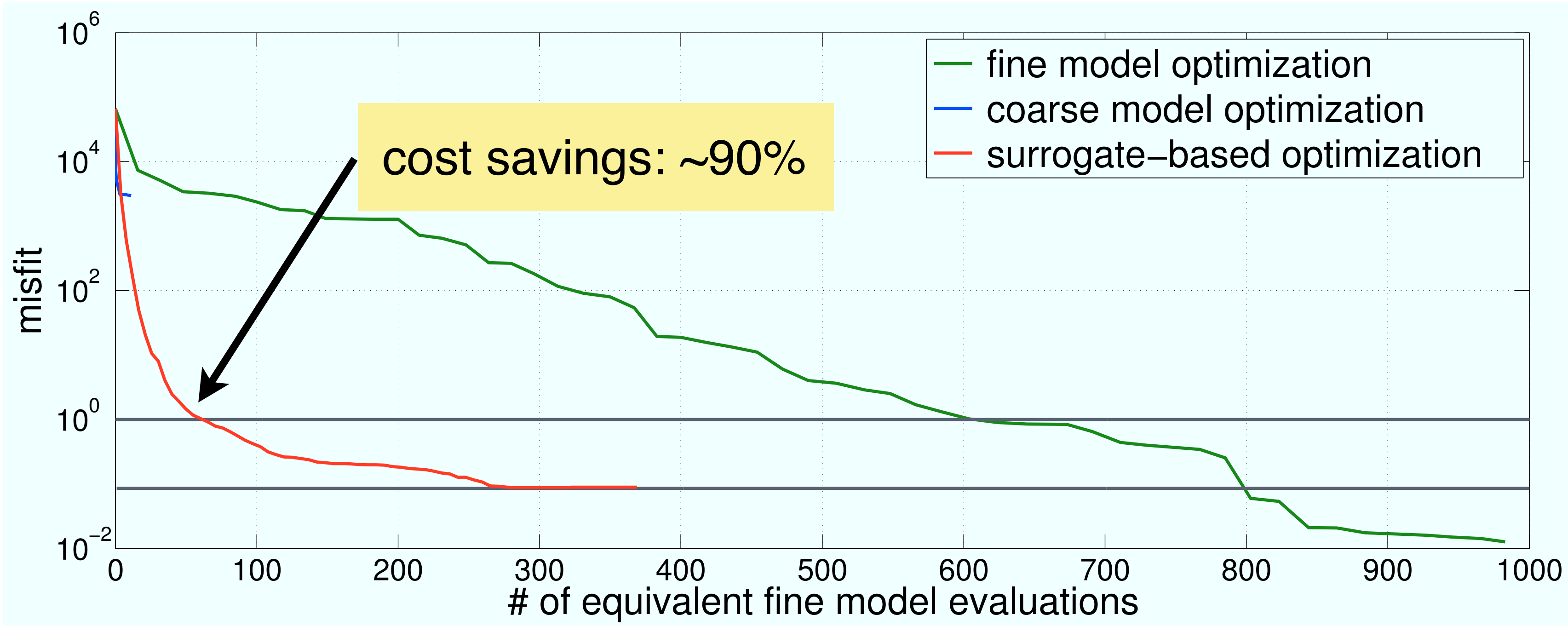

Figure: Convergence history of cost function.